Stem Cells International

Dental-Derived Stem Cells and Their Secretome and Interactions with Bioscaffolds/Biomaterials in Regenerative Medicine: From the In Vitro Research to Translational Applications

Lead Guest Editor: Andrea Ballini
Guest Editors: Marco Tatullo, Antonio Boccaccio, Phuc Van Pham, and Rajiv Saini

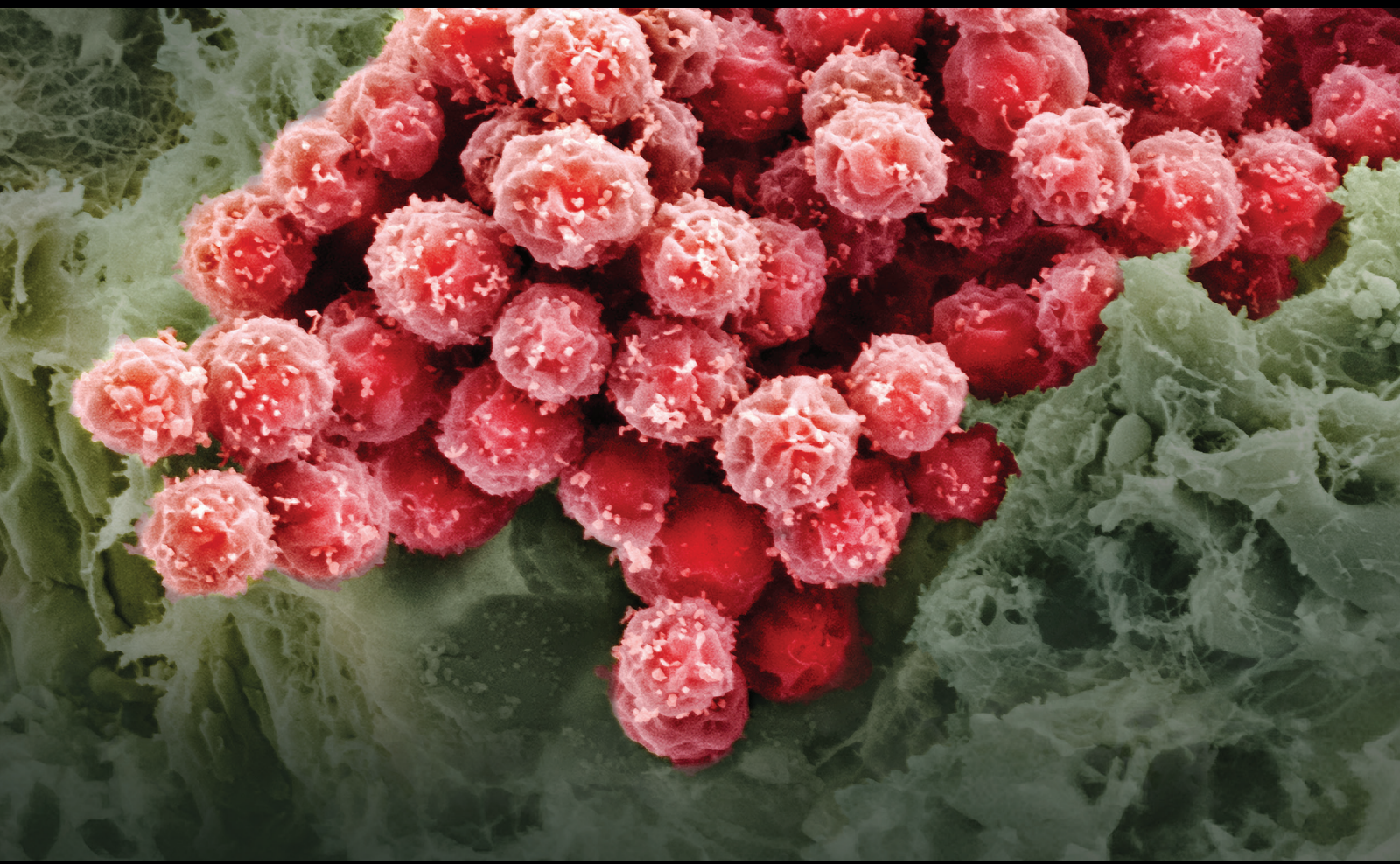

Dental-Derived Stem Cells and Their Secretome and Interactions with Bioscaffolds/Biomaterials in Regenerative Medicine: From the In Vitro Research to Translational Applications

Stem Cells International

Dental-Derived Stem Cells and Their Secretome and Interactions with Bioscaffolds/Biomaterials in Regenerative Medicine: From the In Vitro Research to Translational Applications

Lead Guest Editor: Andrea Ballini
Guest Editors: Marco Tatullo, Antonio Boccaccio, Phuc Van Pham, and Rajiv Saini

Editorial Board

Contents

Hindawi
Stem Cells International
Volume 2017, Article ID 6975251, 3 pages
https://doi.org/10.1155/2017/6975251

Editorial

Dental-Derived Stem Cells and Their Secretome and Interactions with Bioscaffolds/Biomaterials in Regenerative Medicine: From the In Vitro Research to Translational Applications

Andrea Ballini,[1] Antonio Boccaccio,[2] Rajiv Saini,[3] Phuc Van Pham,[4] and Marco Tatullo[5]

[1]*Department of Basic Medical Sciences, Neurosciences and Sense Organs, University of Bari Aldo Moro, Bari, Italy*
[2]*Department of Mechanics, Mathematics and Management, Politecnico di Bari, Bari, Italy*
[3]*Department of Periodontology and Oral Implantology, Pravara Institute of Medical Sciences, Loni, Maharashtra, India*
[4]*Laboratory of Stem Cell Research and Application, University of Science, Vietnam National University, Ho Chi Minh City, Vietnam*
[5]*Biomedical Section, Tecnologica Research Institute, Crotone, Italy*

Correspondence should be addressed to Andrea Ballini; andrea.ballini@uniba.it

Received 19 November 2017; Accepted 20 November 2017; Published 28 December 2017

Regenerative dentistry is an innovative field of medicine that is growing involving both dental and maxillofacial sciences [1, 2].

Clinical healing occurs when new regenerated tissue is well integrated into the previously damaged host tissue: in this context, the reparative and regenerative actions of resident and recruited mesenchymal stem cells (MSCs) have been thoroughly performed.

In the most recent literature, the MSC-produced secretome has been widely studied and it has been even more considered as the strategic promoter of the vast majority of the biological effects derived from stem cell transplantation [3–5].

Dental-derived mesenchymal stem cells (D-dMSCs) are today considered as an intriguing milestone of the regenerative medicine as such cells have been reported to have a strong ability to differentiate into osteogenic, adipogenic, and chondrogenic lineages, with a peculiar ability to improve the bone mineralization [6–9].

Complete healing might be achieved by establishing novel strategies, by using scaffolds in combination with oral-derived MSCs in the presence of secretome and growth [3].

The interaction between stem cells and biomaterials is a crucial topic; recent research trends were focused and developed on the interaction both at superficial macroscopic level and at structural microscopic level. About the first ones, involving the researches on scaffold-related macroscopic features, there are evidences that geometrical and mechanical properties of scaffolds are able to influence the cell behavior and their response to differentiating stimulations [10].

Among the manufacturing processes that can be used to fabricate biomimetic scaffolds, the strategy based on the combination of additive manufacturing and computer-aided design (CAD) modelling seems to be one of the most promising [11]. The possibility to design and create any shape for the newly produced scaffolds, and the scientifically confirmed evidence that scaffold geometry plays a crucial role in influencing the MSC response, led researchers towards an increasing attention to scaffold design; more in details, bioengineers designed complex morphologies able to be reproduced on the surfaces of porous biomaterials [12–15].

Other types of research studies were related to microscopic features of scaffolds, demonstrating that many changes

in scaffold microarchitecture modified, for example, the adhesion of stem cells to the scaffold surfaces [16]. The adhesion of stem cells to scaffold is a biologically guided result of complex cellular, physical, and chemical processes, and it is an essential requirement to guarantee a proper and effective tissue engineering aimed to healing and regenerative applications. Differently from the huge number of studies focused on biochemical reactions that trigger stem cell differentiation, very few studies are reported in the scientific literature about how the mechanical environment affects the adhesion of stem cells on biomaterials' surfaces [17, 18].

We believe that extensive studies will be carried out on this topic in the next few years. However, much still needs to be elucidated in order to be able to create efficient and safe bioartificial substitutes for clinical use.

This special issue has reported articles on D-dMSCs used as therapeutic aid in clinical and surgical applications. The human dental pulp stem cells (hDPSCs) seem to be still the most used cell model by the SI authors.

The most reported translational use of D-dMSC therapy is related to tissue regeneration: in fact, authors have investigated about cytotoxicity, genotoxicity, and biocompatibility of endodontic materials for hDPSCs (A. Victoria-Escandell et al.) or compared using this cell line the efficiencies of osteogenic differentiation and *in vivo* bone formation of hydroxyapatite-tricalcium phosphates (HA-TCPs) and demineralized dentin matrix (DDM) (K.-J. Kang et al.).

An interesting general view has been also given on topics related to issues of general interest, as the potential effect of heavy ethanol consumption can inhibit odontogenic differentiation, a factor that needs to be considered in clinical practice during pulp therapy (W. Qin et al.).

Moreover, other authors have focused their researches to consider that nuclear receptor related 1 (NURR1) plays a key role in switching hDPSC differentiation towards osteoblast rather than neuronal or even other cell lines (A. Di Benedetto et al.).

Finally, some authors have also reported interesting aspects about the role of nephronectin (Npnt) to recruit and conducive to mineralization in hDPSCs, offering a promising approach for hard tissue regeneration (J. Tang and T. Saito).

In this special issue, the editors together with the involved authors have well described the D-dMSCs in their different but fundamental roles of promoters, enhancers, and playmakers of the translational regenerative medicine.

Starting from the contents of our issue, the scientific community will be stimulated to experiment new ideas, to improve the knowledge of D-dMSCs, and to speed up their clinical application, so to improve regenerative medicine approaches.

Andrea Ballini
Antonio Boccaccio
Rajiv Saini
Phuc Van Pham
Marco Tatullo

References

[1] S. Bardelli and M. Moccetti, "Remodeling the human adult stem cell niche for regenerative medicine applications," *Stem Cells International*, vol. 2017, Article ID 6406025, 10 pages, 2017.

[2] T. Squillaro, G. Peluso, and U. Galderisi, "Clinical trials with mesenchymal stem cells: an update," *Cell Transplantation*, vol. 25, no. 5, pp. 829–848, 2016.

[3] B. Parekkadan and J. M. Milwid, "Mesenchymal stem cells as therapeutics," *Annual Review of Biomedical Engineering*, vol. 12, no. 1, pp. 87–117, 2010.

[4] C. Lechanteur, A. Briquet, O. Giet, O. Delloye, E. Baudoux, and Y. Beguin, "Clinical-scale expansion of mesenchymal stromal cells: a large banking experience," *Journal of Translational Medicine*, vol. 14, no. 1, p. 145, 2016.

[5] R. Fazzina, P. Iudicone, D. Fioravanti et al., "Potency testing of mesenchymal stromal cell growth expanded in human platelet lysate from different human tissues," *Stem Cell Research & Therapy*, vol. 7, no. 1, p. 122, 2016.

[6] J. Galipeau, M. Krampera, J. Barrett et al., "International Society for Cellular Therapy perspective on immune functional assays for mesenchymal stromal cells as potency release criterion for advanced phase clinical trials," *Cytotherapy*, vol. 18, no. 2, pp. 151–159, 2016.

[7] M. Marrelli, F. Paduano, and M. Tatullo, "Human periapical cyst-mesenchymal stem cells differentiate into neuronal cells," *Journal of Dental Research*, vol. 94, no. 6, pp. 843–852, 2015.

[8] M. Tatullo, G. Falisi, M. Amantea, C. Rastelli, F. Paduano, and M. Marrelli, "Dental pulp stem cells and human periapical cyst mesenchymal stem cells in bone tissue regeneration: comparison of basal and osteogenic differentiated gene expression of a newly discovered mesenchymal stem cell lineage," *Journal of Biological Regulators & Homeostatic Agents*, vol. 29, no. 3, pp. 713–718, 2015.

[9] A. Ballini, F. Mastrangelo, G. Gastaldi et al., "Osteogenic differentiation and gene expression of dental pulp stem cells under low-level laser irradiation: a good promise for tissue engineering," *Journal of Biological Regulators and Homeostatic Agents*, vol. 29, no. 4, pp. 813–822, 2015.

[10] A. A. Zadpoor, "Bone tissue regeneration: the role of scaffold geometry," *Biomaterials Science*, vol. 3, no. 2, pp. 231–245, 2015.

[11] A. Macchetta, I. G. Turner, and C. R. Bowen, "Fabrication of HA/TCP scaffolds with a graded and porous structure using a camphene-based freeze-casting method," *Acta Biomaterialia*, vol. 5, no. 4, pp. 1319–1327, 2009.

[12] A. Boccaccio, A. E. Uva, M. Fiorentino, L. Lamberti, and G. Monno, "A mechanobiology-based algorithm to optimize the microstructure geometry of bone tissue scaffolds," *International Journal of Biological Sciences*, vol. 12, no. 1, pp. 1–17, 2016.

[13] A. Boccaccio, A. E. Uva, M. Fiorentino, G. Mori, and G. Monno, "Geometry design optimization of functionally graded scaffolds for bone tissue engineering: a mechanobiological approach," *PloS One*, vol. 11, no. 1, article e0146935, 2016.

[14] S. Giannitelli, D. Accoto, M. Trombetta, and A. Rainer, "Current trends in the design of scaffolds for computer-aided tissue engineering," *Acta Biomaterialia*, vol. 10, no. 2, pp. 580–594, 2014.

[15] A. Boccaccio, M. Fiorentino, A. E. Uva, L. N. Laghetti, and G. Monno, "Rhombicuboctahedron unit cell based scaffolds for bone regeneration: geometry optimization with a mechanobiology – driven algorithm," *Materials Science and Engineering: C*, vol. 83, pp. 51–66, 2018.

[16] S. Bose, M. Roy, and A. Bandyopadhyay, "Recent advances in bone tissue engineering scaffolds," *Trends in Biotechnology*, vol. 30, no. 10, pp. 546–554, 2012.

[17] P. P. Provenzano and P. J. Keely, "Mechanical signaling through the cytoskeleton regulates cell proliferation by coordinated focal adhesion and Rho GTPase signaling," *Journal of Cell Science*, vol. 124, no. 8, pp. 1195–1205, 2011.

[18] A. Buxboim and D. E. Discher, "Stem cells feel the difference," *Nature Methods*, vol. 7, no. 9, p. 695, 2010.

Hindawi
Stem Cells International
Volume 2017, Article ID 2546261, 14 pages
https://doi.org/10.1155/2017/2546261

Research Article

The Role of Nephronectin on Proliferation and Differentiation in Human Dental Pulp Stem Cells

Jia Tang[1] and Takashi Saito[2]

[1]*Division of Biochemistry, Department of Oral Biology, School of Dentistry, Health Sciences University of Hokkaido, 1757 Kanazawa, Ishikari-Tobetsu, Hokkaido 061-0293, Japan*
[2]*Division of Clinical Cariology and Endodontology, Department of Oral Rehabilitation, School of Dentistry, Health Sciences University of Hokkaido, 1757 Kanazawa, Ishikari-Tobetsu, Hokkaido 061-0293, Japan*

Correspondence should be addressed to Jia Tang; mathlover2004@163.com

Received 5 June 2017; Revised 28 September 2017; Accepted 16 October 2017; Published 19 November 2017

Academic Editor: Andrea Ballini

Aim. The purpose of the current study was to investigate the effects of nephronectin (Npnt) in human dental pulp stem cells (hDPSCs). *Methodology*. Npnt was coated to nontissue culture-treated polystyrene (non-PS) plates. The presence of immobilized protein on the surface was detected by polyclonal rabbit primary anti-Npnt antibody. Then the cell number was counted and compared with PBS-, bovine serum albumin- (BSA-), fish scale type I collagen- (FCOL1-), and human fibronectin- (Fn-) coated wells. Cell proliferation was assessed using CCK-8 assay. Cell morphology was observed under light microscopy and fluorescence microscopy. Lastly, the mRNA expression profiles of integrins, dentin sialophosphoprotein (DSPP), bone sialoprotein (BSP), and mineralization capacity of hDPSCs were investigated by real time RT-PCR and alizarin red staining, respectively. *Results*. Npnt mediates hDPSC adhesion and spreading partially via the Arg-Gly-Asp (RGD) motif. Npnt enhanced the mRNA expression of ITGA1, ITGA4, ITGA7, and ITGB1 on day five. Npnt downregulated DSPP but significantly upregulated BSP mRNA expression at day 28. Further, Npnt and FCOL1 accelerated the matrix mineralization in hDPSCs. *Conclusions*. The current findings implicate that Npnt would be favorable to recruit hDPSCs and conducive to mineralization in hDPSCs. The combination of Npnt with hDPSCs may offer a promising approach for hard tissue regeneration.

1. Introduction

A healthy dental pulp is of paramount importance to the structural and functional integrity of the tooth. The implications caused by tooth devitalization such as discoloration have driven significant interest in the development of bioactive materials that facilitate the regeneration of damaged dentine tissues by harnessing the capacity of dental pulp for self-repair.

As the regeneration capacities of dental tissue are limited, exposure of pulp, whether caused by injury or caries, requires immediate operative intervention to restore its vitality. The fundamental point of a successful regeneration of dentin is a combination of growth factors, stem cells, and scaffold. The human dental pulp stem cells (hDPSCs) were discovered in 2000 and characterized by their ability to form dentine-like structure when transplanted into immunocompromised mice [1]. On the other hand, hDPSCs were also able to differentiate into adipocyte and neural-like cells [2], highlighting their potentiality to be used in the treatment of neurodegenerative diseases. Recently, it was reported that hDPSC secretome reduces cytotoxicity and apoptosis caused by amyloid beta (Aβ) peptide, a main component of amyloid plaques in Alzheimer's disease (AD), and could possibly be utilized in the treatment of AD [3], a chronic neurodegenerative disease that afflicts 46 million people worldwide nowadays [4]. More importantly, although DPSC shares similar immune-phenotype with the bone marrow stromal

cell (BMSC) *in vitro*, DPSC displayed strikingly higher odontogenic potentiality than BMSC using the same induction factors [5].

Generally, because of the existence of stem cells, tissues or organs retain an innate ability to repair their damaged portions, to a certain degree. Nevertheless, this endogenous capacity is compromised by aging or severe inflammation. Tissue engineering in the dental field is therefore gaining an increasing interest. The past several decades witness a paradigm shift in the conception of the scaffold, which has changed from passive carrier to bioactive signal initiator. Especially, relentless efforts have been ongoing in exploring natural polymers such as extracellular matrix (ECM) scaffold containing cell interactive motifs. To name a few, collagen [6], chitosan [7], hydroxyapatite [8], etc. have all been reported to be appropriate candidates for tissue engineering. Npnt, an Arg-Gly-Asp- (RGD-) containing ECM protein originally identified in embryonic kidney, is intensively expressed in developing tooth and assumes important function in regulating the sox2 expression, a dental epithelial stem cell marker. Importantly, loss of Npnt results in reduced tooth germ size [9], underscoring an indispensable role of Npnt in the process of tooth development. Furthermore, an earlier work from our lab demonstrated that the mRNA expression of Npnt increased with the differentiation of the MDPC-23 cell and Npnt protein itself was effective in promoting the proliferation and differentiation of this specific odontoblast-like cell line [10]. Nevertheless, the precommitted nature of MDPC-23 cell necessitates study using a multipotent type of cell to further confirm the adhesive and inducing capacities of Npnt.

The current experiment was hence designed to clarify the following issues: first, is Npnt a hDPSC adhesive? Second, if yes, is RGD in its sequence involved in the regulation of cell adhesion? Third, is Npnt effective in promoting the differentiation of hDPSCs into odontoblast or at least hard tissue-forming cells? Finally, can the mineralization of hDPSCs be enhanced by Npnt? To answer those questions, we coated Npnt protein to nontreated tissue-cultured polystyrene plates (non-PS) and assessed a number of biochemical parameters such as RGD peptide inhibition assay, CCK-8 assay, real-time RT-PCR, and alizarin red staining to characterize the cellular behavior.

2. Materials and Methods

2.1. Cell Culture. Human dental pulp stem cells (hDPSCs) (catalog number PT-5025; Lot number 0000361427) were purchased from LONZA (Walkersville, MD, USA). Use of hDPSCs was approved and under the guidelines set by the ethical committee of the Health Sciences University of Hokkaido. The characterization of its stem cell phenotypes was carried out using flow cytometry including tests of surface antigens ($CD105^+$, $CD166^+$, $CD29^+$, $CD90^+$, $CD73^+$, $CD133^-$, $CD34^-$, and $CD45^-$) by the manufacturer (see the certificate of analysis in Supplementary file 1 available online at https://doi.org/10.1155/2017/2546261). Cells were maintained in Dulbecco's Modified Eagle's Medium (DMEM) (D5796, Sigma) supplemented with 10% fetal bovine serum (FBS) (10270-106, Gibco). All media were supplemented with 50 units/mL penicillin and 50 μg/mL streptomycin (catalog number 15070063, Gibco). Cells were cultivated at 37°C under humidified 5% CO_2 and 95% air atmospheric conditions. Mineralization reagent including β-glycerophosphate (β-GP, 10 mM) (191-02042, Wako) and ascorbic acid (AA, 50 μg/mL) (013-19641, Wako) was incorporated upon confluence.

2.2. ECM Proteins and Coating Procedure. Non-PS plates (24-well plate: 1820-024, Iwaki; 12-well plate: 351143, Falcon) were coated with nephronectin (Npnt, 10 μg/mL, 1 μg/cm^2, 4298-NP-050, R&D systems), fibronectin (Fn, human plasma, 10 μg/mL, 1 μg/cm^2, 33016015, Gibco), and fish scale type I collagen (FCOL1, 10 μg/mL, 1 μg/cm^2, Cellcampus AQ-3LE, Taki Chemical) diluted in phosphate-buffered saline (PBS) (REF 10010-023, Gibco), water (pH 7.4), or sterile acidic water (pH 3.0), respectively. PBS- and bovine serum albumin (BSA, 1%) (A9418, Sigma)-coated substrate(s) were served as controls. Surfaces were coated with ECM proteins solution for 48 hours at room temperature inside clean bench, washed twice with PBS before cell inoculation.

2.3. Confirmation of the Presence of Coated Npnt by Immunofluorescence Staining. Primary polyclonal rabbit anti-Npnt (1 μg/mL, ab110230, Abcam) was added to Npnt- or PBS-coated polystyrene at room temperature for 2 h. PBS was used to wash the first antibody-treated surfaces twice. Afterwards, the surfaces were incubated for 1 h in PBS with Alex Flour 488 goat anti-rabbit IgG (2 μg/mL, A11034, Invitrogen). Surfaces were rinsed twice by PBS and imaged using fluorescence microscopy (EVOS® FL Cell Imaging System, catalog number AMF4300, Thermo Fisher Scientific).

2.4. Fluorescence Staining of Actin Cytoskeleton. hDPSCs were seeded into 24-well plates (surface area: 2 cm^2, non-PS) at the concentration of 4×10^3/well in DMEM containing 10% FBS. At day five, culture media were aspirated and cell monolayer was rinsed by PBS (Gibco) twice preceding fixation. Fixation of cells was performed using methanol-free formaldehyde (16%, *w*/*v*, catalog number 28906, Thermo Fisher Scientific) diluted to a concentration of 4% (*v*/*v*) in PBS (200 μL/well) for 15 min at room temperature. Cells were rinsed briefly by PBS three times before addition of permeabilisation reagent Triton X-100 (0.1%, *v*/*v*, in PBS) (400 μL/well). Five minutes following the permeabilisation treatment, BSA at the concentration of 1% (*w*/*v*, in PBS) was poured into each well (400 μL/well) to block any nonspecific binding for 30 min at room temperature. Phalloidin (catalog number A12380, Invitrogen) (working concentration: 2 U/200 μL, 200 μL/well), a highly toxic and specific cytoskeleton probe conjugated to red-orange fluorescent Alexa Fluor® (AF) 568 dye, was used to localize F-actin. Nucleus was counterstained using 4,6-diamidino-2-phenylindole (DAPI, D9542, Sigma) (working concentration: 300 nM, 200 μL/well) for 5 min. Finally, cells were immersed

Table 1: Primer sequence, fragment size, and annealing temperature.

Gene name	Forward	Backward	Fragment size (bp)	Annealing temperature (°C)
hGAPDH (NM_001289746.1)	CACTAGGCGCTCACTGTTC TCT	CGTTCTCAGCCTTGACGGT	250	66
hDSPP (NM_014208.3)	TGCTGGCCTGGATAATTCCG	CTCCTGGCCCTTGCTGTTAT	136	66
hBSP (NM_004967.3)	AAGGGCACCTCGAAGACAAC	CCCTCGTATTCAACGGTGGT	119	62.8
hITGA1 (NM_181501.1)	CTCACTGTTGTTCTACGCTGC	ACGACTTGAAATGTGGGGCT	419	59.9
hITGA2 (NM_002203.3)	GTGGCTTTCCTGAGAACCGA	GAAGCTGGCTGAGAGCTGAA	278	62.8
hITGA3 (NM_002204.3)	ATGGCAAGTGGCTGCTGTAT	GCACTCTAGCCACACACAGT	272	59.9
hITGA4 (NM_000885.5)	AATCCCGGGGCGATTTACAG	TCCAGCTTGACATGATGCA AAA	354	59.9
hITGA5 (NM_002205.4)	CCCTCATCTCCGGGACACTA	ATCCAACTCCAGGCCCTTTG	397	56.3
hITGA6 (NM_000210.3)	CTCGCTGGGATCTTGATGCT	TCAGATGGCTGAGCATGGAT	128	59.9
hITGA7 (NM_002206.2)	GGAAGACCGACAGCAGTTCA	ATCTTGATGCGACACCAGCA	264	59.9
hITGA8 (NM_003638.2)	GCCTATGCCGAGTTCTCTCC	CCCAGTAAACTCCCCAGCAG	297	59.9
hITGB1 (NM_002211.3)	GCCGCGCGGAAAAGATGAAT	TGCTGTTCCTTTGCTACGGT	323	59.9
hITGB3 (NM_000212.2)	GAAGCAGAGTGTGTCACGGA	ACATGACACTGCCCGTCATT	201	59.9

in PBS to avoid drying up and photographed using EVOS FL Cell Imaging Station System. Four different fields were selected under fluorescence microscopy to count the number of DAPI-stained nucleus. The average number was calculated and compared between each group.

2.5. Cell Proliferation Assay. For the cell viability test, fifty microliters of recombinant Npnt (10 μg/mL) solution was coated onto a 96-well plate (351172, Falcon) for two days at room temperature. The wells were dried up and rinsed twice with PBS. hDPSCs were rinsed once with PBS, harvested using trypsin for eight minutes at 37°C, collected by centrifugation (500g, 5 min, 2800, Kubota), and then resuspended in serum-free DMEM. Cells were seeded into non-, BSA-, Npnt-, Fn- and FCOL1-coated wells at the concentration of 8×10^3/well. At 18 h, 41 h, and 64 h, CCK-8 reagent was added to each well (10 μL/well) and incubated for 1 h and 20 min in the incubator. Absorbance was read at the wavelength of 450 nm (iMark™, Bio-Rad).

2.6. Inhibition Test Using Npnt-Derived Soluble RGD Peptide. The RGD-containing hexapeptide, KPRGDV, was designed based on the amino acid sequence of mouse Npnt (NCBI reference sequence NP_001025007.1). KPRGDV and its aberrant counterpart KPRGEV with final purity over 97% were generated from Sigma-Aldrich, Japan. The peptides were dissolved in PBS to a final concentration of 10 mM and stored at 4°C until use. Npnt (10 μg/mL) solution was poured into a 24-well plate (200 μL/well), and the plate was dried up with a cover open in the clean bench for two days. Prior to cell inoculation, the coated plate was rinsed briefly with PBS twice (400 μL/well each time). hDPSCs were preincubated with KPRGDV (1 mM) or KPRGEV (1 mM) or PBS vehicle for 10 min at 37°C in the incubator. After incubation, the cells were seeded into Npnt-coated wells at the concentration of 2×10^4/well in serum-depleted DMEM. The cell photos were taken after 19 h incubation; afterwards, the media were changed into DMEM containing 10% FBS. Cells were photographed at 43 h and 67 h as well.

2.7. Quantitative Reverse Transcriptase Polymerase Chain Reaction (qRT-PCR). hDPSCs were seeded into 12-well plates coated by either Npnt or the other proteins (BSA, Fn, and COL-1) at the concentration of 2×10^4/well and incubated at 37°C in 5% CO_2. After five and 28 days in culture, cells were lysed by TRIzol (Invitrogen) and total RNA extracted from each sample using the acid guanidinium thiocyanate-phenol-chloroform method. After the precipitation step, RNA was washed with 75% ethanol and reconstituted in RNase-free water. Quantification of RNA was measured by absorbance using Nanodrop 1000 (Thermo Fisher Scientific). Total RNA was reverse transcribed into complementary DNA (cDNA) and amplified in a 20 μL reaction system. Real-time RT-PCR was carried out in LightCycler® Nano (Roche) using FastStart Essential DNA Probes Master (2x) (Roche). Housekeeping gene GAPDH was taken to be the internal control. The primers used are shown in Table 1. The SYBR green amplification consisted in an initial denaturation of 10 min at 95°C and followed by 50 cycles of 15 s at 95°C (denaturation), 30 s at annealing temperature (refer to Table 1 for each set of primer) and 40s at 72°C (extension).

2.8. Alizarin Red Staining (ARS). ARS is a method of detecting calcium-rich deposits in cell cultures. The media were aspirated before the staining procedure, cells were rinsed briefly with PBS twice and fixed by adding 10% neutral buffered formalin (200 μL/well in a 24-well plate; 400 μL/well in a 12-well plate) (060-01667, Wako) at room temperature for 20 min. Fixative residues were removed by washing with distilled water. ARS solution (1%, pH 4.0) (011-01192, Wako) was added, at the same volume of fixative poured, and incubated at 37°C for 5–10 min. ARS solution was discarded

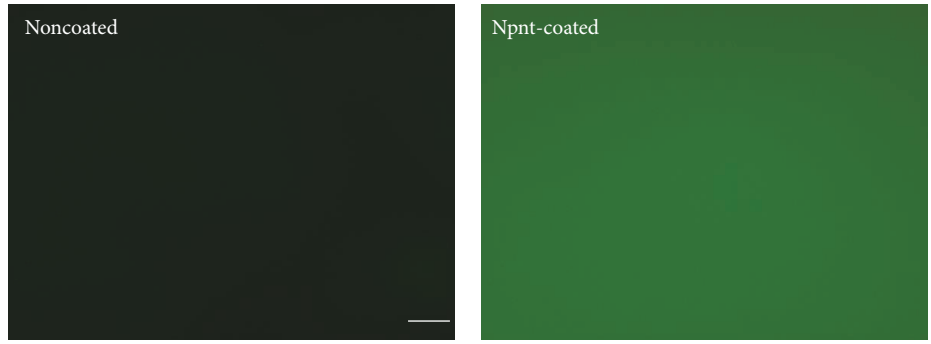

Figure 1: Fluorescence visualization of coated Npnt. Npnt-coated polystyrene was positive for anti-Npnt (b). No fluorescence was observed in the noncoated control (a) (scale bar: 50 μm).

afterwards; the cells were washed using distilled water for another 1 hour and photographed. To quantify the staining intensity, cetylpyridinium chloride (CPC) (10%, *w*/*v*, in distilled water) (C0732-100G, Sigma) was added to each well (700 μL/well) to extract the stain. After 1 h incubation under 37°C, the CPC solution was transferred to a new 96-well plate (200 μL/well) for absorbance reading at 570 nm.

2.9. Statistical Analysis. Statistical analyses were performed by post hoc Tukey's HSD test. The results were considered statistically significant for $p < 0.05$.

3. Results

3.1. Confirmation of the Presence of Npnt on Polystyrene Surface. The Npnt-coated polystyrene was positive for anti-Npnt-generating green fluorescence light, while no fluorescence was observed in the PBS-coated control (Figure 1).

3.2. Cell Morphology Observation and Cell Number on Different ECMs. The light microscopy photos of cells seeded on five different substrate(s) are shown in Figure 2(a). Until 116 h, it was observed that cells in noncoated and BSA-coated groups remain to be round in shape, no cells were found to be spread in the two groups. Cells in Npnt-, Fn-, and FCOL1-modified surfaces were successfully attached, spread, and adopted-flattened or spindle-shaped; the cells continued to grow during the five-time points of observation in the three groups. A significant difference in cell number was observed in Npnt- $(1.95 \pm 0.13 \times 10^4)$, Fn- $(3.00 \pm 0.27 \times 10^4)$, and FCOL1- $(3.25 \pm 0.41 \times 10^4)$ coated substrate(s) as compared to PBS- $(0.10 \pm 0.04 \times 10^4)$ and BSA- $(0.38 \pm 0.20 \times 10^4)$ coated control groups at day five. The cell number in the Npnt-coated group was slightly lower than that in Fn- and FCOL1-coated groups ($p < 0.01$), while no difference was detected between Fn- and FCOL1-coated surfaces (Figure 2(b)).

3.3. Cytoskeleton Visualization. Well-developed actin stress fibers were formed and clearly observed in Npnt-, Fn-, and FCOL1-coated non-PS wells (Figure 3).

3.4. Cell Growth in the Absence of Serum. The proliferation rates of hDPSCs were analyzed in response to various substrate(s) using the CCK-8 assay. The three matrix proteins (Npnt, Fn, and FCOL1) significantly promoted the proliferation of cells in the absence of serum at 18 h, and this effect persisted to 64 h (Figure 4). At 18 h, the viability of hDPSCs in Npnt (0.33 ± 0.01) was slightly lower than that of FCOL1 (0.36 ± 0.00). Forty-one hours postinoculation, the viability of the cell in Npnt (0.50 ± 0.03) was at the same level as the FCOL1 group (0.51 ± 0.02). At 64 h, cell viability of Npnt (0.70 ± 0.06) achieved the highest among the five groups, while the viability of cells in Fn was only slightly augmented; in the FCOL1 group, cell growth entered a static stage since the value at 64 h was almost unchanged as compared to that at 41 h (41 h: 0.51 ± 0.02 versus 64 h: 0.50 ± 0.02). Cells in the two negative control groups stopped to grow as illustrated by the viability number. Notably, at 64 h, viability of cells in noncoated (0.23 ± 0.01) and BSA-coated (0.15 ± 0.01) decreased as compared to their earlier time points data (noncoated: 0.29 ± 0.00 at 18 h, 0.33 ± 0.00 at 41 h; BSA-coated: 0.17 ± 0.01 at 18 h, 0.18 ± 0.01 at 41 h).

3.5. Peptide Inhibition Test. Figure 5 shows that adhesion and spreading of hDPSCs was inhibited by KPRGDV (Figure 5(a), middle photo of the upper panel, and 5(b)); cells were successfully attached and spread on Npnt-coated surfaces in KPRGEV- or PBS-treated groups. The counting of DAPI-stained nucleus further confirmed a significant reduction of attached cell number in Npnt-RGD preincubated group, indicating adhesion of cells to the Npnt-coated substrate(s) was partly mediated by the RGD domain within Npnt (Figure 5(b)). Moreover, addition of KPRGDV hampered the spreading of hDPSCs as well (Figure 5(d)). A change of aspartic acid (D) into glutamic acid (E) completely abrogated the inhibition: cells in control peptide-KPRGEV group had no adverse effect on the parameter measured (Figures 5(a), 19 h FBS-, 5(b), and 5(e)). To test whether the inhibitory effect of RGD peptide is reversible, after 19 h of adhesion, the serum-free DMEM was replaced by the serum-containing complete medium. As shown in Figure 5(a) (middle and lower panel) that, at 43 h and 67 h,

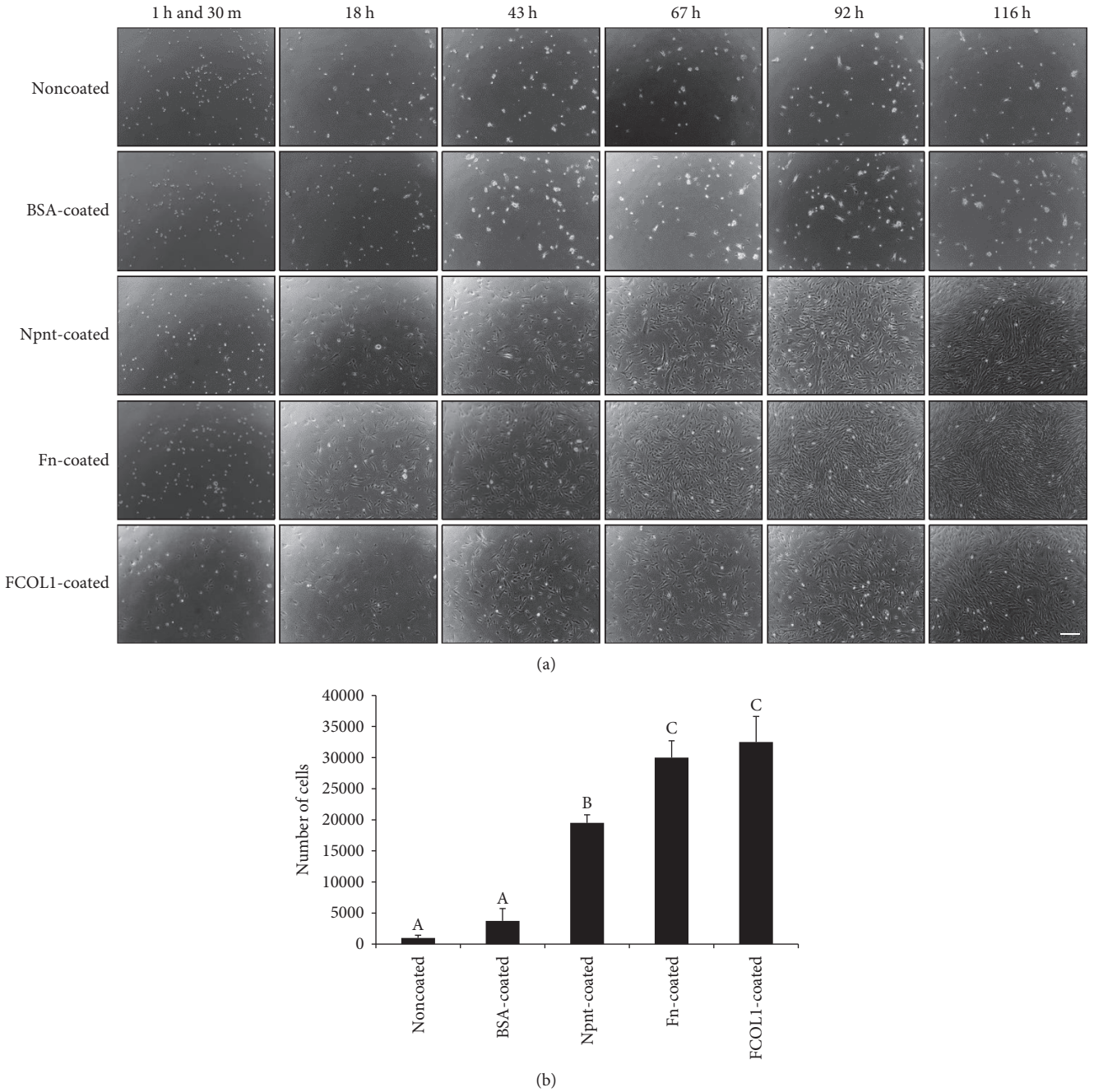

Figure 2: Microscopic observation and cell number counting. (a) hDPSCs were seeded into PBS-, BSA-, Npnt-, Fn-, or FCOL1-coated 24-well plates (non-PS) at the concentration of 4×10^3/well in DMEM supplemented with 10% FBS, penicillin/streptomycin (50 U/mL; 50 μg/mL) (scale bar: 200 μm). Cell morphology was observed at 1 h and 30 m, 18 h, 43 h, 67 h, 92 h, and 116 h. (b) hDPSCs were seeded into 24-well plates (non-PS) at the concentration of 4×10^3/well in the same culture media as illustrated in (a), cell number was counted at day five. Different symbols represent significant differences, $p < 0.01$ by post hoc Tukey's HSD test.

the cell adhesion and spreading in the Npnt-RGD group was recovered after incorporation of FBS, implicating this inhibitory activity of cell adhesion was reversible.

3.6. Real-Time RT-PCR. The gene expression profile of integrin(s) at an early stage (day five) was characterized. It is shown in Figure 6 that ITGA1 and ITGB1 were simultaneously upregulated to 1.31 ± 0.04-fold ($p < 0.01$) and 1.87 ± 0.09-fold ($p < 0.01$) by Npnt, respectively. Interestingly, expression of ITGA8, the reported potent receptor for Npnt, was found to be unaltered in Npnt-coated well. ITGA2 was downregulated in the Npnt-coated group (0.86 ± 0.01-fold, $p < 0.01$). There was no change in the expression of ITGA5 in the Npnt-coated group, while in the Fn-coated group, its expression was moderately attenuated as compared to control. On day 28, the expression of

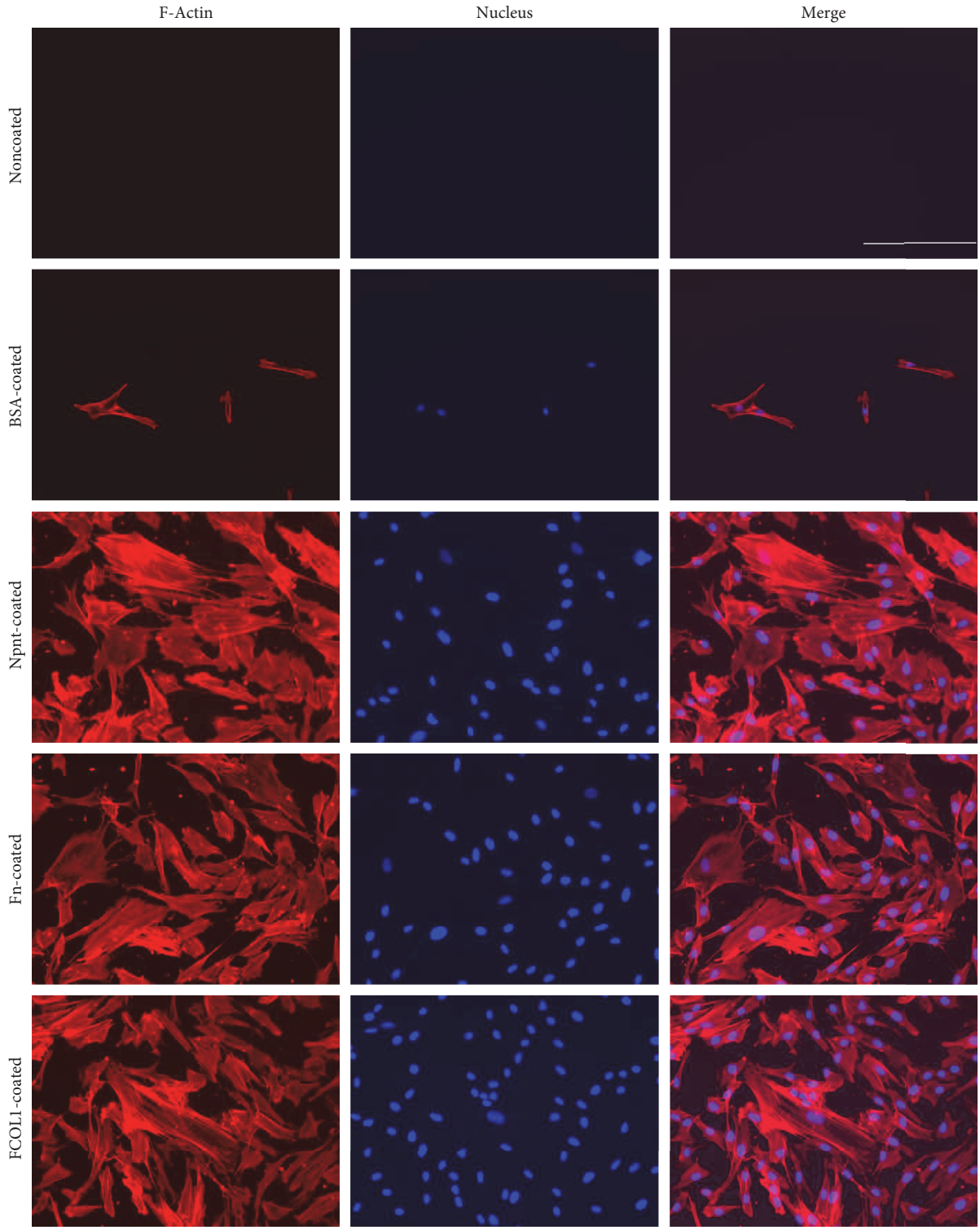

Figure 3: Organization of actin stress fibers. Fluorescence microscopy photographs of hDPSCs that adhered and spread on polystyrene presenting Npnt. As positive controls, cells attached to substrate(s) having adsorbed layers of Fn and FCOL1. Actin stress fibers were visualized with Alexa Fluor 568-conjugated phalloidin (red-orange), and nuclei were visualized with DAPI (blue). The scale bar in merge photo of noncoated group applies to all panels (scale bar: 200 μm).

hard tissue-forming markers including DSPP, BSP, and four integrins that were upregulated by Npnt on day five was assessed (Figure 7). Fn and FCOL1 significantly promoted the expression of DSPP to 2.02 ± 0.06-fold and 1.39 ± 0.11-fold, respectively, while Npnt downregulated the expression (0.77 ± 0.07). On the other hand, BSP was found to be augmented by all the three matrix proteins to a different extent (Npnt: 2.31 ± 0.14-fold; Fn: 1.60 ± 0.03-fold; and FCOL1:

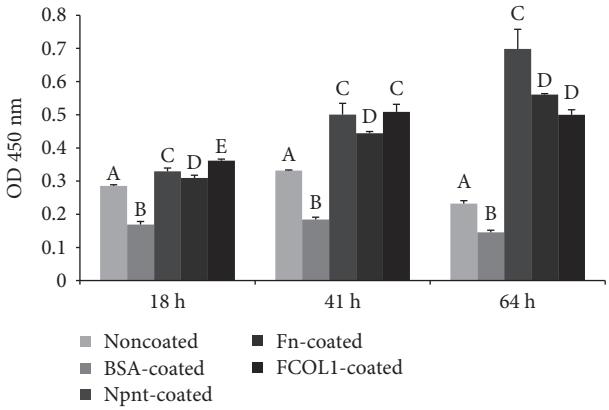

Figure 4: Cell proliferation in the absence of serum. hDPSCs (passage number 5) were seeded into 96-well plates (non-PS) at the concentration of 8×10^3/well in FBS-free DMEM. Cell proliferation was recorded using CCK-8 reagent at 18 h, 41 h, and 64 h postinoculation. Different symbols represent significant differences in each separate time point, $p < 0.01$ by post hoc Tukey's HSD test.

1.81 ± 0.09-fold). As for the four subtypes of integrin, it was found that ITGA7 was the one that has been significantly promoted by Npnt (3.31 ± 0.10-fold); on the contrary, FCOL1 repressed its expression by 53% compared to noncoated control. Slight upregulation of ITGA1 and ITGA4 was detected in the Npnt group, while ITGB1 was moderately suppressed.

3.7. Alizarin Red Staining. Figure 8(a) shows hDPSCs underwent mineralization when cultured on tissue culture polystyrene plates in osteogenic media for 19 days (total 23 days in culture), denoting that hDPSCs were able to differentiate into mineralized tissue-forming cells *in vitro*. Subsequently, it was found that mineralization occurred in cells (high seeding number 6×10^3/well) cultured on Npnt- and FCOL1-coated substrate(s) (non-PS), albeit at a longer culture period (total 30 culture days and 25 days in osteogenic media). The cells grown on negative controls and Fn failed to facilitate appreciable mineralization nodules even in the presence of osteogenic media (Figures 8(b) and 8(c)).

4. Discussion

We used nontissue culture-treated polystyrene (non-PS), a highly hydrophobic substrate to study the roles of three matrix proteins in hDPSCs. For the surface modification of polystyrene, a variety of methods are available: physical adsorption (PA), chemical crosslinking, plasma modification, photochemical immobilization, and layer-by-layer self-assembly [11]. Among the methods listed, PA, also called physisorption, is the simplest and fastest way of achieving immobilization of a target polymer. The primary mechanism of PA lies in intermolecular interaction—the van der Waals force [12]. We hence selected the PA method because of its convenience and safety. The proteins were all prepared in solution form and immobilized by applying to non-PS at the same concentration of 10 μg/mL. The coated surfaces were left dried up at room temperature. Primary antibody specific to Npnt was used to verify that the protein had undergone efficient immobilization (Figure 1). The cells were allowed to adhere to 24-well plates (non-PS) presenting Npnt, Fn, and FCOL1, simultaneously; those grown on PBS and BSA-coated wells were taken to be negative controls. Notably, a considerable number of cells started to adhere and spread as early as 1 h 30 m in the FCOL1 group: cells in FCOL1 formed membrane protrusions to adhere and attach to the underlying substratum, while those in the negative controls and Fn group remained round in shape. In the Npnt-coated group, although less in number than the FCOL1 group, cell membrane protrusions could still be observed.

Early observation of cell protrusions formed by actin polymerization in the FCOL1 and Npnt groups indicated potential positive effects adopted by these two proteins in directing differentiation of cells, which were echoed by the later ARS staining data. Eighteen hours post inoculation, all the three matrix protein ligands mediated efficient adhesion of cells and spreading to result in a flattened morphology. Therefore, for non-PS presenting the proteins at this specific concentration (10 μg/mL), each protein could efficiently facilitate cell adhesion and spreading. As negative controls, PBS and BSA failed to assist efficient cell adhesion and spreading throughout the time points observed, suggesting that neither PBS nor BSA possessed cell adhesive motifs and hence did not impart cell adhesion activities. Cell number of the five groups further revealed that significant higher numbers of cells were attached in Npnt, Fn, and FCOL1 groups as compared to PBS and BSA controls (Figure 2(b)).

Next, cells were allowed to attach to substrata presenting the three types of protein and fixed to permit imaging of the cytoskeletal structures. We used phalloidin AF 568 (red fluorescence) to visualize actin stress fibers. hDPSCs had well-spread shape, with actin fibers that spanned the dimensions of cells in Npnt, Fn, and FCOL1-coated surfaces (Figure 3). However, cells cultured in PBS- or BSA-coated wells failed to generate similar cytoskeletal structure as shown in the matrix protein-coated groups. It is well-documented that the driving force for the formation of membrane protrusion is polymerization of actin filaments [13]. Remodeling of actin cytoskeleton plays a central role in a number of biological activities, especially, the importance of actin polymerization is underscored in the osteogenic commitment of stem cells, for example, osteogenic differentiation of mesenchymal stem cells was interrupted by the inhibition of actin polymerization using *Cytochalasin D* (an actin polymerization blocking reagent) [14, 15], while induction of actin polymerization in MC3T3-E1 cell by *Jasplakinolide* contributes to an enhanced mRNA expression of alkaline phosphatase (ALP) and osteocalcin (OCN) [16]. Moreover, inhibition of actin depolymerization promoted the differentiation [17]. The current results highlighted that Npnt could mediate similar cytoskeletal phenotypes as did the Fn and FCOL1, while PBS and BSA could not. Furthermore, we characterize the cell proliferation profile in the absence of serum in 96-well plates (non-PS) (Figure 4). It was shown that growth of cells seeded in PBS and BSA groups stagnated, as the absorbance reading for the three-time points in the two groups remained almost the same. In contrast, cells in the Npnt

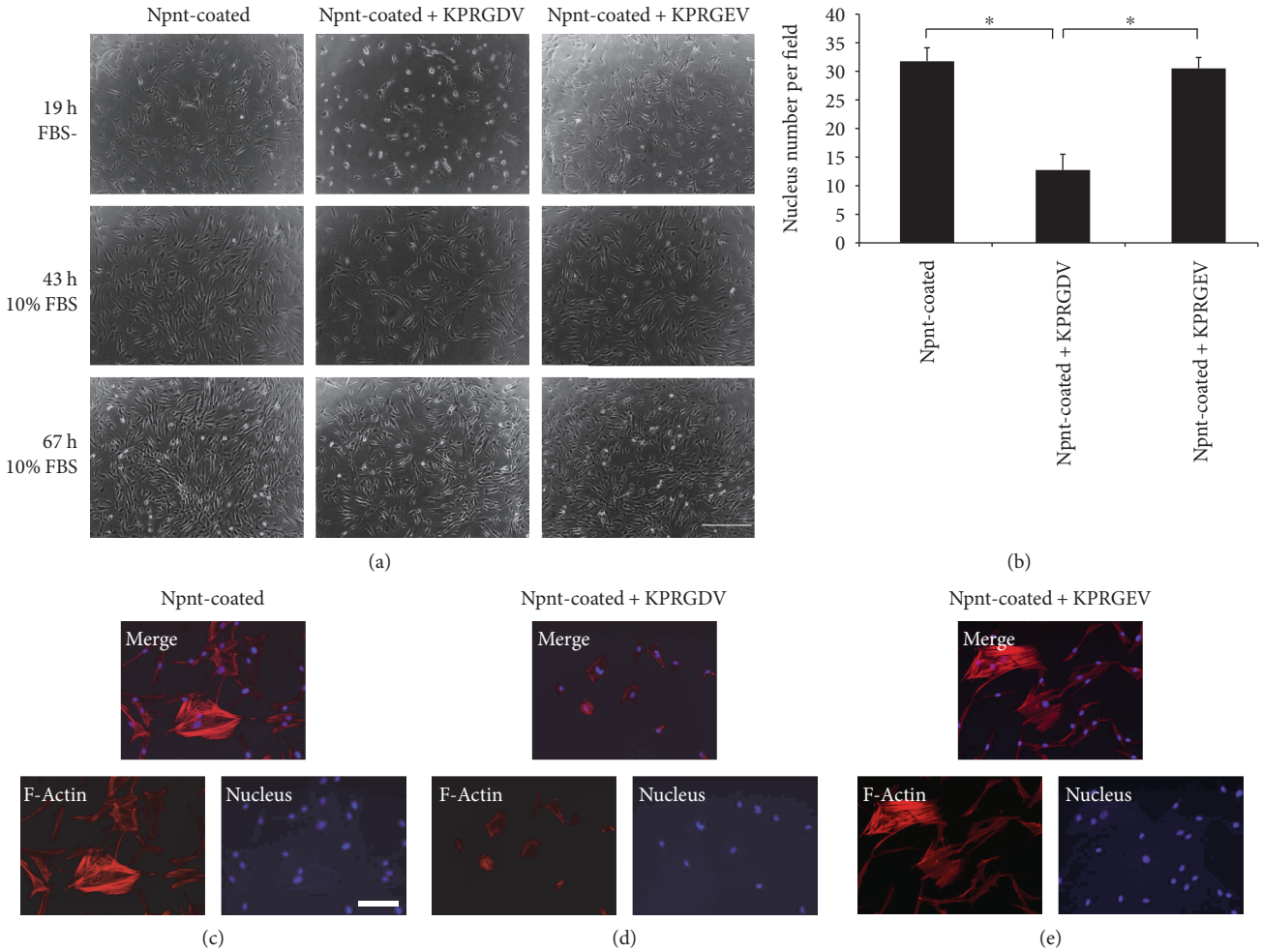

Figure 5: RGD was the key peptide that allowed hDPSCs to bind with Npnt. (a) hDPSCs (passage number 5) were treated with KPRGDV (1 mM in PBS) (a, middle), KPRGEV (1 mM in PBS) (a, right), or equal volume of PBS (Control) (a, left) for 10 min and were then seeded onto Npnt (10 μg/mL)-coated substrate(s) (24-well plate) in serum-free DMEM, and media were changed into FBS (10%) containing DMEM after 19 h. Scrambled peptide (KPRGEV) did not inhibit cell adhesion (a, 19 h right). KPRGDV abrogated cell adhesion and spreading (a, 19 h middle). The abrogation was reversible when serum-free DMEM was replaced with 10% FBS containing DMEM (a, 43 h and 67 h) (scale bar: 400 μm). (b) Nucleus number determination in four separate fields under microscopy for each group. $^*p < 0.01$ by post hoc Tukey' HSD test. (c) hDPSCs were first treated with PBS (c), KPRGDV (d), and KPRGEV (e) and subsequently seeded into Npnt-coated substrate(s) in serum-free DMEM for 24 h. Fluorescence staining was conducted to visualize actin stress fibers and nucleus. Well-development actin stress fibers were observed in (c) and (e), whereas cells remain round in (d) (scale bar: 100 μm).

group continued to grow and reached the highest viability at 64 h as compared to the other groups. The above data shed novel light on the capacity of Npnt to support the growth of hDPSCs in the presence or even absence of serum, featuring its potential to facilitate cell attachment and growth in the exposed pulp, where the blood supply is usually compromised by aging or inflammation.

To further elucidate the specific cell adhesive motif within Npnt, we investigated whether synthetic hexapeptide KPRGDV derived from mouse Npnt (Npnt-RGD) and its mutant counterpart KPRGEV (Npnt-RGE) in soluble form could block the adhesion of hDPSCs to surface-presenting Npnt (Figure 5). We found that the Npnt-RGD could block cell adhesion and spreading to a surface presenting Npnt (Figures 5(a), 19 h FBS-, 5(b), and 5(d)), while the mutant Npnt-RGE did not (Figures 5(a), 19 h FBS-, 5(b), and 5(e)). Further, although Npnt-RGD inhibited the adhesion of cells in short-term (19 h), the presence of this peptide did not prevent cells from adhering and thriving in long-term culture (43 h and 67 h), when the media was replaced from serum-free DMEM to DMEM containing 10% FBS (Figure 5(a), 43 h and 67 h). With the advancing of technology such as chemical microchip array [18], more cell adhesion and functional peptides are being identified. Nevertheless, proteins harboring the RGD motif constitute a major recognition system for cell adhesion. The RGD motif is present in a large number of adhesive extracellular matrix proteins and recognized by over 20 known integrins [19]. The RGD-integrin binding-activity can be reproduced by short synthetic peptides containing RGD sequence, under the condition that it is stably immobilized to a substrate instead of simple addition to culture media [20]. Hence,

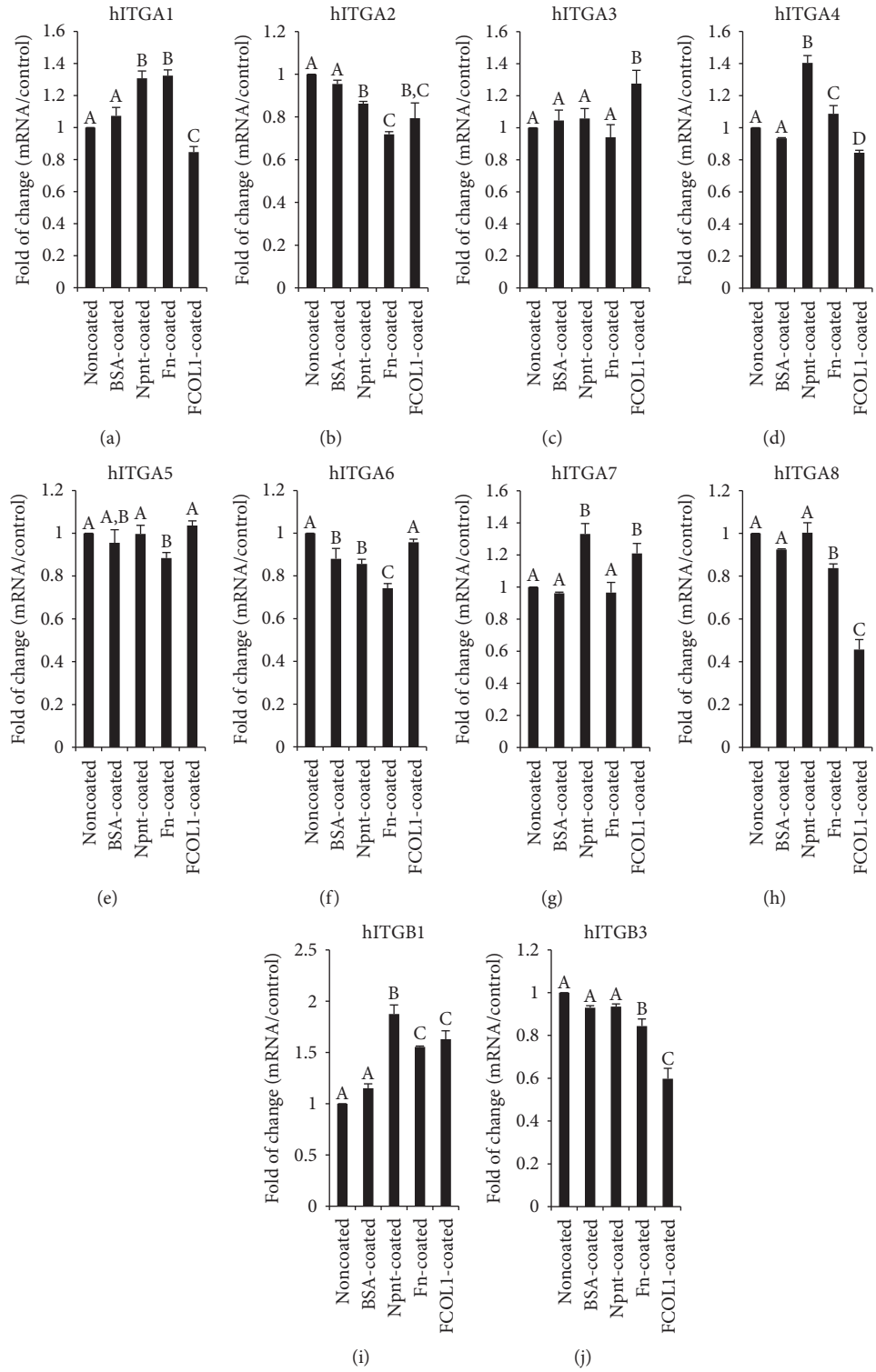

Figure 6: Real-time RT-PCR of integrins on day five. hDPSCs (passage number 2) were inoculated at the concentration of 1×10^4/mL in 12-well plates (nontissue culture-treated polystyrene, Falcon) in DMEM supplemented with 10% FBS and penicillin/streptomycin (pen: 50 U/mL; strep: 50 μg/mL) and cultured for five days. RNA was isolated at day five and reverse transcribed into cDNA. The quantitative mRNA expression of integrin α1 (ITGA1, (a)), α2 (ITGA2, (b)), α3 (ITGA3, (c)), α4 (ITGA4, (d)), α5 (ITGA5, (e)), α6 (ITGA6, (f)), α7 (ITGA7, (g)), α8 (ITGA8, (h)), β1 (ITGB1, (i)), and β3 (ITGB3, (j)) was determined by real-time RT-PCR. Results are shown as fold increase in relation to the noncoated control and represent the mean ± STD of three independent experiments. Different symbols mean significant differences in each separate panel, $p < 0.01$ (except for $p < 0.05$ between BSA-coated and Npnt-coated in (b); noncoated and Fn-coated and BSA-coated and FCOL1-coated in (d); Noncoated and Fn-coated and Npnt-coated and Fn-coated in (e); BSA-coated and FCOL1-coated in (f); BSA-coated and Fn-coated in (h); and BSA-coated and Fn-coated in (j)) by post hoc Tukey's HSD test.

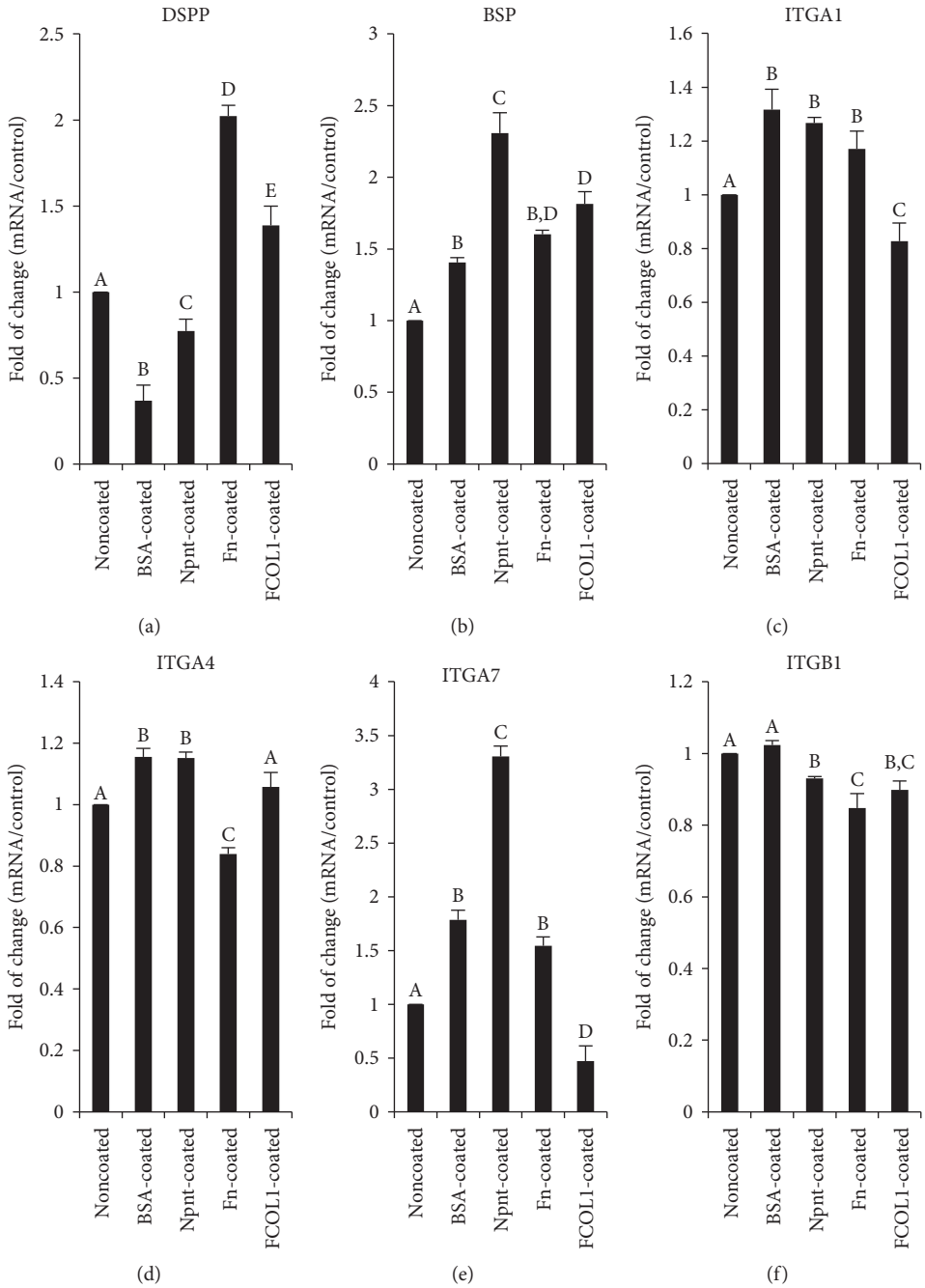

Figure 7: Real-time RT-PCR of DSPP, BSP, and integrins on day 28. hDPSCs (passage number 4) were cultured in different substrate(s) in DMEM supplemented with 10% FBS for five days. Mineralization reagent including β-GP and AA was incorporated on day five. Dexamethasone (100 nM) (D2915, Sigma) was started to be added on day nine. The total culture time was 28 days. DSPP (a), BSP (b) and ITGA1 (c), ITGA4 (d), ITGA7 (e), and ITGB1 (f) mRNA expression was investigated. Different symbols represent significant differences, $p < 0.01$ (except for $p < 0.05$ between noncoated and Npnt-coated in (a); noncoated and BSA-coated and BSA-coated and FCOL1-coated in (b); noncoated and Fn-coated and noncoated and FCOL1-coated in (c); BSA-coated and FCOL1-coated in (d); noncoated and Fn-coated in (e); and noncoated and Npnt-coated in (f)) by post hoc Tukey's HSD test.

small synthetic RGD sequence is usually utilized to test whether the adhesion of a specific type of cell to certain matrix protein is RGD-dependent. A previous work by Kulkarni et al. using soluble peptide (GRGDNP versus GRGESP) revealed that dentin matrix protein 1 (DMP1) promotes the cell attachment in MC3T3-E1 via the RGD domain [21]. Here, our results demonstrated for the first time that upon treatment by a soluble RGD peptide derived from Npnt, the adhesion and spreading of hDPSCs to Npnt was remarkably abrogated, denoting a cell adhesion activity mediated by RGD motif. Additionally, considering the inhibition of adhesion and spreading by RGD was partial, involvement of active sequences other than RGD is suggested therein. Indeed, aside from RGD, new evidence

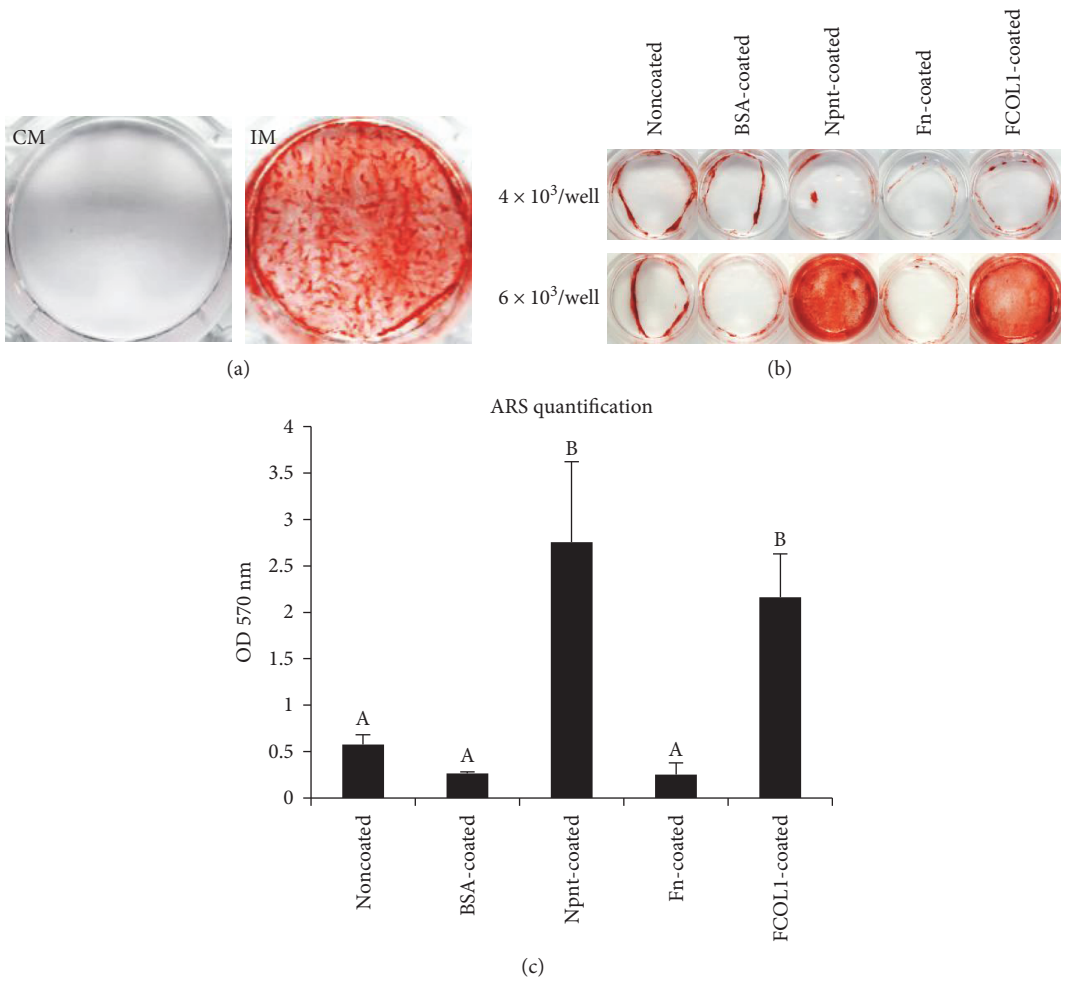

Figure 8: Evaluation of mineralization capacity in hDPSCs. (a) The mineralization capacity of hDPSCs was confirmed. hDPSCs (passage number 1) were seeded in 6-well plates (tissue culture-treated polystyrene, Iwaki) at the concentration of 3×10^4/well in DMEM supplemented with 10% FBS and penicillin/streptomycin (50 U/mL penicillin; 50 μg/mL streptomycin). Media were changed into DMEM supplemented with 5% FBS, penicillin/streptomycin and mineralization reagent (10 mM β-GP and 50 μg/mL AA) (IM), or PBS vehicle (CM) at day four. The photo shows the alizarin red staining of cells at 23 days. (b) Alizarin red staining of hDPSCs (passage number 4) cultured on various protein-coated nontissue culture-treated polystyrene at day 30. hDPSCs were seeded to modified surfaces at the concentration of 4×10^3/well (upper) or 6×10^3/well (lower) in a 24-well plate (nontissue culture-treated polystyrene, Iwaki). Cells were cultured in DMEM supplemented with 10% FBS and penicillin/streptomycin. Mineralization reagent (β-GP and AA) was added at day 4 with 5% FBS containing DMEM. (c) Quantification of alizarin red staining for the lower panel in (b). Significant higher level of mineralization of hDPSCs was detected in Npnt-coated and FCOL1-coated substrate(s). Different symbols represent significant differences, $p < 0.01$ by post hoc Tukey's HSD test.

uncovered that the Phe-Glu-IIe (FEI) domain at the downstream of RGD acts synergistically with RGD to support the adhesion of the human brain neuroglioma cell (H4 cell) [22] to the Npnt-coated substratum. However, whether the FEI plays a similar role in hDPSCs awaits further scrutinization.

An ideal scaffold should be able to promote attachment and proliferation of a specific cell population needed for structural and functional restoration of the damaged tissue. The non-PS is highly hydrophobic, which is usually used for mammalian cells that grow in suspension and bacterial cell culture where attachment is not required. The above results conclude that Npnt is a hDPSC adhesive and supports hDPSC growth in either serum-containing or serum-free conditions. This potential of Npnt to initiate cell growth may yield novel approaches to recruit stem cells in situ.

Integrin, comprising α and β transmembrane glycoprotein subunits, is a complex family of cell adhesion receptors regulating a diverse array of functions. The cytoplasmic domains of integrin connect to the actin cytoskeleton. Accumulating evidences have shown that the cross talk between integrin and environmental clues such as extracellular matrix protein is important in mediating cell proliferation and differentiation [23]. In an effort to clarify gene expression profile of ten types of integrin (eight alpha integrins and two beta integrins), real-time RT-PCR was carried out at an early stage (day five) after cell inoculation. The results highlighted that Npnt triggered the upregulation of ITGA1 (1.31 ± 0.04-fold), ITGA4 (1.40 ± 0.05-fold), ITGA7 (1.33 ± 0.07-fold),

and ITGB1 (1.87 ± 0.09-fold). As a ubiquitously expressed integrin and common partner to almost all the alpha integrins, $\beta 1$ integrin (ITGB1 or CD29) is the primary plasma membrane receptor transmitting cues from the extracellular matrix to intracellular signaling pathways; here, the upregulation of ITGB1 correlates well with our previous data using MDPC-23 cell line [10]. Ozeki et al. reported enhanced ITGA1 expression leads to the differentiation of human skeletal muscle stem cells (hSMSCs) into odontoblasts evidenced by upregulation of dentin sialophosphoprotein (DSPP), dentin sialoprotein (DSP), and alkaline phosphatase (ALP) [24]. In addition, dentin phosphoprotein-(DPP-) coated polystyrene can augment the expression of ITGA4 in rat preodontoblast cell line (T4-4) [25]. Another study showed that ITGA7 positive hSMSCs have the potential of differentiation into odontoblasts under appropriate inductive conditions (retinoic acid and bone morphogenetic protein-4 (BMP4)) [26]. The findings in the present experiment suggest that $\alpha 1\beta 1$, $\alpha 4\beta 1$, and $\alpha 7\beta 1$ might be involved during early stages of Npnt-mediated adhesion and intracellular signaling. In contrast, there was no elevation in the expression of ITGA8 as measured by quantitative RT-PCR in the Npnt-coated group. The unaffected expression of ITGA8 in the Npnt group suggests either a compensatory effect from other alpha integrins, such as ITGA1, ITGA4, and ITGA7 forming heterodimers with integrin $\beta 1$ or/and an earlier role of ITGA8 that was not detected because of its late downregulation. Additionally, mild attenuation of ITGA2 and ITGA6 expression was observed in the Npnt-treated group. Except for the elevation of ITGA3 and ITGA7, FCOL1 downregulates the rest alpha integrins (ITGA1, ITGA2, ITGA4, and ITGA8) without impacting ITGA5 and ITGA6. Notably, the expression ITGA8 (0.46 ± 0.05-fold, $p < 0.01$) was found to be remarkably reduced under the influence of FCOL1. Fn (1.55 ± 0.01-fold, $p < 0.01$) and FCOL1 (1.63 ± 0.08-fold, $p < 0.01$) both enhanced the expression of ITGB1 at a level of statistical significance, while there was no difference between the two groups. With regard to ITGB3, it was found that its mRNA expression remains constant in noncoated, BSA-coated, and Npnt-coated groups and was inhibited by both Fn and FCOL1. The data demonstrated Npnt selectively upregulated mRNA expression of ITGA1, ITGA4, and ITGA7. However, it remains to be clarified which specific integrin receptor ($\alpha 1\beta 1$, $\alpha 4\beta 1$, or $\alpha 7\beta 1$) plays a predominant role in mediating the adhesion and differentiation of hDPSCs. To answer this question, inhibition experiment is necessary using antibodies against $\alpha 1\beta 1$, $\alpha 4\beta 1$, and $\alpha 7\beta 1$ in the future study.

Further, the late-stage gene expression analysis in Figure 7 revealed that Npnt tended to direct the hDPSCs' differentiation toward osteoblastic lineage instead of odontoblastic lineage, as the DSPP, a well-established odontoblast differentiation marker [27], was moderately suppressed by Npnt, but BSP, a widely recognized osteoblast marker, [28] was markedly enhanced by Npnt compared to the other groups. The result correlates well with a previous work from Kahai et al. [29], indicating that Npnt induces the differentiation of hDPSCs into osteoblast rather than odontoblast. Nevertheless, Npnt still holds sound potential for its application in the pulp capping treatment, as a coating of Npnt significantly augments the matrix mineralization of hDPSCs. In addition, ITGA7 was found to be remarkably increased by Npnt as much as threefold more than the noncoated control, denoting that the ITGA7 may be required in the interaction between Npnt and hDPSCs at the late stage of osteoblastic differentiation.

To examine whether a coating of polystyrene by the matrix proteins might cause an enhanced mineralization, the *in vitro* mineralization capabilities of hDPSCs in various substrate(s) were monitored. As expected, the induction of differentiation of cells in Npnt and FCOL1 resulted in the appearance of mineralized nodules revealed by alizarin red staining at day 30. Moreover, we observed that a low initial seeding number fail to initiate the mineralization after culturing for the same period of time, be it noncoated or protein-coated surfaces, denoting a sufficient number of cells (in the present work: 6×10^3/mL in 24-well plates) are required to ensure the onset of appreciable late-stage calcific deposition. In terms of mineralization activity, a comparison of Npnt, Fn, and FCOL1 revealed that both Npnt and FCOL1 were promising in eliciting intensive calcific deposition. The finding suggested Npnt assumes a comparable mineralization-inducing capacity with FCOL1, which is a well-documented tissue engineering material [30, 31]. Interestingly, although the RGD-containing Fn supported hDPSC proliferation, cells grown on it did not undergo an appreciable mineralization as did Npnt and FCOL1. An earlier work demonstrated that Fn promotes the mineralization, albeit to a lesser extent than COL1, in bovine vascular cells [32]. A possible explanation for the observed phenomena might be attributable to a different type of cell used. Moreover, except RGD, there are other cell adhesive motifs in the protein, namely, PHSRN. The interaction of Fn with cells was not merely via RGD but from a synergistic action of RGD, PHSRN, and other potential motifs. Further, there are various adhesive proteins in FBS and those secreted by cells; the coated proteins did not exert their influence in isolation: cells exposed to the immobilized proteins were interacting against a background of various native integrin-binding proteins. The alizarin red staining data revealed that an accelerated cell adhesion and proliferation does not necessarily leads to the final enhancement of mineralization.

Based on the findings, it is suggested that Npnt possesses comparable capacity to FCOL1 in promoting proliferation and eliciting intensive mineralization in hDPSCs. However, with regard to the cost-effectiveness, FCOL1 stands a better chance of future application, as the price for FCOL1 is much cheaper than Npnt. Despite this limitation, the present experiment has clarified a novel role for Npnt in modulating hDPSC integrin expression and altering their interaction with the microenvironment, leading to mineralization.

5. Conclusion

Taken together, the results demonstrated that Npnt facilitates hDPSC adhesion and spreading to hydrophobic

nontissue culture-treated polystyrene. The adhesion and spreading of hDPSCs to Npnt was partially mediated by RGD motif. Moreover, Npnt acts as a bioactive signal to initiate the upregulation of ITGA1, ITGA4, ITGA7, and ITGB1 as early as day five. Further, the mRNA expression of DSPP was slightly downregulated by Npnt, while BSP was significantly enhanced. Finally, late-stage mineralization was significantly enhanced in cells cultured in Npnt-coated and FCOL1-coated wells as compared to negative controls.

Conflicts of Interest

The authors declare that there are no conflicts of interest with regard to the publication of this article.

Acknowledgments

This work was supported by JSPS KAKENHI Grant nos. JP15H05024 to Takashi Saito and JP17K17139 to Jia Tang.

References

[1] S. Gronthos, M. Mankani, J. Brahim, P. G. Robey, and S. Shi, "Postnatal human dental pulp stem cells (DPSCs) *in vitro* and *in vivo*," *Proceedings of the National Academy of Sciences of the United States of America*, vol. 97, pp. 13625–13630, 2000.

[2] S. Gronthos, J. Brahim, W. Li et al., "Stem cell properties of human dental pulp stem cells," *Journal of Dental Research*, vol. 81, pp. 531–535, 2002.

[3] N.-M. Ahmed, M. Murakami, Y. Hirose, and M. Nakashima, "Therapeutic potential of dental pulp stem cell secretome for Alzheimer's disease treatment: an in vitro study," *Stem Cells International*, vol. 2016, Article ID 8102478, 11 pages, 2016.

[4] M. Prince, A. Wimo, M. Guerchet, G. C. Ali, Y. T. Wu, and M. Prina, "World Alzheimer Report 2015, The Global Impact of Dementia: an analysis of prevalence, incidence, cost and trends," 2015, May 2017, https://www.alz.co.uk/research/WorldAlzheimerReport2015.pdf.

[5] J. Yu, Y. Wang, Z. Deng et al., "Odontogenic capability: bone marrow stromal stem cells versus dental pulp stem cells," *Biology of the Cell*, vol. 99, pp. 465–474, 2007.

[6] B. Kong, W. Sun, G. Chen et al., "Tissue-engineered cornea constructed with compressed collagen and laser-perforated electrospun mat," *Scientific Reports*, vol. 7, p. 970, 2017.

[7] D. Cao, Z. Xu, Y. Chen, Q. Ke, C. Zhang, and Y. Guo, "Ag-loaded MgSrFe-layered double hydroxide/chitosan composite scaffold with enhanced osteogenic and antibacterial property for bone engineering tissue," *Journal of Biomedical Materials Research Part B: Applied Biomaterials*, 2017.

[8] Y. Y. Jo, S. G. Kim, K. J. Kwon et al., "Silk fibroin-alginate-hydroxyapatite composite particles in bone tissue engineering applications in vivo," *International Journal of Molecular Sciences*, vol. 18, p. 858, 2017.

[9] C. Arai, K. Yoshizaki, K. Miyazaki et al., "Nephronectin plays critical roles in Sox2 expression and proliferation in dental epithelial stem cells via EGF-like repeat domains," *Scientific Reports*, vol. 7, article 45181, 2017.

[10] J. Tang and T. Saito, "Nephronectin stimulates the differentiation of MDPC-23 cells into an odontoblast-like phenotype," *Journal of Endodontics*, vol. 43, pp. 263–271, 2017.

[11] Q. Huang, G. P. M. Cheng, K. Chiu, and G. Q. Wang, "Surface modification of intraocular lenses," *Chinese Medical Journal*, vol. 129, pp. 206–214, 2016.

[12] V. P. Zhdanov and B. Kasemo, "Van der Waals interaction during protein adsorption on a solid covered by a thin film," *Langmuir*, vol. 17, pp. 5407–5409, 2001.

[13] K. A. DeMali and K. Burridge, "Coupling membrane protrusion and cell adhesion," *Journal of Cell Science*, vol. 116, Part 12, pp. 2389–2397, 2003.

[14] J. F. Casella, M. D. Flanagan, and S. Lin, "Cytochalasin D inhibits actin polymerization and induces depolymerization of actin filaments formed during platelet shape change," *Nature*, vol. 293, pp. 302–305, 1981.

[15] H. Sonowal, A. Kumar, J. Bhattacharyya, P. K. Gogoi, and B. G. Jaganathan, "Inhibition of actin polymerization decreases osteogeneic differentiation of mesenchymal stem cells through p38 MAPK pathway," *Journal of Biomedical Science*, vol. 20, p. 71, 2013.

[16] T. Honjo, S. Kubota, H. Kamioka et al., "Promotion of *Ccn2* expression and osteoblastic differentiation by actin polymerization, which is induced by laminar fluid flow stress," *Journal of Cell Communication and Signaling*, vol. 6, pp. 225–232, 2012.

[17] L. Chen, K. Shi, C. E. Frary et al., "Inhibiting actin depolymerization enhances osteoblast differentiation and bone formation in human stromal stem cells," *Stem Cell Research*, vol. 15, pp. 281–289, 2015.

[18] J. R. Falsey, M. Renil, S. Park, S. Li, and K. S. Lam, "Peptide and small molecule microarray for high throughput cell adhesion and functional assays," *Bioconjugate Chemistry*, vol. 12, pp. 346–353, 2001.

[19] E. Ruoslahti, "RGD and other recognition sequences for integrins," *Annual Review of Cell and Developmental Biology*, vol. 12, pp. 697–715, 1996.

[20] U. Hersel, C. Dahmen, and H. Kessler, "RGD modified polymers: biomaterials for stimulated cell adhesion and beyond," *Biomaterials*, vol. 24, pp. 4385–4415, 2003.

[21] G. V. Kulkarni, B. Chen, J. P. Malone, A. S. Narayanan, and A. George, "Promotion of selective cell attachment by the RGD sequence in dentine matrix protein 1," *Archives of Oral Biology*, vol. 45, pp. 475–484, 2000.

[22] J. Sánchez-Cortés and M. Mrksich, "Using self-assembled monolayers to understand $\alpha 8\beta 1$-mediated cell adhesion to RGD and FEI motifs in nephronectin," *ACS Chemical Biology*, vol. 6, pp. 1078–1086, 2011.

[23] H. Wang, X. Luo, and J. Leighton, "Extracellular matrix and integrins in embryonic stem cell differentiation," *Biochemistry Insights*, vol. 8, Supplement 2, pp. 15–21, 2015.

[24] N. Ozeki, M. Mogi, H. Yamaguchi et al., "Differentiation of human skeletal muscle stem cells into odontoblasts is dependent on induction of $\alpha 1$ integrin expression," *Journal of Biological Chemistry*, vol. 289, pp. 14380–14391, 2014.

[25] A. Eapen and A. George, "Dentin phosphophoryn in the matrix activates AKT and mTOR signaling pathway to promote preodontoblast survival and differentiation," *Frontiers in Physiology*, vol. 6, p. 221, 2015.

[26] N. Ozeki, R. Kawai, T. Tanaka, K. Ishizuka, K. Nakata, and H. Nakamura, "Odontogenic potential of $\alpha 7$ integrin positive human skeletal muscle stem cells," *The Japanese Society of Conservative Dentistry*, vol. 52, pp. 319–329, 2009.

[27] Z. Chen, W. Li, H. Wang et al., "Klf10 regulates odontoblast differentiation and mineralization via promoting expression of dentin matrix protein 1 and dentin sialophosphoprotein genes," *Cell and Tissue Research*, vol. 363, pp. 385–398, 2016.

[28] J. A. Gordon, C. E. Tye, A. V. Sampaio, T. M. Underhill, G. K. Hunter, and H. A. Goldberg, "Bone sialoprotein expression enhances osteoblast differentiation and matrix mineralization *in vitro*," *Bone*, vol. 41, pp. 462–473, 2007.

[29] S. Kahai, S. C. Lee, A. Seth, and B. B. Yang, "Nephronectin promotes osteoblast differentiation via the epidermal growth factor-like repeats," *FEBS Letters*, vol. 584, pp. 233–238, 2010.

[30] S. Yamada, K. Yamamoto, T. Ikeda, K. Yanagiguchi, and Y. Hayashi, "Potency of fish collagen as a scaffold for regenerative medicine," *BioMed Research International*, vol. 2014, Article ID 302392, 8 pages, 2014.

[31] J. Tang and T. Saito, "Effect of type I collagen derived from tilapia scale on odontoblast-like cells," *Tissue Engineering and Regenerative Medicine*, vol. 12, pp. 231–238, 2015.

[32] K. E. Watson, F. Parhami, V. Shin, and L. L. Demer, "Fibronectin and collagen I matrixes promote calcification of vascular cells in vitro, whereas collagen IV matrix is inhibitory," *Arteriosclerosis, Thrombosis, and Vascular Biology*, vol. 18, pp. 1964–1971, 1998.

Hindawi
Stem Cells International
Volume 2017, Article ID 8717454, 10 pages
https://doi.org/10.1155/2017/8717454

Research Article

Alcohol Inhibits Odontogenic Differentiation of Human Dental Pulp Cells by Activating mTOR Signaling

Wei Qin,[1,2] Qi-Ting Huang,[1,2] Michael D. Weir,[2] Zhi Song,[1] Ashraf F. Fouad,[3] Zheng-Mei Lin,[1] Liang Zhao,[2,4] and Hockin H. K. Xu[2,5,6]

[1]*Department of Operative Dentistry and Endodontics, Guanghua School of Stomatology, Sun Yat-sen University and Guangdong Provincial Key Laboratory of Stomatology, Guangzhou 510055, China*
[2]*Biomaterials and Tissue Engineering Division, Department of Endodontics, Periodontics and Prosthodontics, University of Maryland School of Dentistry, Baltimore, MD 21201, USA*
[3]*Department of Endodontics, School of Dentistry, University of North Carolina, Chapel Hill, NC 27599-7450, USA*
[4]*Department of Orthopedic Surgery, Nanfang Hospital, Southern Medical University, Guangzhou, Guangdong 510515, China*
[5]*Center for Stem Cell Biology & Regenerative Medicine, University of Maryland School of Medicine, Baltimore, MD 21201, USA*
[6]*Department of Mechanical Engineering, University of Maryland, Baltimore County, Baltimore County, MD 21250, USA*

Correspondence should be addressed to Zheng-Mei Lin; linzhm@mail.sysu.edu.cn, Liang Zhao; lzhaonf@126.com, and Hockin H. K. Xu; hxu@umaryland.edu

Received 20 April 2017; Revised 5 July 2017; Accepted 16 July 2017; Published 14 September 2017

Academic Editor: Antonio Boccaccio

Long-term heavy alcohol consumption could result in a range of health, social, and behavioral problems. People who abuse alcohol are at high risks of seriously having osteopenia, periodontal disease, and compromised oral health. However, the role of ethanol (EtOH) in the biological functions of human dental pulp cells (DPCs) is unknown. Whether EtOH affects the odontoblastic differentiation of DPCs through the mechanistic target of rapamycin (mTOR) remains unexplored. The objective of this study was to investigate the effects of EtOH on DPC differentiation and mineralization. DPCs were isolated and purified from human dental pulps. The proliferation and odontoblastic differentiation of DPCs treated with EtOH were subsequently investigated. Different doses of EtOH were shown to be cytocompatible with DPCs. EtOH significantly activated the mTOR pathway in a dose-dependent manner. In addition, EtOH downregulated the alkaline phosphatase activity, attenuated the mineralized nodule formation, and suppressed the expression of odontoblastic markers including ALP, DSPP, DMP-1, Runx2, and OCN. Moreover, the pretreatment with rapamycin, a specific mTOR inhibitor, markedly reversed the EtOH-induced odontoblastic differentiation and cell mineralization. Our findings show for the first time that EtOH can suppress DPC differentiation and mineralization in a mTOR-dependent manner, indicating that EtOH may be involved in negatively regulating the dental pulp repair.

1. Introduction

Alcohol is widely consumed throughout the world and has attracted human concernment for thousands of years. Alcohol abuse can place the health of an individual at risk for a series of diseases. According to the World Health Organization, heavy alcohol consumptions are associated with many chronic diseases, including low bone mass, hepatitis, and cardiovascular diseases [1]. Chronic and heavy alcohol consumption is known to result in bone loss, decreased bone formation, increased risks for bone fracture, and delayed fracture healing [2–4]. Moderate alcohol consumption may actually have a modest favorable effect on bone density, particularly in postmenopausal women, although not all studies agree [5–8]. However, alcohol intake of three or more drinks per day is detrimental to bone health [9]. Recent experimental evidences indicated that the mammalian target of rapamycin (mTOR) signal may contribute to the maintenance of bone homeostasis and the differentiation of mesenchymal stem cells [10, 11].

DPCs possess multipotent differentiation potential and the ability to form dentin-pulp-like complexes throughout

life. When the dental pulp is confronted with trauma, microbes, or chemicals, a host of inflammatory cytokines are released [12]. These insults can stimulate the underlying progenitor pulp cells to differentiate into odontoblasts [13], which are capable of secreting dentin matrix proteins as part of the reparative dentinogenesis [14]. Odontoblasts secrete several collagenous and noncollagenous proteins, such as type I collagen, osteopontin, dentin matrix protein 1 (DMP1), and dentin sialophosphoprotein (DSPP), which are special biological markers for the odontoblast/osteoblast-like differentiation of DPCs [15, 16]. Studies have shown that a variety of signal pathways participate in the regulation of dental pulp cell differentiation, such as BMP, Wnt, and Notch signaling [17–19]. However, the impact of alcohol on odontoblastic differentiation of human dental pulp cells (DPCs) remains unclear.

Therefore, the objective of the present study was to investigate the effects of ethanol (EtOH) on the proliferation and odontoblastic differentiation of DPCs. The role of mTOR signaling in EtOH-mediated odontoblastic differentiation was also investigated. The results of this study will shed light on the role of alcohol consumption on the health of human dental pulp cells and their ability in tissue repair and regeneration.

2. Materials and Methods

2.1. Cell Cultures. DPCs were isolated and characterized as described previously [20, 21]. Dental pulp tissues were obtained from explants of clinically healthy dental pulps from human adult third molars that were removed from individuals undergoing tooth extraction for orthodontic treatment. The procedure was approved by the Institutional Review Board of the University of Maryland Baltimore. The pulp tissue was digested in a solution of 3 mg/mL collagenase type I (Worthington Biochem, Freehold, NJ, USA) and 4 mg/mL dispase (Boehringer Mannheim, Indianapolis, IN, USA) for 1 h at 37°C. In the present study, DPCs were cultured in alpha modified Eagle's medium (Invitrogen, Carlsbad, CA, USA) supplemented with 10% foetal calf serum (FCS; Invitrogen), 10 mM L-ascorbic acid 2-phosphate (AA), 2 mM L-glutamate, 100 units/mL penicillin, and 100 μg/mL streptomycin at 37°C in a humidified atmosphere of 5% CO_2 and 95% air. When the cells reached 80% confluence, they were harvested using trypsin/ethylene diamine tetraacetic acid (EDTA) (Gibco, Carlsbad, CA, USA) and subcultured at a ratio of 1 : 3. The 4th passage DPCs were used in the following experiments.

2.2. Cell Viability. DPCs were seeded in 24-well plates at a density of 3×10^4 cells/well. Cells were stained by live/dead viability assay kit (Life Technologies) after culture for 1, 7, and 14 d as described previously [22]. Cells were washed with PBS, followed by incubation with the dye. Live cells were stained green with 2 mM calcein AM and dead cells were marked red with 4 mM ethidium homodimer-1, and they were examined using epifluorescence microscopy (Eclipse TE2000-S, Nikon, Melville, NY). The percentage of live cells and the live cell density were calculated as previously described [21]. Three random sections were analyzed for each sample.

2.3. Cell Proliferation Assays. A cell counting kit (CCK-8, Dojindo, Tokyo, Japan) was used to evaluate cell proliferation at 1, 3, 5, and 7 d. Four replicates in each group were used for this assay. CCK-8 is based on the WST-8 reaction that produces an orange formazan dye in an amount that is directly related with the number of viable cells. The cell proliferative rate was determined via the absorbance at an optical density of 450 nm (OD_{450nm}) using a microplate reader (SpectraMax M5, Molecular Devices, Sunnyvale, CA) according to the manufacturer's protocol.

2.4. Western Blot Analysis. Cells were harvested and lysed in lysis buffer: 20 mmol/L Na_2PO_4 at pH 7.4, 150 mmol/L NaCl, 1% Triton X-100, 1% aprotinin, 1 mmol/L phenymethysulfonyl fluoride, 10 mg/mL leupeptin, 100 mmol/L NaF, and 2 mmol/L Na_3VO_4. Lysates were centrifuged at 12,000 rpm for 15 min. The supernatant was collected, and the protein content was determined using the Bio-Rad protein assay. SDS-PAGE sample buffer (10 mM Tris-HCl, pH 6.8, 2% SDS, 10% glycerol, and 0.2 M DTT) was added to the lysates. Lysates were heated to 100°C for 8 min, and 20 μg of the total protein was loaded in each well of a 10% SDS-PAGE gel. Western blot analysis was performed as reported previously [23, 24]. The following primary antibodies were used: phospho-mTOR (p-mTOR), and total mTOR antibody (Cell Signaling Technology, Beverly, MA, USA).

2.5. Alkaline Phosphatase Activity. DPCs were preincubated with 50 mM rapamycin 1 hour and then exposed to 50 mM EtOH; this procedure was repeated at day 3. After the treatment, the cells were scraped into cold PBS and then sonicated in an ice bath and centrifuged at 1500 ×g for 5 min. Then, the ALP activity was measured in the supernatant using ALP assay mixtures containing 0.1 M diethanolamine, 1 mM $MgCl_2$, and 10 mg/mL p-nitrophenyl phosphate. After incubation at 37°C for 30 min, the reaction was stopped by the addition of NaOH, and the absorbance was measured at 410 nm using the microplate reader (SpectraMax M5).

2.6. Reverse Transcriptase PCR (RT-PCR) and Real-Time Quantitative PCR (qPCR). The expression levels of ALP, DSPP, DMP-1, Runx2, and OCN mRNA were determined by SYBR green real-time reverse transcription-PCR (RT-PCR) as described previously [25]. Total RNA were extracted using TRIzol reagent. Quantitative determination of RNA levels were performed in triplicate in three independent experiments. Real-time PCR and data collection were performed with an ABI PRISM 7500 sequence detection system. The housekeeping gene GAPDH was used as an internal control to normalize the expression levels of different genes. For each primer set, the melting curves were performed to ensure that a single peak was produced. The data for gene expression were analyzed with the $\triangle\triangle$Ct method. The primers used for the amplification of the indicated genes are listed in Table 1.

2.7. Von Kossa Staining. Specific calcifications were detected by von Kossa staining [26, 27]. Briefly, DPCs were plated in

Table 1: List of reverse transcriptase polymerase chain reaction primers.

Gene	Forward	Reverse
ALP	CTATCCTGGCTCCGTGCTC	GCTGGCAGTGGTCAGATGTT
DSPP	TGGAGCCACAAACAGAAGCAA	TCCAGCTACTTGAGGTCCATC
DMP-1	GTGAGTGAGTCCAGGGGAGATAA	TTTTGAGTGGGAGAGTGTGTGC
Runx2	GACTGTGGTTACCGTCATGGC	ACTTGGTTTTTCATAACAGCGGA
OCN	CTCACACTCCTCGCCCTATT	TTGGACACAAAGGCTGCAC
GAPDH	TCAACGACCCCTTCATTGAC	ATGCAGGGATGATGTTCTGG

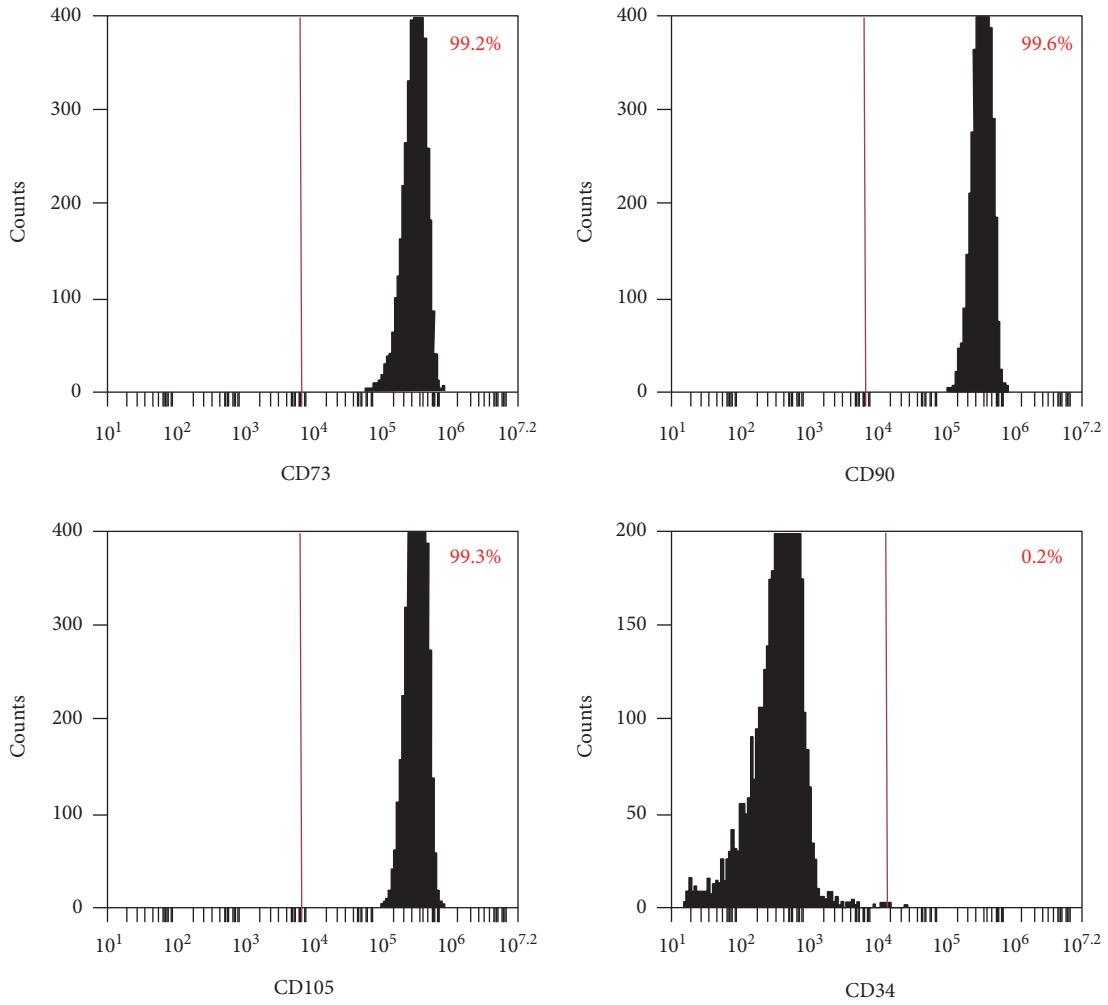

Figure 1: DPCs phenotype via flow cytometry. The expression of a series of cell surface markers associated with the mesenchymal stem cell (MSC) phenotype was investigated using flow cytometry. Analysis of molecular surface antigen markers in DPCs by flow cytometry indicated that the cells were negative for CD34, whereas they were positive for CD73, CD90, and CD105.

six-well plates at a density of 1×10^5 cells per well and cultured in DMEM supplemented with 10% FBS, 50 mg/mL ascorbic acid, 10 mmol/L sodium β-glycerophosphate, and 10 nmol/L dexamethasone. DPCs were then pretreated with 50 mM rapamycin for 1 hour prior to the addition of 50 mM EtOH. This treatment was repeated every 3 d. After 14 d of treatment, the cells were treated with a 5% silver nitrate solution and exposed to ultraviolet light for 30 min. This solution was then neutralized with 5% sodium thiosulfate for 2 min, and the cells were rinsed with distilled water for 5 min. Finally, the cells were stained with nuclear fast red (Sigma, Deisenhofen, Germany) for 1 min. To quantify the mineralization, the calcium content was measured by a quantitative colorimetric method using a calcium assay kit following the manufacturer's instructions. The calcium content of the cell layer was determined at

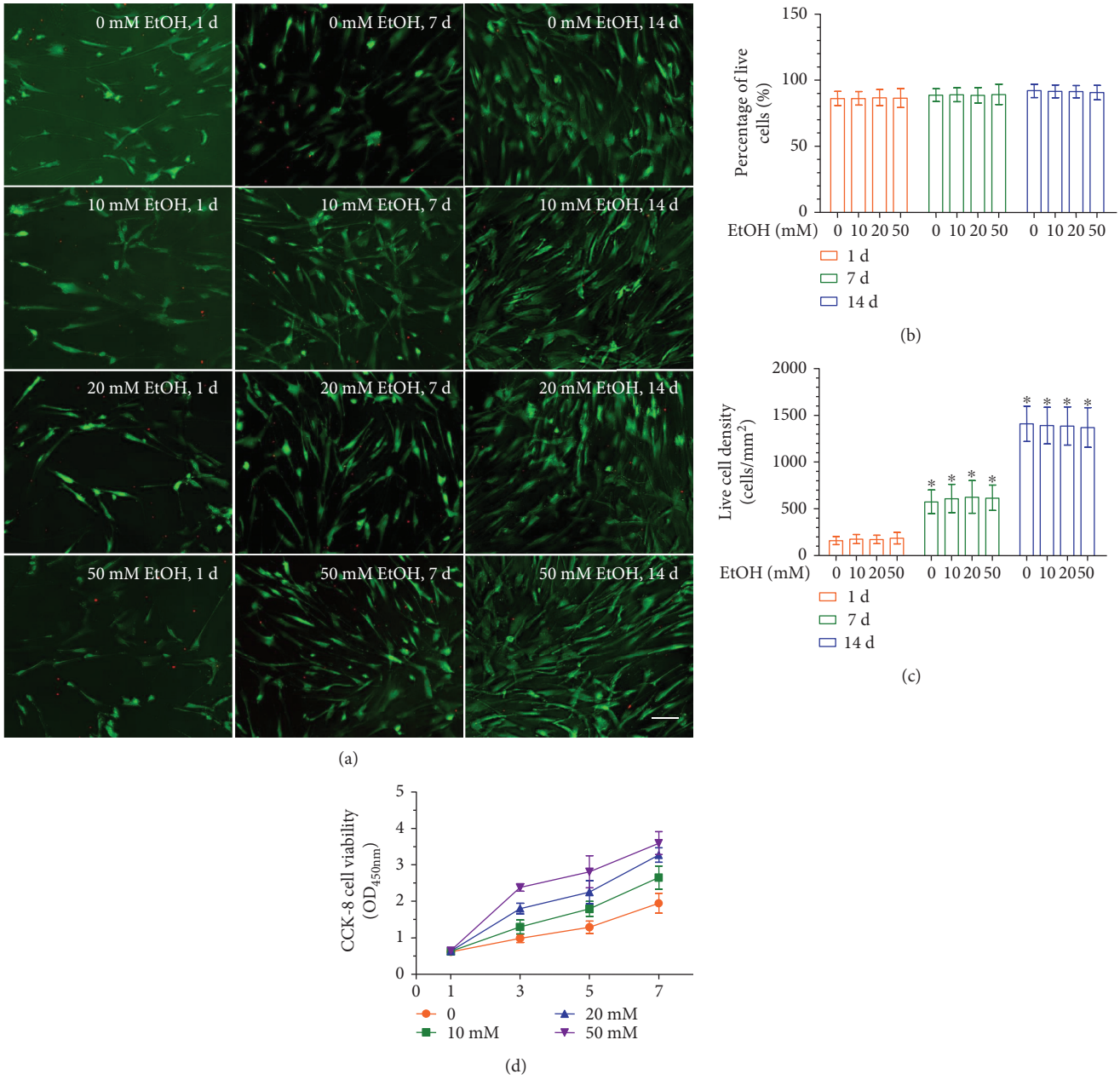

Figure 2: Effect of EtOH on cell viability and proliferation of DPCs. (a) Representative live/dead images of EtOH-treated DPCs after days 1, 7, and 14 of culture. Live cells were stained in green and dead cells were stained in red. In all four groups, live cells were abundant, and dead cells were few (scale bar = 50 μm). (b) Percentage of live cells of DPCs was around 90%. Data represent mean ± SD of 3 experiments with triplicates. (c) EtOH increased the cell proliferation. Data represent mean ± SD of 3 experiments with triplicates. $^*p < 0.05$ versus control group.

day 14 of odontogenic culture. The absorbance of the solutions was read at 570 nm using a UV-visible light spectrophotometer.

2.8. Statistical Analysis. All experiments were repeated at least three times. Data are expressed as mean ± standard deviation (SD). Results of at least three independent experiments (always performed with cells isolated from different donors) were compared by one-way ANOVA. Differences between groups were evaluated with Tukey's posttest. p values < 0.05 were considered significant.

3. Results

3.1. Identification of Stem Cell Phenotypic Markers in Primary DPCs. The surface markers of DPCs were analyzed using flow cytometry. Consistent with other mesenchymal stem cell populations (Figure 1), the majority of DPCs exhibited intense expression of mesenchymal surface molecular markers (CD73—99.2%, CD90—99.6%, and CD105—99.3%). On the other hand, DPCs exhibited weak expression of surface markers (CD34—0.2%), indicating that the DPCs contained mesenchymal progenitors.

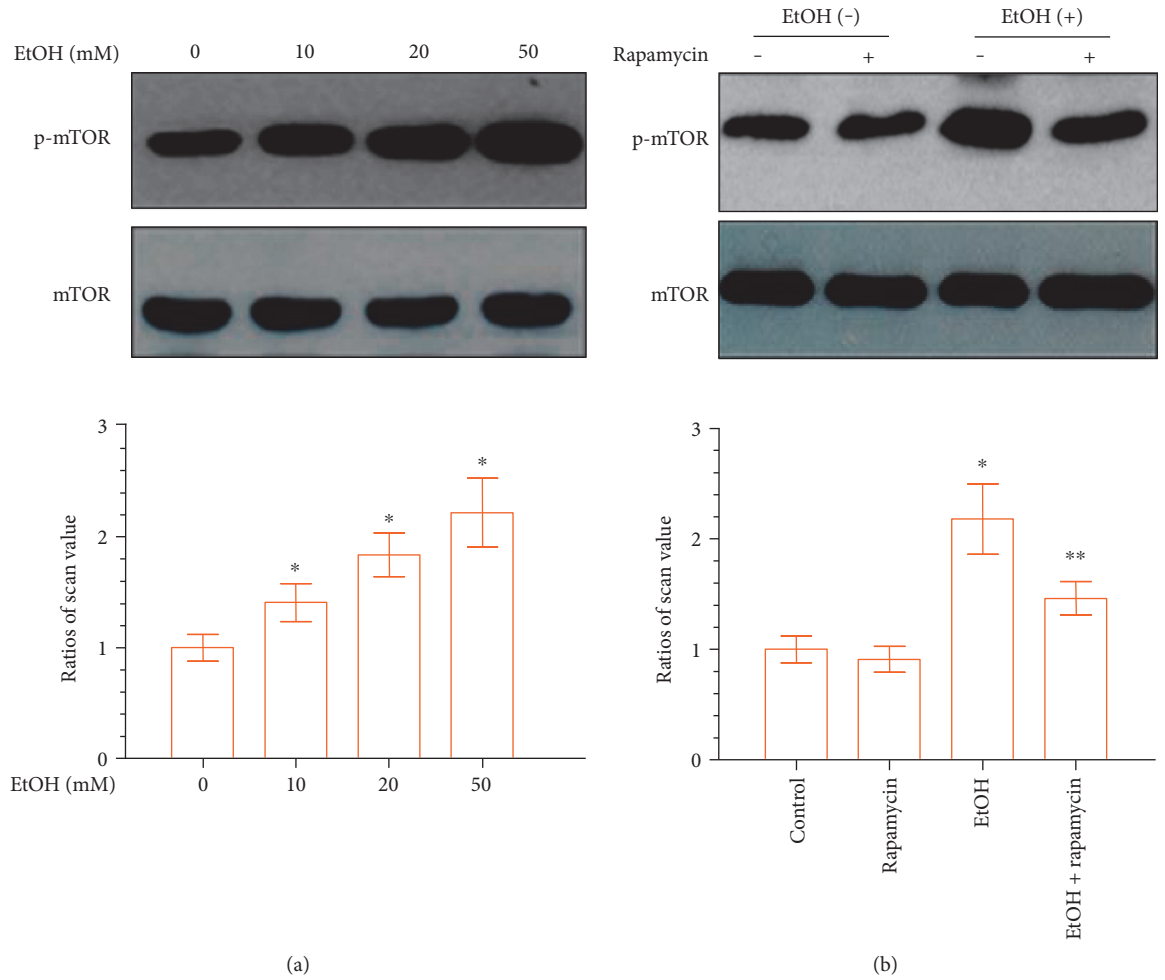

Figure 3: EtOH upregulates mTOR phosphorylation in DPCs in a dose-dependent manner. (a) DPCs were treated with different concentrations of EtOH for 24 hours. Lower panels show the ratios of band densities of phosphor-mTOR to mTOR. (b) Confluent DPCs cells were preincubated with the mTOR inhibitor rapamycin (50 mM) for 1 hour before treatment with EtOH. Rapamycin decreases EtOH-induced mTOR phosphorylation. Data represent mean ± SD of 3 experiments with triplicates. $^{*}p < 0.05$ versus control group. $^{**}p < 0.05$ versus EtOH group.

3.2. DPC Viability and Cell Proliferation. In order to evaluate the effects of EtOH treatment on DPC cytocompatibility, cellular viability was assessed using live/dead staining after 24 hours of culture. Representative live/dead staining images are shown in Figure 2(a). There were numerous live cells (stained green) and a few dead cells (stained red). In Figure 2(b), the percentages of live cells in all four groups were approximately 90% and were not significantly different among the three doses of EtOH ($p > 0.1$). Cell number significantly increased from day 1 to day 14, most likely due to cell proliferation (Figure 2(c)). The concentrations of EtOH of up to 50 mM enhanced cell proliferation compared to the untreated DPCs (Figure 2(d)). Overall, these results demonstrate that 50 mM EtOH, used in the other experiments of the present study, was not cytotoxic to DPCs.

3.3. mTOR Activation in Response to EtOH in DPCs. To determine whether the mTOR signaling pathway is involved in the EtOH-mediated differentiation of DPCs, DPCs were treated with EtOH for 24 hours. EtOH treatment elevated the expression levels of phospho-mTOR signaling with increasing doses, compared to the control group, as shown in Figure 3(a). The small molecule rapamycin has been widely used as a selective mTOR inhibitor [28]. We used rapamycin to prevent mTOR phosphorylation in response to EtOH. As depicted in Figure 3(b), EtOH-induced phospho-mTOR was downregulated following pretreatment with 50 mM rapamycin. These results confirmed that in DPCs EtOH triggers the activation of the mTOR pathway as confirmed by the inhibitory action of rapamycin.

3.4. EtOH-Induced mTOR Activation Increases Alkaline Phosphatase Activity, Alkaline Phosphatase mRNA Expression, and Mineralization. To understand whether EtOH affects the odontogenic differentiation of DPCs, an ALP activity assay was performed. To this end, ALP activity significantly decreased in the EtOH-treated group until day 14, compared to the control group (Figure 4(a)). The decreased ALP activity

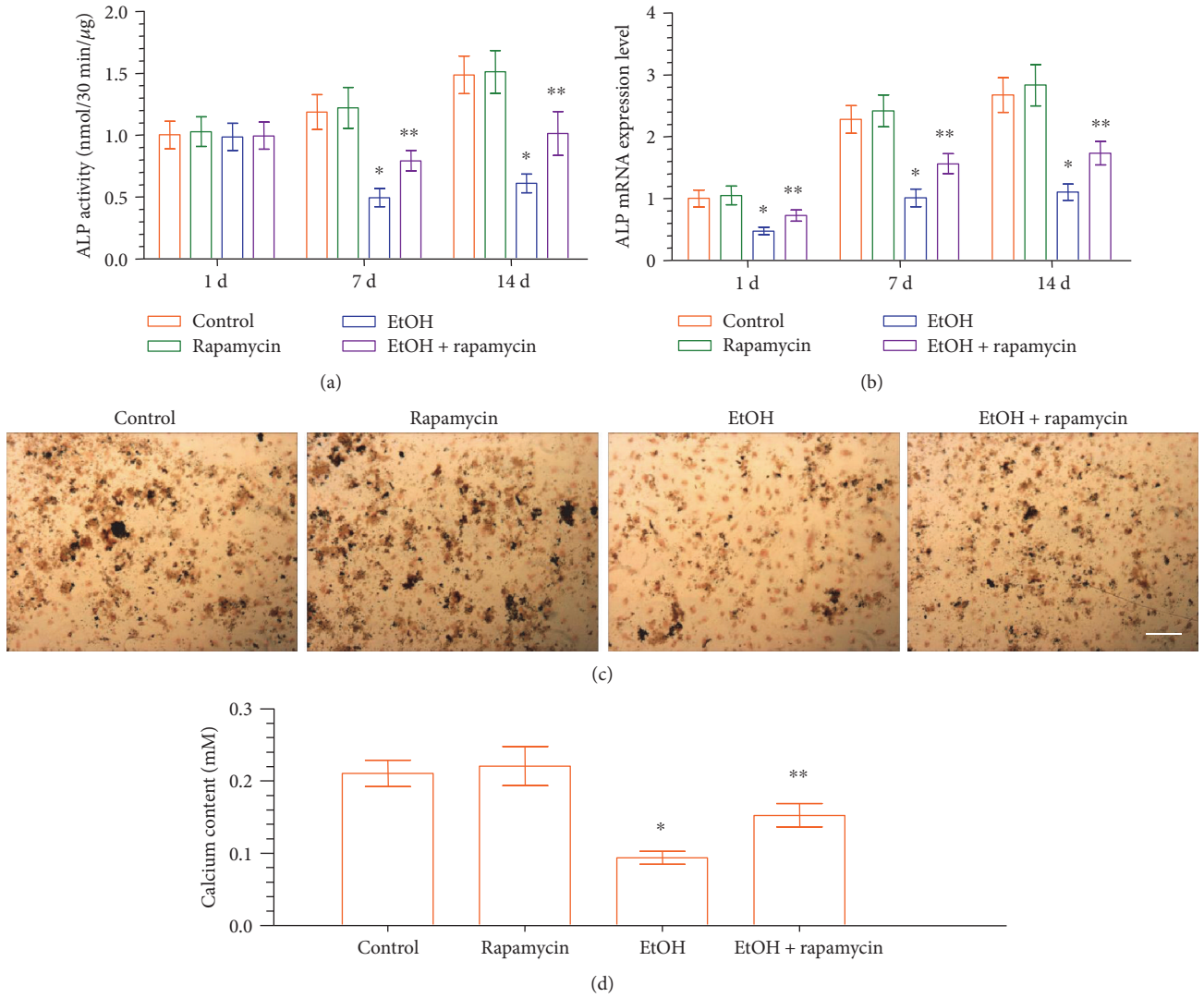

FIGURE 4: Effect of EtOH-induced ALP activity and mineralized nodule formation in DPCs. (a, b) DPCs were treated with EtOH (50 mM) in the absence or presence of rapamycin (50 mM, pretreatment for 1 h). Cells were retreated every 3 days. ALP activity (a) and ALP mRNA expression (b) were measured at each time point. (c) DPCs were cultured in osteogenic induction medium for 14 days, and the mineralized nodule formation was assessed by von Kossa staining (scale bar = 100 μm). (d) On 14 days, the calcium content was determined. Data represent mean ± SD of 3 experiments with triplicates. $^{*}p < 0.05$ versus control group. $^{**}p < 0.05$ versus EtOH group.

was significantly enhanced following pretreatment with rapamycin. The results of the ALP mRNA expression were consistent with ALP assay (Figure 4(b)). Next, we investigated the mineralized nodule formation, an index of terminal odontoblastic differentiation, in DPCs after 14 d of incubation with EtOH in the absence or presence of rapamycin. Treatment of DPCs with EtOH decreased the mineralized nodule formation and calcium content. Conversely, an increase in calcified nodule formation (Figure 4(c)) and calcium content (Figure 4(d)) was observed in cells treated with EtOH in the presence of rapamycin. These results suggest that the downstream effects of EtOH on the odontoblastic maturation of DPCs were mediated through the activation of the mTOR signaling pathway.

3.5. EtOH Triggers DPC Odontoblastic Differentiation in an mTOR-Dependent Manner. To further investigate the effects of EtOH on odontoblastic differentiation of DPCs, cells were exposed to EtOH for 1, 7, and 14 d. EtOH markedly downregulated the mRNA expression of critical odontoblastic genes including DSPP, DMP-1, Runx2, and OCN mRNA. In contrast, expression of these genes was significantly elevated by the addition of rapamycin prior to EtOH treatment (Figure 5). These results further indicate that mTOR is a key mediating factor controlling EtOH-induced odontoblastic differentiation of DPCs.

4. Discussion

The long-term detrimental effects of alcoholism on bone mass have been relatively well established [29]. Previous studies showed that heavy chronic alcohol consumption is associated with a variety of risk factors that may contribute to the pathogenesis of bone disease, including malabsorption, hypogonadism, poor nutrition, vitamin D deficiency, liver

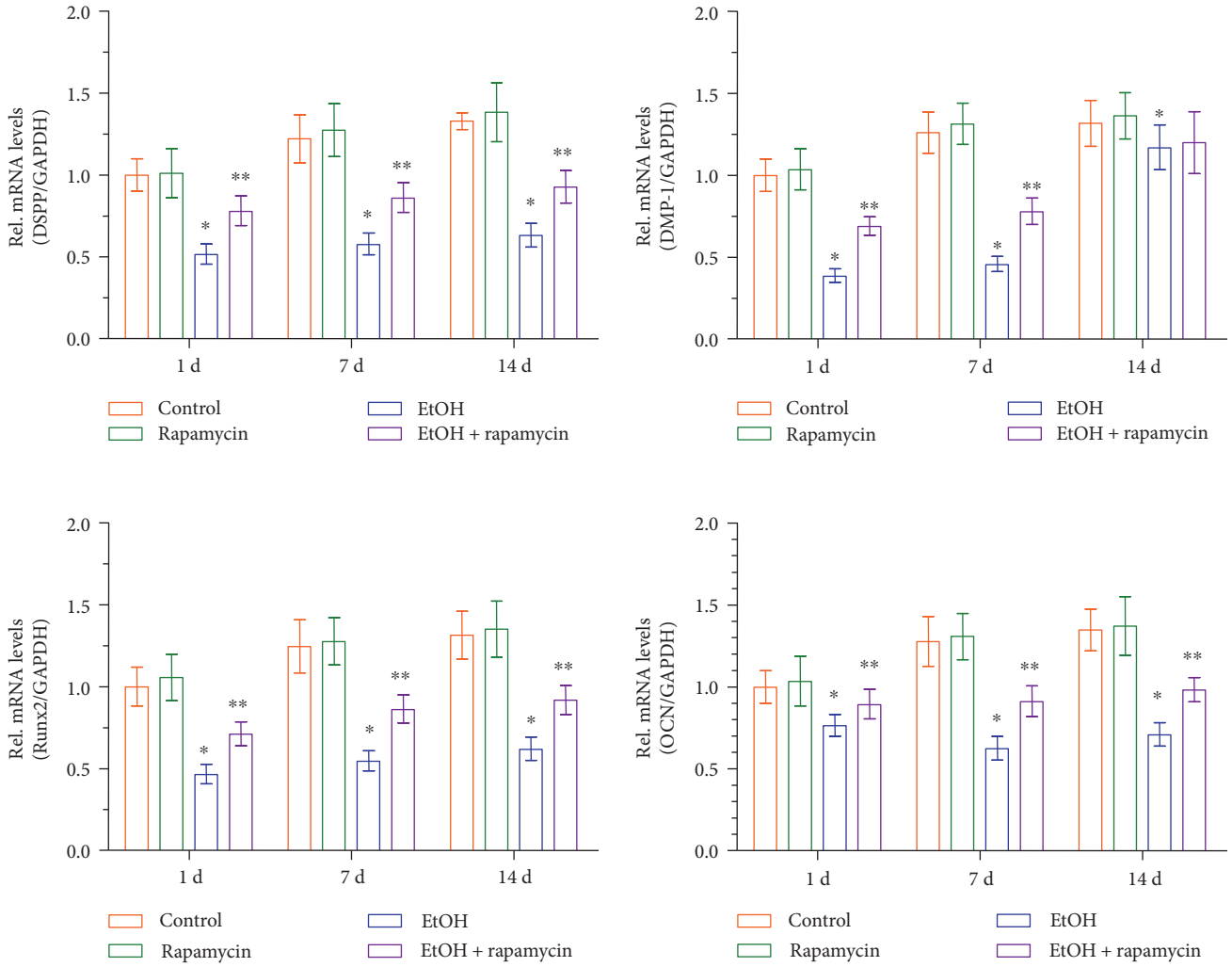

Figure 5: Effects of EtOH treatment on the odontoblastic differentiation of DPCs. DPCs cells were pre-incubated with rapamycin (50 mM) for 1 hour before treatment with EtOH. The mRNA expression of DSPP, DMP-1, Runx2, and OCN was analyzed using real-time RT-PCR. Data represent mean ± SD of 3 experiments with triplicates. $^{*}p < 0.05$ versus control group. $^{**}p < 0.05$ versus EtOH group.

disease, and parathyroid dysfunction [30]. The effect of alcohol on cell proliferation has been reported for various types of cells [31–33]. Our observations in the present study indicate that alcohol treatment was able to increase the proliferation rate of DPCs. Furthermore, The concentrations of EtOH of up to 50 mM was found to not alter the viability of DPCs. Liu et al. reported that treatment of marrow mesenchymal stem cells with alcohol led to an increase in cell proliferation as determined by the methylthiazolyldiphenyl-tetrazolium bromide assay [34]. The effect of EtOH on the proliferation of DPCs is also consistent with that reported for mouse bone marrow mesenchymal stem cells.

Alcohol has been reported to activate mTOR in bone marrow mesenchymal cells [34]. Interestingly, this study showed that the addition of rapamycin, a widely used mTOR inhibitor [35], attenuated the alcohol-induced responses. These results suggested that alcohol decreased the differentiation and mineralization of osteoblast-like cells via the activation of mTOR signaling. To investigate whether mTOR signaling pathway is involved in EtOH-induced odontogenic differentiation of DPCs, we assessed the activation of mTOR signaling in EtOH-treated DPCs under conditions designed to induce odontoblastic differentiation and its role in odontoblastic differentiation with the use of mTOR inhibitors. Among the concentration gradients in our experiment, we found that 50 mM EtOH significantly upregulated phospho-mTOR activity in DPCs. Thus, this concentration was selected for subsequent experiments in the present study. Rapamycin was also used to test the effect of alcohol on mTOR phosphorylation. The phosphorylation of mTOR was partially inhibited by rapamycin. The mechanism of how EtOH regulates the odontoblast differentiation of DPCs is complicated and has not yet been elucidated completely. In addition, whether mTOR signaling participates in odontoblast differentiation of DPCs has not yet been elucidated completely.

DPCs from dental pulp tissues represent a population of mesenchymal stem/progenitor cells. The high proliferative potential of DPCs makes this population of cells suitable

for cell-based regeneration and especially for dentin repair. DPCs could form the dentin-like tissues and bone-like tissues *in vivo* [36]. Several studies have showed that dentin-like tissue formation is associated with DPCs [37–39]. ALP activity is most often used as an early marker of odontoblastic differentiation and plays an important role in dentin-like tissue formation. In the present study, greater ALP activity and ALP mRNA were achieved when the mTOR signaling pathway was inhibited by rapamycin. Consistent with this finding, more mineralized nodules were also observed in DPCs treated with rapamycin at the late stage of odontoblastic differentiation. These results indicate that the mTOR signaling pathway is partly controlling the effects of EtOH on the odontoblastic differentiation of DPCs.

Furthermore, the gene expression levels of the related odontoblastic markers such as DSPP, DMP-1, Runx2, and OCN were measured to investigate the effects of mTOR signaling on the differentiation ability of odontoblasts *in vitro*. Runx2, of the runt domain gene family, is an essential transcription factor that controls bone and tooth development by regulating osteoblast and odontoblast differentiation [40, 41]. DSPP and DMP-1 are members of the small integrin-binding ligand N-linked glycoprotein (SIBLING) family. DSPP was originally considered to be dentin-specific. Although several studies have recently shown its expression in bone [42–44], DSPP remains a major marker of odontoblastic differentiation. In addition, DMP-1 is essential for the mineralization of bone and dentin [45, 46]. Furthermore, OCN can be expressed by odontoblasts and is present in the dentin matrix, and it is also thought to be a reparative molecule within the dental pulp [47]. In the present study, DSPP, DMP-1, Runx2, and OCN mRNA levels were downregulated in the EtOH-treated DPCs. However, rapamycin significantly reversed the EtOH-induced downregulation of DSPP, DMP-1, Runx2, and OCN mRNAs. This provided further evidence that the mTOR signaling pathway plays an important role in EtOH-mediated DPC odontoblastic differentiation. Our study provides a basis that high doses of alcohol may be detrimental to DPCs' repair and regenerative capability.

However, the level of odontogenic differentiation of DPCs can be regulated also by other important factors. Paduano et al. demonstrated that hydrogel scaffolds derived from bone extracellular matrix (bECM) promoted odontogenic differentiation of dental pulp stem cells in the absence of external inducers, and these scaffolds could be combined with osteo/odontogenic medium or growth factors [48]. Qu and Liu demonstrated that gelatin/bioactive glass hybrid scaffolds provided an excellent environment for dental pulp stem cells for odontogenic differentiation [49]. Moreover, dental-derived mesenchymal stem cells exhibited a predisposition toward other phenotypes when cultured in the appropriate media [50–53]. Interestingly, the polyphenolic fractions isolated from the beer brewing process enhanced the antioxidant and antitumor activity. Further study is needed to determine whether the positive bioactive compounds of beer and other agents could regulate the odontogenic differentiation of DPCs and their underlying mechanisms.

In conclusion, the present study demonstrated for the first time that EtOH can downregulate the odontoblastic differentiation of DPCs through activation of the mTOR signaling pathway, suggesting that EtOH plays an important role during the odontoblastic differentiation. Regenerating dentin is an important target for the treatment of dental pulp exposure [54]. The primary objective of vital pulp therapy is to maintain the health of pulp tissues and to stimulate the remaining pulp to regenerate the dentin-pulp complex [55]. Therefore, the aim of the present study was to investigate the potential effect of heavy EtOH consumption on pulp therapy as a factor that needs to be considered in clinical practice. Further research is needed to fully understand and support the clinical indications suggesting that heavy alcoholic consumption should be discouraged during vital pulp therapy in adults.

Conflicts of Interest

The authors declare that they have no competing interests.

Authors' Contributions

Wei Qin and Qi-Ting Huang contributed equally as co-first authors to this study.

Acknowledgments

This study was in part supported by NIH R01 DE14190 (Hockin H. K. Xu), the University of Maryland School of Dentistry bridge fund (Hockin H. K. Xu), the Guandong Natural Science Foundation (2015A030310079) (Wei Qin), and the Young Teacher Training Program of Sun Yat-sen University (15ykpy40) (Wei Qin).

References

[1] P. E. Molina, J. D. Gardner, F. M. Souza-Smith, and A. M. Whitaker, "Alcohol abuse: critical pathophysiological processes and contribution to disease burden," *Physiology (Bethesda)*, vol. 29, no. 3, pp. 203–215, 2014.

[2] J. M. Barragry, R. G. Long, M. W. France, M. R. Wills, B. J. Boucher, and S. Sherlock, "Intestinal absorption of cholecalciferol in alcoholic liver disease and primary biliary cirrhosis," *Gut*, vol. 20, no. 7, pp. 559–564, 1979.

[3] D. D. Bikle, H. K. Genant, C. Cann, R. R. Recker, B. P. Halloran, and G. J. Strewler, "Bone disease in alcohol abuse," *Annals of Internal Medicine*, vol. 103, no. 1, pp. 42–48, 1985.

[4] R. T. Turner, "Skeletal response to alcohol," *Alcoholism, Clinical and Experimental Research*, vol. 24, no. 11, pp. 1693–1701, 2000.

[5] J. D. Pedrera-Zamorano, J. M. Lavado-Garcia, R. Roncero-Martin, J. F. Calderon-Garcia, T. Rodriguez-Dominguez, and M. L. Canal-Macias, "Effect of beer drinking on ultrasound bone mass in women," *Nutrition*, vol. 25, no. 10, pp. 1057–1063, 2009.

[6] K. L. Tucker, R. Jugdaohsingh, J. J. Powell et al., "Effects of beer, wine, and liquor intakes on bone mineral density in older men and women," *The American Journal of Clinical Nutrition*, vol. 89, no. 4, pp. 1188–1196, 2009.

[7] R. Jugdaohsingh, M. A. O'Connell, S. Sripanyakorn, and J. J. Powell, "Moderate alcohol consumption and increased bone mineral density: potential ethanol and non-ethanol mechanisms," *The Proceedings of the Nutrition Society*, vol. 65, no. 3, pp. 291–310, 2006.

[8] J. Alvisa-Negrin, E. Gonzalez-Reimers, F. Santolaria-Fernandez et al., "Osteopenia in alcoholics: effect of alcohol abstinence," *Alcohol and Alcoholism*, vol. 44, no. 5, pp. 468–475, 2009.

[9] L. J. Dominguez, R. Scalisi, and M. Barbagallo, "Therapeutic options in osteoporosis," *Acta Biomed*, vol. 81, no. 1, pp. 55–65, 2010.

[10] P. Hadji, R. Coleman, and M. Gnant, "Bone effects of mammalian target of rapamycin (mTOR) inhibition with everolimus," *Critical Reviews in Oncology/Hematology*, vol. 87, no. 2, pp. 101–111, 2013.

[11] C. Chen, K. Akiyama, D. Wang et al., "mTOR inhibition rescues osteopenia in mice with systemic sclerosis," *The Journal of Experimental Medicine*, vol. 212, no. 1, pp. 73–91, 2015.

[12] J. J. Chidiac, B. Al-Asmar, K. Rifai, S. J. Jabbur, and N. E. Saadé, "Inflammatory mediators released following application of irritants on the rat injured incisors. The effect of treatment with anti-inflammatory drugs," *Cytokine*, vol. 46, no. 2, pp. 194–200, 2009.

[13] A. J. Sloan and A. J. Smith, "Stem cells and the dental pulp: potential roles in dentine regeneration and repair," *Oral Diseases*, vol. 13, no. 2, pp. 151–157, 2007.

[14] A. J. Smith, "Vitality of the dentin-pulp complex in health and disease: growth factors as key mediators," *Journal of Dental Education*, vol. 67, no. 6, pp. 678–689, 2003.

[15] Y. C. Hwang, I. N. Hwang, W. M. Oh, J. C. Park, D. S. Lee, and H. H. Son, "Influence of TGF-beta1 on the expression of BSP, DSP, TGF-beta1 receptor I and Smad proteins during reparative dentinogenesis," *Journal of Molecular Histology*, vol. 39, no. 2, pp. 153–160, 2008.

[16] P. Papagerakis, A. Berdal, M. Mesbah et al., "Investigation of osteocalcin, osteonectin, and dentin sialophosphoprotein in developing human teeth," *Bone*, vol. 30, no. 2, pp. 377–385, 2002.

[17] J. Yang, L. Ye, T. Q. Hui et al., "Bone morphogenetic protein 2-induced human dental pulp cell differentiation involves p38 mitogen-activated protein kinase-activated canonical WNT pathway," *International Journal of Oral Science*, vol. 7, no. 2, pp. 95–102, 2015.

[18] F. He, Z. Yang, Y. Tan et al., "Effects of Notch ligand Delta1 on the proliferation and differentiation of human dental pulp stem cells in vitro," *Archives of Oral Biology*, vol. 54, no. 3, pp. 216–222, 2009.

[19] W. Qin, F. Yang, R. Deng et al., "Smad 1/5 is involved in bone morphogenetic protein-2-induced odontoblastic differentiation in human dental pulp cells," *Journal of Endodontia*, vol. 38, no. 1, pp. 66–71, 2012.

[20] Y. Y. Chen, S. T. He, F. H. Yan et al., "Dental pulp stem cells express tendon markers under mechanical loading and are a potential cell source for tissue engineering of tendon-like tissue," *International Journal of Oral Science*, vol. 8, no. 4, pp. 213–222, 2016.

[21] L. Wang, C. Zhang, C. Li et al., "Injectable calcium phosphate with hydrogel fibers encapsulating induced pluripotent, dental pulp and bone marrow stem cells for bone repair," *Materials Science & Engineering. C, Materials for Biological Applications*, vol. 69, pp. 1125–1136, 2016.

[22] P. Wang, X. Liu, L. Zhao et al., "Bone tissue engineering via human induced pluripotent, umbilical cord and bone marrow mesenchymal stem cells in rat cranium," *Acta Biomaterialia*, vol. 18, pp. 236–248, 2015.

[23] J. Guo, W. Qin, Q. Xing et al., "TRIM33 is essential for osteoblast proliferation and differentiation via BMP pathway," *Journal of Cellular Physiology*, vol. 232, pp. 3158–3169, 2017.

[24] C. G. Pfeifer, A. Karl, A. Berner et al., "Expression of BMP and actin membrane bound inhibitor is increased during terminal differentiation of MSCs," *Stem Cells International*, vol. 2016, Article ID 2685147, 9 pages, 2016.

[25] T. Nakamura, Y. Chiba, M. Naruse, K. Saito, H. Harada, and S. Fukumoto, "Globoside accelerates the differentiation of dental epithelial cells into ameloblasts," *International Journal of Oral Science*, vol. 8, no. 4, pp. 205–212, 2016.

[26] W. Qin, P. Liu, R. Zhang et al., "JNK MAPK is involved in BMP-2-induced odontoblastic differentiation of human dental pulp cells," *Connective Tissue Research*, vol. 55, no. 3, pp. 217–224, 2014.

[27] W. Qin, Z. M. Lin, R. Deng et al., "p38a MAPK is involved in BMP-2-induced odontoblastic differentiation of human dental pulp cells," *International Endodontic Journal*, vol. 45, no. 3, pp. 224–233, 2012.

[28] A. R. Martin, R. A. Pollack, A. Capoferri, R. F. Ambinder, C. M. Durand, and R. F. Siliciano, "Rapamycin-mediated mTOR inhibition uncouples HIV-1 latency reversal from cytokine-associated toxicity," *The Journal of Clinical Investigation*, vol. 127, no. 2, pp. 651–656, 2017.

[29] D. Feskanich, S. A. Korrick, S. L. Greenspan, H. N. Rosen, and G. A. Colditz, "Moderate alcohol consumption and bone density among postmenopausal women," *Journal of Women's Health*, vol. 8, no. 1, pp. 65–73, 1999.

[30] M. J. Kim, M. S. Shim, M. K. Kim et al., "Effect of chronic alcohol ingestion on bone mineral density in males without liver cirrhosis," *The Korean Journal of Internal Medicine*, vol. 18, no. 3, pp. 174–180, 2003.

[31] J. Lee, M. S. Shin, M. O. Kim et al., "Apple ethanol extract promotes proliferation of human adult stem cells, which involves the regenerative potential of stem cells," *Nutrition Research*, vol. 36, no. 9, pp. 925–936, 2016.

[32] P. D. Narayanan, S. K. Nandabalan, and L. S. Baddireddi, "Role of STAT3 phosphorylation in ethanol-mediated proliferation of breast cancer cells," *Journal of Breast Cancer*, vol. 19, no. 2, pp. 122–132, 2016.

[33] H. S. Kim, S. J. Kim, J. Bae et al., "The p90rsk-mediated signaling of ethanol-induced cell proliferation in HepG2 cell line," *The Korean Journal of Physiology and Pharmacology*, vol. 20, no. 6, pp. 595–603, 2016.

[34] Y. Liu, X. Kou, C. Chen et al., "Chronic high dose alcohol induces osteopenia via activation of mTOR signaling in bone marrow mesenchymal stem cells," *Stem Cells*, vol. 34, no. 8, pp. 2157–2168, 2016.

[35] K. J. Kinghorn, S. Gronke, J. I. Castillo-Quan et al., "A drosophila model of neuronopathic gaucher disease demonstrates lysosomal-autophagic defects and altered mTOR signalling and is functionally rescued by rapamycin," *Journal of Neuroscience*, vol. 36, no. 46, pp. 11654–11670, 2016.

[36] G. T. Huang, S. Gronthos, and S. Shi, "Mesenchymal stem cells derived from dental tissues vs. those from other sources: their biology and role in regenerative medicine," *Journal of Dental Research*, vol. 88, no. 9, pp. 792–806, 2009.

[37] J. Caton, N. Bostanci, E. Remboutsika, C. De Bari, and T. A. Mitsiadis, "Future dentistry: cell therapy meets tooth and periodontal repair and regeneration," *Journal of Cellular and Molecular Medicine*, vol. 15, no. 5, pp. 1054–1065, 2011.

[38] A. A. Volponi, Y. Pang, and P. T. Sharpe, "Stem cell-based biological tooth repair and regeneration," *Trends in Cell Biology*, vol. 20, no. 12, pp. 715–722, 2010.

[39] N. E. Abou, W. Chrzanowski, V. M. Salih, H. W. Kim, and J. C. Knowles, "Tissue engineering in dentistry," *Journal of Dentistry*, vol. 42, no. 8, pp. 915–928, 2014.

[40] B. Jin and P. H. Choung, "Recombinant human plasminogen activator inhibitor-1 accelerates odontoblastic differentiation of human stem cells from apical papilla," *Tissue Engineering Part A*, vol. 22, no. 9-10, pp. 721–732, 2016.

[41] F. Posa, A. Benedetto, and G. Colaianni, "Vitamin D effects on osteoblastic differentiation of mesenchymal stem cells from dental tissues," *Stem Cells International*, vol. 2016, Article ID 9150819, 9 pages, 2016.

[42] O. Baba, C. Qin, J. C. Brunn et al., "Detection of dentin sialoprotein in rat periodontium," *European Journal of Oral Sciences*, vol. 112, no. 2, pp. 163–170, 2004.

[43] J. K. Kim, R. Shukla, L. Casagrande et al., "Differentiating dental pulp cells via RGD-dendrimer conjugates," *Journal of Dental Research*, vol. 89, no. 12, pp. 1433–1438, 2010.

[44] I. S. Kim, Y. M. Song, and S. J. Hwang, "Osteogenic responses of human mesenchymal stromal cells to static stretch," *Journal of Dental Research*, vol. 89, no. 10, pp. 1129–1134, 2010.

[45] L. W. Fisher, "DMP1 and DSPP: evidence for duplication and convergent evolution of two SIBLING proteins," *Cells, Tissues, Organs*, vol. 194, no. 2–4, pp. 113–118, 2011.

[46] A. Balic and M. Mina, "Identification of secretory odontoblasts using DMP1-GFP transgenic mice," *Bone*, vol. 48, no. 4, pp. 927–937, 2011.

[47] N. Goto, K. Fujimoto, and S. Fujii, "Role of MSX1 in osteogenic differentiation of human dental pulp stem cells," *Stem Cells International*, vol. 2016, Article ID 8035759, 13 pages, 2016.

[48] F. Paduano, M. Marrelli, L. J. White, K. M. Shakesheff, and M. Tatullo, "Odontogenic differentiation of human dental pulp stem cells on hydrogel scaffolds derived from decellularized bone extracellular matrix and collagen type I," *PLoS One*, vol. 11, no. 2, article e148225, 2016.

[49] T. Qu and X. Liu, "Nano-structured gelatin/bioactive glass hybrid scaffolds for the enhancement of odontogenic differentiation of human dental pulp stem cells," *Journal of Materials Chemistry. B, Materials for Biology and Medicine*, vol. 1, no. 37, pp. 4764–4772, 2013.

[50] M. Marrelli, F. Paduano, and M. Tatullo, "Human periapical cyst-mesenchymal stem cells differentiate into neuronal cells," *Journal of Dental Research*, vol. 94, no. 6, pp. 843–852, 2015.

[51] M. Tatullo, M. Marrelli, K. M. Shakesheff, and L. J. White, "Dental pulp stem cells: function, isolation and applications in regenerative medicine," *Journal of Tissue Engineering and Regenerative Medicine*, vol. 9, no. 11, pp. 1205–1216, 2015.

[52] C. Gandia, A. Arminan, J. M. Garcia-Verdugo et al., "Human dental pulp stem cells improve left ventricular function, induce angiogenesis, and reduce infarct size in rats with acute myocardial infarction," *Stem Cells*, vol. 26, no. 3, pp. 638–645, 2008.

[53] G. Carnevale, M. Riccio, A. Pisciotta et al., "In vitro differentiation into insulin-producing beta-cells of stem cells isolated from human amniotic fluid and dental pulp," *Digestive and Liver Disease*, vol. 45, no. 8, pp. 669–676, 2013.

[54] A. Nowicka, M. Lipski, M. Parafiniuk et al., "Response of human dental pulp capped with biodentine and mineral trioxide aggregate," *Journal of Endodontia*, vol. 39, no. 6, pp. 743–747, 2013.

[55] F. Schwendicke, F. Brouwer, and M. Stolpe, "Calcium hydroxide versus mineral trioxide aggregate for direct pulp capping: a cost-effectiveness analysis," *Journal of Endodontia*, vol. 41, no. 12, pp. 1969–1974, 2015.

Hindawi
Stem Cells International
Volume 2017, Article ID 7617048, 10 pages
https://doi.org/10.1155/2017/7617048

Research Article

NURR1 Downregulation Favors Osteoblastic Differentiation of MSCs

Adriana Di Benedetto,[1] Francesca Posa,[1,2] Claudia Carbone,[3] Stefania Cantore,[3] Giacomina Brunetti,[3] Matteo Centonze,[4] Maria Grano,[5] Lorenzo Lo Muzio,[1] Elisabetta A. Cavalcanti-Adam,[2] and Giorgio Mori[1]

[1]*Department of Clinical and Experimental Medicine, Medical School, University of Foggia, Foggia, Italy*
[2]*Institute of Physical Chemistry, Department of Biophysical Chemistry, University of Heidelberg and Max Planck Institute for Intelligent Systems, Stuttgart, Germany*
[3]*Department of Basic and Medical Sciences, Neurosciences and Sense Organs, University of Bari, Bari, Italy*
[4]*IRCCS Istituto Tumori Giovannoi Paolo II, Bari, Italy*
[5]*Department of Emergency and Organ Transplantation, University of Bari, Bari, Italy*

Correspondence should be addressed to Giorgio Mori; giorgio.mori@unifg.it

Received 30 April 2017; Accepted 12 June 2017; Published 9 July 2017

Academic Editor: Rajiv Saini

Mesenchymal stem cells (MSCs) have been identified in human dental tissues. Dental pulp stem cells (DPSCs) were classified within MSC family, are multipotent, can be isolated from adult teeth, and have been shown to differentiate, under particular conditions, into various cell types including osteoblasts. In this work, we investigated how the differentiation process of DPSCs toward osteoblasts is controlled. Recent literature data attributed to the nuclear receptor related 1 (NURR1), a still unclarified role in osteoblast differentiation, while NURR1 is primarily involved in dopaminergic neuron differentiation and activity. Thus, in order to verify if NURR1 had a role in DPSC osteoblastic differentiation, we silenced it during all the processes and compared the expression of the main osteoblastic markers with control cultures. Our results showed that the inhibition of NURR1 significantly increased the expression of osteoblast markers collagen I and alkaline phosphatase. Further, in long time cultures, the mineral matrix deposition was strongly enhanced in NURR1-silenced cultures. These results suggest that NURR1 plays a key role in switching DPSC differentiation toward osteoblasts rather than neuronal or even other cell lines. In conclusion, DPSCs represent a source of osteoblast-like cells and downregulation of NURR1 strongly prompted their differentiation toward the osteoblastogenesis process.

1. Introduction

The regenerative medicine is increasing its interest in using adult stem cells for the regeneration of mineralized tissues. Specifically, wide variety of postnatal MSCs have been identified in the dental tissues in the past decade. In particular, DPSCs can be isolated from the dental pulp of adults, a tissue containing the progenitors of the dentinogenic lineage and thus physiologically involved in the reparative processes of dentin [1–3]. Although the regenerative process of the dentin/pulp complex is not well understood, it is known that the reparative dentin is deposed as a protective barrier for the pulp as a consequence of trauma or cavity [4, 5]. DPSCs are normally quiescent, but, following injuries that cause odontoblast death, they can resume their biological activity. Thus, in response to stimuli located on pulp-dentin interface, DPSCs are recruited at the site of the lesion and differentiate into odontoblasts synthesizing reparative dentin and preserving tooth vitality. Previous works showed that DPSCs can be considered odontoblast/osteoblast precursors because they express osteogenic markers and are responsive to many growth factors for osteo/odontogenic differentiation [6–8].

In addition, dental pulp cells are capable of forming mineral matrix nodules [2, 9–11]. Actually, it has been demonstrated that DPSCs can differentiate toward multiple cell lineages; hence, when stimulated with the appropriate culture media, they showed the capacity to differentiate into chondrocyte-like, adipocyte-like, and osteoblast-like cells [12–17]. Consistently, more studies showed that DPSCs, when properly stimulated, can be induced to differentiate into neuronal-like and glial cells expressing the typical markers nestin and glial fibrillary acidic protein (GFAP) [18–21]. In addition, DPSCs showed to differentiate into osteoblast-like cells, express the main bone matrix protein collagen I (Col1), the typical osteoblast enzyme alkaline phosphatase (ALP), and form nodules of mineralized matrix [2, 15, 22–24]. This suggests the presence of different niches of progenitors/stem cells in the pulp with a multipotency of differentiation that can be intercepted and altered by the appropriate stimuli. Morphological characteristics of DPSCs were compared to those of mesenchymal stem cells (MSCs) from bone marrow; the comparison showed many similarities [2, 13]; it is also relevant that gene expression profiles of the two cell populations were very similar [25–27]. The finding of the differentiation potential of DPSCs led the scientists to consider them as an alternative source of postnatal stem cells. In particular, the ability to differentiate into osteoblast-like cells, which are able to deposit a mineralized matrix, has revolutionized the dental research and opened new perspectives for reconstructive surgery and calcified tissue bioengineering. The literature data on dental stem cells are so promising that American companies, with the approval by the Food and Drug Administration (FDA), provide a service of isolation and preservation of these cells where the onset of disease would make their use beneficial in therapy. Although the plasticity of DPSCs and their ability to generate many different cell lines are already known, what genes are involved in the multilineage differentiation ability of these cells and in their osteoblastic differentiation process remains unclear and needs to be deeply investigated, since osteoblastogenesis is influenced by many cytokines and genes [28, 29]. We have reported in a previous work that DPSCs express the nuclear receptor NURR1 in basal and in osteogenic conditions [23], a surprising finding, considering that NURR1 is a member of the nuclear steroid/thyroid receptor superfamily, expressed primarily in the central nervous system, essential for the survival and development function of dopaminergic neurons of the ventral nuclei of the brain [30]. Indeed, the expression of NURR1 was already described in DPSCs and SHEDs, but a role for the receptor was mostly attributed during the differentiation toward a neuronal phenotype [19, 31–33]. Actually, a couple of works reported, in mice calvarial osteoblast and MC3T3-E1, that NURR1 increased the expression of osteoblastic markers [34, 35]. Conversely, a more recent work described a cross talk between NURR1 and β-catenin where NURR1 inhibited β-catenin-mediated expression and β-catenin was capable of inhibiting the transcriptional activity of NURR1 [36]. So far, NURR1 is expressed in DPSCs, but its role in the osteogenic differentiation is still controversial and needs more investigations. Thus, having established that DPSCs are an excellent model for studying the osteoblast differentiation [2, 15, 22–24], in this work, we knock down NURR1 in DPSCs, by using the gene silencing technology, and elucidated the effect and the role of Nurr1 in osteoblast differentiation.

2. Results

2.1. Osteogenic Trigger Inhibits Neuronal Markers Expression in DPSCs. To confirm that DPSCs, following the osteogenic differentiation treatment, commit to osteoblastic lineage and lose their multipotency, we analyzed the expression of the neuronal protein nestin and the astrocytes marker GFAP. The cells were cultured in presence of osteogenic media, and the total cell lysates were collected at different time points (T0, 4, 8, and 12 days) to be analyzed by Western blotting. Figure 1 shows that both nestin and GFAP are expressed during the first phases of osteogenic differentiation, but their expression became dramatically reduced after 8 days of culture. These results demonstrated that, during the first days (4–8) of osteogenic differentiation, DPSCs continue to maintain neural potentials, or perhaps not all the cells are already committed while, after 8 days of culture in osteogenic medium, the neuronal potential of DPSCs appeared completely suppressed.

2.2. NURR1 Expression Was Knocked Down in DPSCs. Our previous work, showing that NURR1 was expressed in DPSCs in basal conditions and still present when the cells differentiated into osteoblast-like cells [23], prompted us to deeper investigate the role of NURR1 in DPSCs during the differentiation toward osteoblastic lineage. To this purpose, we used siRNA to knock down NURR1 expression in DPSCs from time zero (T0) during the whole differentiation process. The cells were seeded in osteogenic medium and the silencing sequences NURR1 (SIL) or scramble (CTR) were added every 48 hrs in order to keep NURR1 downregulated. All cell lysates were collected and subjected to qPCR showing a dramatic reduction of Nurr1 mRNA in silenced samples relative to CTR at the all analyzed time points (2, 4, 6, and 8 days) (Figure 2(a)). Detection of NURR1 protein levels was performed by Western blotting, confirming the decrease of the protein in NURR1 silenced cells (Figure 2(b)).

2.3. NURR1 Downregulation Favors the Osteogenic Differentiation of DPSCs. Once verified that NURR1expression was silenced during the osteoblastic differentiation of DPSCs, we analyzed how NURR1 knockdown could influence the osteogenic differentiation of DPSCs. Osteoblastic markers such as ALP, Col1, Runx-2, osteoprotegerin (OPG), osteopontin (OPN), and osteocalcin (OCN) were studied by qPCR: a schematic panel of the results is shown in Table 1.

However, the osteogenic markers that were significantly influenced by NURR1 downregulation have been described in details below. The expression of the typical osteoblast early markers Col1 and ALP was determined by qPCR (Figure 3). Col1 mRNA level increased in the CTR cells, along the

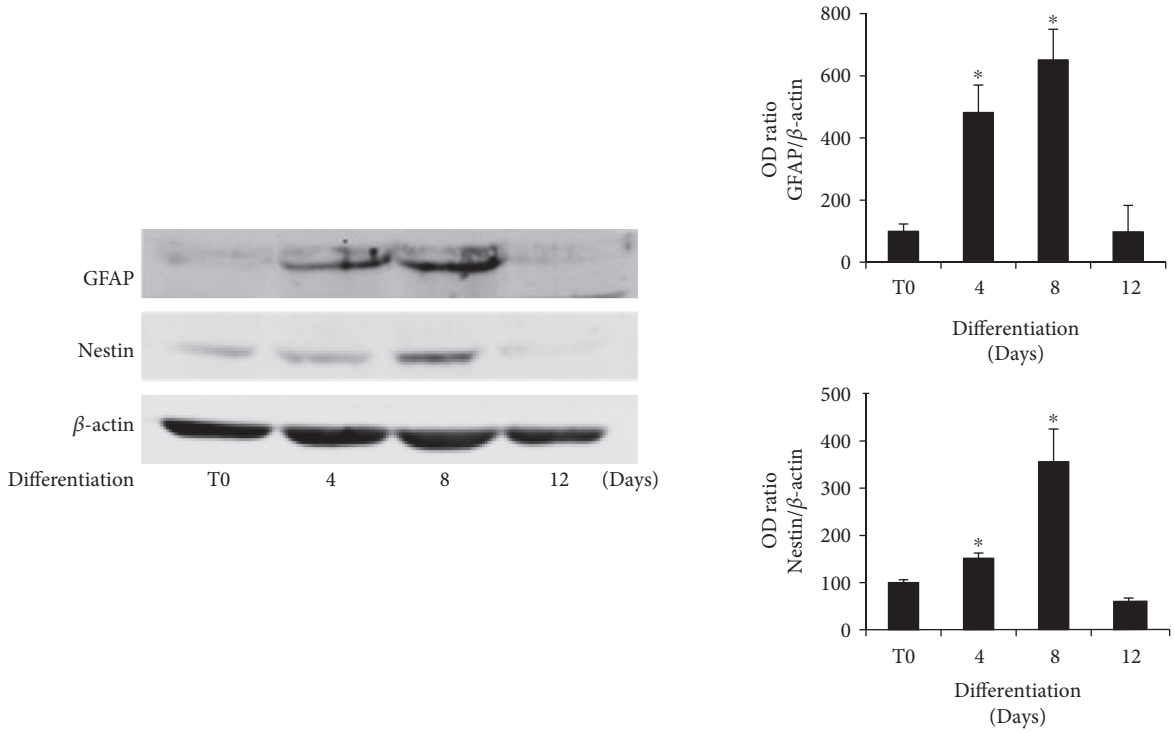

Figure 1: Expression of GFAP and nestin during osteogenic differentiation of DPSCs. Immunoblots show the protein expression trend of GFAP and nestin in DPSCs cultivated in osteogenic conditions for 4, 8, and 12 days. Both proteins were expressed during the first phases of osteogenic differentiation (4–8 days), but their expression dramatically dropped after 8 days of culture. Data are presented as means ± SE of 3 independent donors. $^*P < 0.01$ compared to T0. Statistics: unpaired Student's t-test.

analyzed differentiation steps (Figure 3(a)), as well as ALP (Figure 3(b)), confirming that DPSCs cultivated in osteogenic medium acquired the typical osteoblastic features. Intriguingly, the expression of Col1 significantly increased in NURR1 silenced cells compared to CTR cells with a significant trend at 6 and 8 days, as did ALP at 8 days, suggesting that NURR1 downregulation favors the osteogenic differentiation of DPSCs. The expression trend of Col1 was further confirmed, in NURR1 silenced and CTR cells, by Western blot analysis. As shown in Figure 3(c), Col1 protein level increased in NURR1 silenced cells if compared with CTR cells at 2–6 days, thus confirming the mRNA data. The molecular result of ALP trend was further supported by the histochemical evaluation of ALP expression. The histochemical assay was performed on DPSCs CTR and siNURR1 after 8 days of osteogenic differentiation (Figure 4(a)). As revealed by the purple staining, ALP expression was significantly more abundant in siNURR1 cells compared to CTR cells (~150%) corroborating the idea that NURR1 expression must be downregulated to prompt the cells to osteogenic lineage.

2.4. Downregulation of NURR1 in DPSCs Favors the Mineral Matrix Deposition Ability. To further investigate the role of NURR1 in osteoblast differentiation of DPSCs, we cultured CTR and NURR1 silenced cells in mineralizing conditions. The silencing sequences (siNURR1) or scramble (CTR) were added every 48 hrs in order to keep NURR1 downregulated. A histochemical assay was used to analyze how NURR1 knockdown could influence the ability of DPSCs to mineralize. As showed in Figure 4(b), the capacity of DPSCs to mineralize was highly enhanced in NURR1 silenced cells compared to CTR cells (200%). These results are in agreement with the increased expression of osteoblast markers Col1 and ALP and confirmed the finding that NURR1 is expressed in undifferentiated DPSCs, but down levels of the receptor prompt the differentiation of the cells toward the osteoblastic lineage and mineral matrix deposition.

3. Discussion

So far, NURR1 has been considered primarily involved in dopaminergic neurons differentiation and activity. Interestingly, a key role for the receptor was attributed during the differentiation of DPSCs toward a neuronal phenotype [19, 31–33]. Indeed, NURR1 is crucial for dopaminergic neuron function [37] and its malfunction has been correlated with neurological and inflammatory disease [38, 39]. By contrast, literature data about NURR1 role in osteoblasts are controversial: studies in mice highlighted an effect in increasing the osteoblastic phenotype of primary culture and osteoblastic cell lines [34, 35], while a more recent work indicated that NURR1 downregulated the main osteoblastic differentiation pathway, involving β-catenin, in a human osteoblastic cell line [36]. In addition, we found that MSCs such as DPSCs express NURR1 in basal and osteogenic conditions [23]. Thus, NURR1 is expressed in DPSCs, with a prominent role

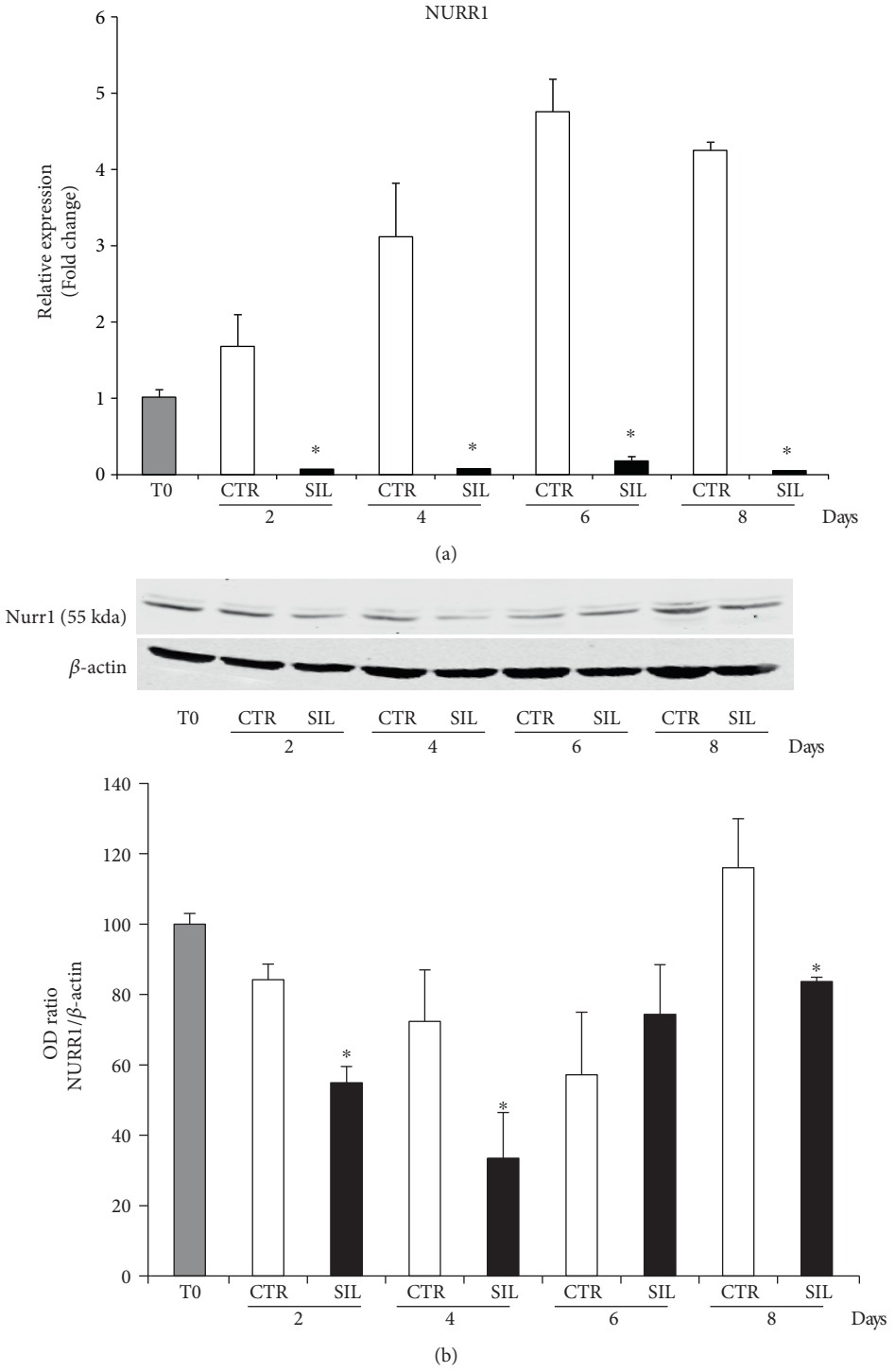

Figure 2: Effect of NURR1 short-interfering knockdown. (a) qPCR of DPSCs differentiated in osteogenic conditions and transfected with NURR1-specific siRNA (black bars) or scrambled sequences as control (white bars) showed the effective knockdown of NURR1 mRNA. A time course demonstrated that NURR1 expression remained downregulated along the culture. Expression was normalized to GAPDH. $^{*}P < 0.01$ compared to CTR. (b) NURR1 mRNA downregulation was confirmed and validated by Western blotting indicating that NURR1 protein was knocked down. Each graph represents means ± SE of 3 independent donors. $^{*}P < 0.01$ compared to CTR. Student's *t*-test was used for single comparison.

in neuronal differentiation, but its role in the osteogenic differentiation needs more investigations. Consistent with the essential role played by NURR1 in nervous tissue, we speculated if the molecule could, in some way, influence the DPSC differentiation toward the osteoblastic phenotype and, more precisely, if NURR1 inhibition could interfere with DPSC osteoblastogenesis. Primarily, we studied the neuronal marker nestin and the neuroglia marker G-Fap during DPSC

Table 1: Osteogenic markers in DPSC cultures: NURR1 silenced versus CTRs.

	2 days	4 days	6 days	8 days
ALP	UN	+	++	++
Col1	UN	++	++	++
Runx-2	+	UN	+	−
OPG	UN	−	−	++
OPN	+	−	−	UN
OCN	NF	NF	+	+

The table reports the osteogenic markers analyzed at 2, 4, 6, and 8 days of differentiation in NURR1 silenced and CTR cultures. The symbols indicate the ratio of NURR1 SIL compared to CTR cultures (expressed as %). + corresponds to an increase 10–50%; ++ corresponds to an increase higher than 50%; − corresponds to a decrease 10–50%; UN indicates a not significant variation; NF indicates a not relevant detection of the marker.

osteogenic process. Both markers were expressed in DPSCs during the first phases of osteogenic differentiation, perhaps the cells still retaining a neuronal potency, but dramatically decreased after 8 days of culture, indicating the expected result that osteoblast differentiation triggers decreased DPSC neuronal potential. Tissue regeneration, based on adult stem cells approach, is still facing with strategies directed to control and increase their differentiation capacity; thus, the discovery of target molecules to modulate, in order to address the desired commitment, is still an open challenge [40]. Mainly, MSC multipotency has the problem in regeneration therapy to drive cell differentiation to the correct lineage, reconstructing the expected mature tissue. The role of NURR1 in osteoblast differentiation is not yet clearly established and is intriguing, since it is expressed in MSCs during osteoblastogenesis [23, 34, 36], but it is also involved in neuronal differentiation [19, 41]. To unambiguously establish the role of this receptor in osteogenic differentiation of MSCs, we inhibited NURR1 during all the processes submitting DPSCs to a repeated multistep silencing treatment. Primarily, we checked the successful of NURR1 silencing treatment at each time of the experiment. Hence, the main osteogenic markers were studied. Col1 expression indicated that DPSCs acquired the capacity to secrete the main bone matrix protein and we found that NURR1 silencing increased both mRNA and protein expression. ALP mRNA levels dramatically increased in silenced cells and the histochemical assay confirmed the different enzyme quantities, indicating that NURR1 downregulation had a strong effect on the expression of the molecule crucial for osteoblast during the matrix deposition. The final crucial step in the bone regenerative process is the inorganic matrix formation [42]. Thus, mature osteoblasts, after the secretion of organic matrix components, begin the mineralization phase. MSCs from dental tissues have been demonstrated to correctly undergo to mineralization process [43]: some substances such as vitamin D could increase the mineral matrix deposition [44]; we found that inhibiting NURR1 enhanced DPSC mineralization. In summary, NURR1 is expressed in DPSCs, but to pursuit the cells toward a greater matrix deposition, proper of mature osteoblast, the receptor can be downregulated. MSC differentiation fate can be artificially modulated, in vitro, by the appropriate culture conditions and compounds. Apparently, the epigenetic science indicates that different stimuli can interfere with gene expression; in vivo, this issue regards also cell differentiation. In conclusion, our results showed the expression of nestin and GFAP in DPSCs confirming their neural potential. In addition, we demonstrated that such neural and glial markers are still present during the first steps of osteogenic differentiation, suggesting that DPSCs still maintain quite a multipotency or perhaps not all the cells in the culture are yet committed to osteogenic lineage. After 8 days, the expression of these markers dramatically decreased, suggesting that the cells lose their neural potential. In the same way, we found that NURR1 is expressed in DPSCs, but keeping down its expression during the osteogenic differentiation, the expression of typical osteoblastic markers is increased, culminating in higher production of mineralized matrix. We demonstrated that one of the mechanisms regulating MSC plasticity, influencing their phenotype, is NURR1 expression; in particular, its inhibition promotes osteoblastogenesis and enhances mineral matrix deposition. Discovering an appropriate in vivo method for inhibiting NURR1 during MSC osteogenic differentiation could improve an adult stem cell based tissue engineering, enhancing bone tissue regeneration.

4. Patients, Materials, and Methods

4.1. Cell Cultures. Human pulp tissues were collected from the third molars of twenty healthy young adults aged between eighteen and twenty-six years. The study was approved by the Institutional Review Board of the Department of Dental Science and Surgery—Unit of Periodontology, University of Bari; the patients gave written informed consent. Once the teeth were extracted, the pulp tissues were dissected, enzymatically digested, and filtered to obtain single-cell suspensions. DPSCs harvested were seeded and expanded as previously described [2, 23, 45, 46]. For differentiation toward osteogenic lineage, cell culture medium was supplemented with 10^{-8} M dexamethasone and 50 μg/ml ascorbic acid (Sigma Aldrich, Milan, Italy). For induction of matrix mineralization, we supplemented the cell culture medium with 10^{-8} M dexamethasone, 50 μg/ml ascorbic acid, and 10 mM β-glycerophosphate.

4.2. Short-Interfering RNA Knockdown. DPSCs were transfected with NURR1-specific siRNA or scrambled sequences as control (50 nM) (Life Technologies) using RNAi Max Lipofectamine (Life Technologies). Both specific and control sequences were added on each medium change every 2 days, until the end of the culture, in order to keep the protein downregulated, reaching an optimal knockdown of NURR1 mRNA and protein (Figures 2(a) and 2(b)).

4.3. Real-Time RT-PCR. Total RNA was isolated using spin columns (RNasy, Qiagen, Hilden, Germany) according to the manufacturer's instructions and reverse transcribed (2 μg) using the Superscript First-Strand Synthesis System kit (Invitrogen Life Technologies, Carlsbad, CA, USA); the resulting cDNA (20 ng) was subjected to quantitative PCR

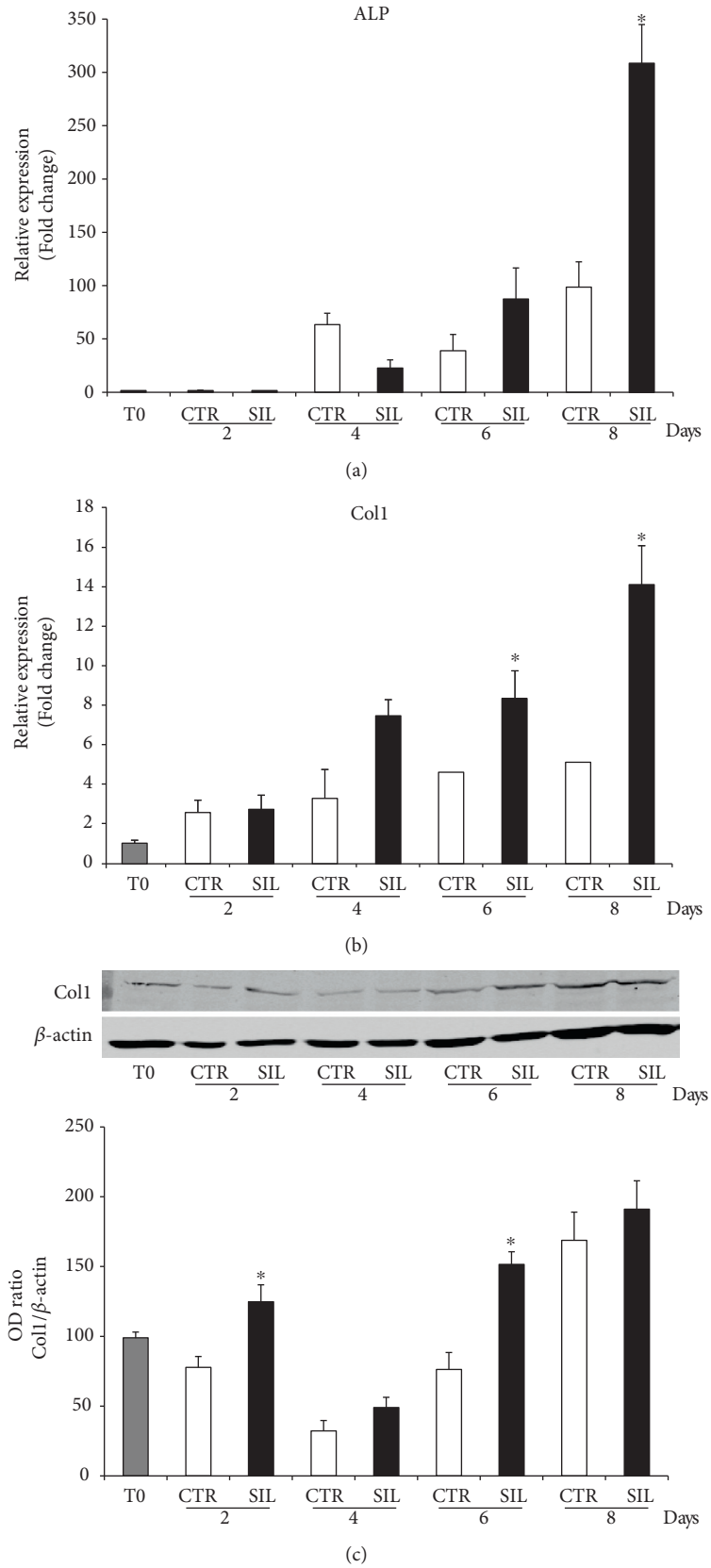

Figure 3: Effect of NURR1 downregulation on osteoblast markers. (a)-(b) qPCR performed on si-NURR1 or CTR cells showed that NURR1 downregulation significantly increased the expression of the two osteoblast markers ALP (8 days) (a) and Col1 (6–8 days) (b). Expression was normalized to GAPDH. $^*P < 0.01$ compared to CTR. (c) Immunoblotting confirmed that the expression of Col1 protein increased in NURR1 silenced cells relative to CTR cells ($^*P < 0.01$). Each graph represents means ± SE of 3 independent donors. Statistics: unpaired Student's t-test.

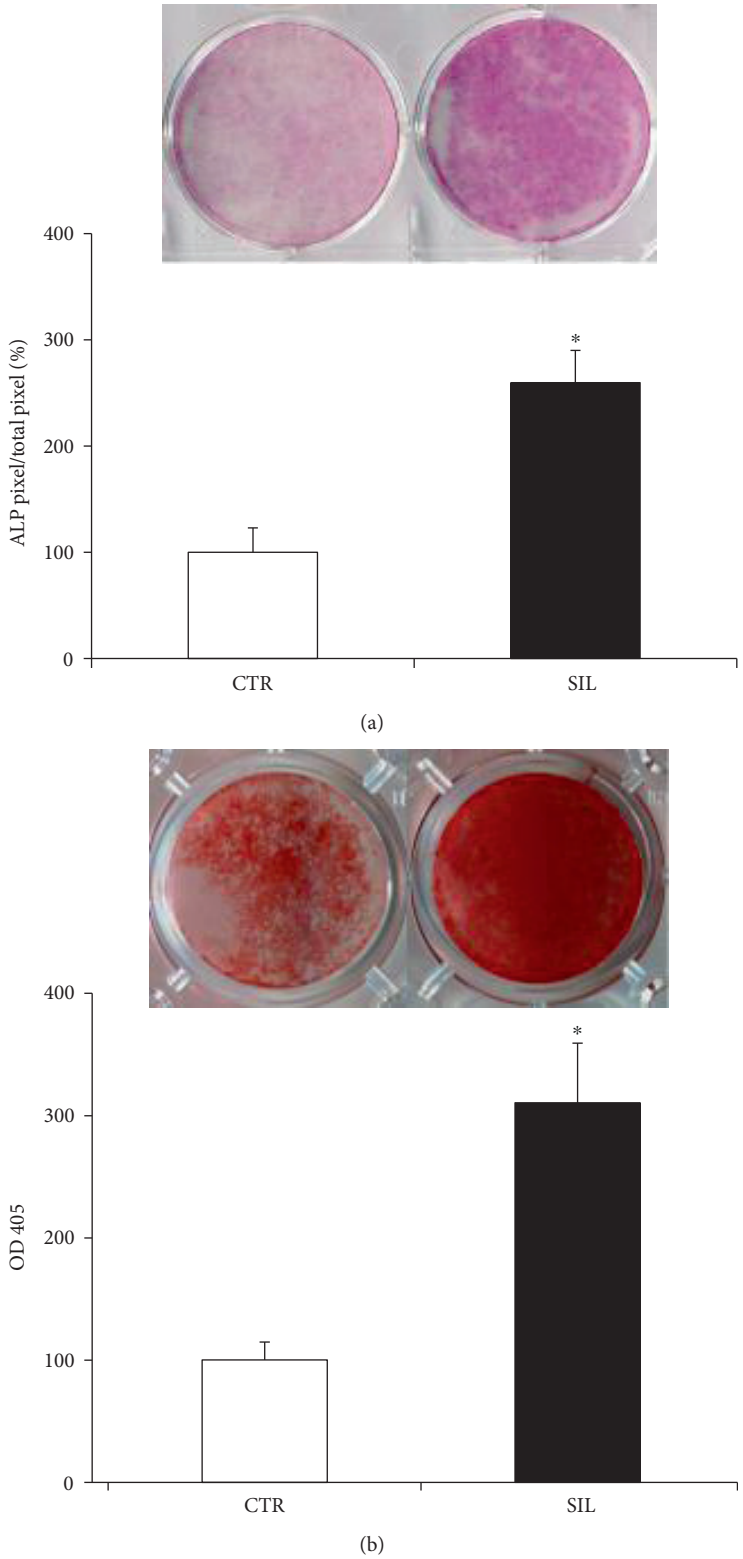

Figure 4: Effect of NURR1 downregulation on ALP and mineralization. (a) ALP histochemical assay (purple staining) performed on DPSCs transfected with NURR1-specific siRNA or scrambled sequences and maintained in osteogenic conditions for 7 days. The graph represents the quantification of positive staining as percentage compared to CTR ($^*P < 0.01$) and is representative for 3 independent donors. Data are presented as mean ± SEM. Student's *t*-test was used for single comparisons. (b) Mineral matrix deposition assayed by ARS (red staining) in siNURR1 and CTR cells after 21 days in osteogenic conditions. The graph shows the OD quantification of extracted dye from stained cell layers as percentage compared to CTR ($^*P < 0.001$) and is representative for 3 independent donors. Data are presented as mean ± SEM. Student's *t*-test was used for single comparisons.

as described. Real-time PCR analysis of mRNA was performed using a BioRad CFX96 Real Time System using the SYBR green PCR method according to the manufacturer's instruction (BioRad iScript Reverse Transcription Supermix cat. 170-8841). The mean cycle threshold value (Ct) from triplicate samples was used to calculate gene expression, and PCR products were normalized to GAPDH levels for each reaction.

4.4. Immunoblotting. Total cell lysates were obtained as previously described [44, 45]. Total protein concentration was measured using the Bio-Rad Protein Assay kit, and cell lysates were separated by SDS-PAGE before transfer onto nitrocellulose membranes (Invitrogen, Carlsbad, CA). After immunoblotting with the appropriate antibodies, immune complexes were visualized by incubation with IRDye-labeled secondary antibodies (680/800CW) (LI-COR Biosciences, NE). For immunoblotting, the Odyssey infrared imaging system was used (LI-COR Corp., Lincoln, NE).

4.5. Alkaline Phosphatase (ALP). The levels of the biochemical marker for the osteoblast activity, ALP, was tested in DPSC cultures differentiated with osteogenic factors, using the Leukocyte Alkaline Phosphatase Kit (Sigma Aldrich). Cells were fixed, gently washed with deionized water, and stained with ALP solution according to the manufacturer's instructions for 15′. After incubation, the cells were rinsed with water, air-dried, and then analyzed under the microscope. ALP-positive cells show a purple color. ALP quantification was performed by ImageJ, analyzing the number of colored pixels corresponding to the positive stained cells.

4.6. Alizarin Red Staining (ARS). The capacity of differentiated DPSCs to produce calcium-rich deposits was analyzed by using alizarin red staining. The cells were gently rinsed with PBS, fixed with 10% formalin at room temperature for 10 minutes, and then rinsed again with deionized water. The staining was performed by adding 1% of ARS solution at room temperature for 10 minutes. After discarding the ARS solution, the wells were rinsed twice with deionized water and air-dried. Calcium-rich deposits appeared red stained. As previously described, the dye was extracted from the stained cell layer and assayed for quantification at 405 nm [46, 47]. Briefly, 10% acetic acid was added for 30 min at room temperature with shaking, the solution incubated 10 min at 85°C and then kept on wet ice for 5 min. Before reading the optical density at 405 nm, 10% ammonium hydroxide was added to neutralize the acid. The results were evaluated for statistical analysis.

Conflicts of Interest

The authors declare no conflicting financial or other competing interests.

Authors' Contributions

Adriana Di Benedetto and Francesca Posa contributed equally to this work.

Acknowledgments

This work was partially awarded from Ministero dell'Istruzione, dell'Università e della Ricerca—PRIN 20098KM9RN, and Giorgio Mori (Progetto di Ricerca d'Interesse Nazionale—Grant 2009).

References

[1] S. Gronthos, J. Brahim, W. Li et al., "Stem cell properties of human dental pulp stem cells," *Journal of Dental Research*, vol. 81, no. 8, pp. 531–535, 2002.

[2] S. Gronthos, M. Mankani, J. Brahim, P. G. Robey, and S. Shi, "Postnatal human dental pulp stem cells (DPSCs) in vitro and in vivo," *Proceedings of the National Academy of Sciences of the United States of America*, vol. 97, no. 25, pp. 13625–13630, 2000.

[3] A. J. Sloan and A. J. Smith, "Stem cells and the dental pulp: potential roles in dentine regeneration and repair," *Oral Diseases*, vol. 13, no. 2, pp. 151–157, 2007.

[4] I. About, P. E. Murray, J. C. Franquin, M. Remusat, and A. J. Smith, "The effect of cavity restoration variables on odontoblast cell numbers and dental repair," *Journal of Dentistry*, vol. 29, no. 2, pp. 109–117, 2001.

[5] P. E. Murray, I. About, J. C. Franquin, M. Remusat, and A. J. Smith, "Restorative pulpal and repair responses," *Journal of the American Dental Association (1939)*, vol. 132, no. 4, pp. 482–491, 2001.

[6] C. T. Hanks, D. Fang, Z. Sun, C. A. Edwards, and W. T. Butler, "Dentin-specific proteins in MDPC-23 cell line," *European Journal of Oral Sciences*, vol. 106, Supplement 1, pp. 260–266, 1998.

[7] A. Ueno, Y. Kitase, K. Moriyama, and H. Inoue, "MC3T3-E1-conditioned medium-induced mineralization by clonal rat dental pulp cells," *Matrix Biology: Journal of the International Society for Matrix Biology*, vol. 20, no. 5-6, pp. 347–355, 2001.

[8] F. J. Unda, A. Martin, E. Hilario, C. Begue-Kirn, J. V. Ruch, and J. Arechaga, "Dissection of the odontoblast differentiation process in vitro by a combination of FGF1, FGF2, and TGFbeta1," *Developmental Dynamics: An Official Publication of the American Association of Anatomists*, vol. 218, no. 3, pp. 480–489, 2000.

[9] I. About, M. J. Bottero, P. Denatode, J. Camps, J. C. Franquin, and T. A. Mitsiadis, "Human dentin production in vitro," *Experimental Cell Research*, vol. 258, no. 1, pp. 33–41, 2000.

[10] M. L. Couble, J. C. Farges, F. Bleicher, B. Perrat-Mabillon, M. Boudeulle, and H. Magloire, "Odontoblast differentiation of human dental pulp cells in explant cultures," *Calcified Tissue International*, vol. 66, no. 2, pp. 129–138, 2000.

[11] E. Giorgini, C. Conti, P. Ferraris et al., "FT-IR microscopic analysis on human dental pulp stem cells," *Vibrational Spectroscopy*, vol. 57, no. 1, pp. 30–34, 2011.

[12] R. d'Aquino, A. RosaDe, G. Laino et al., "Human dental pulp stem cells: from biology to clinical applications," *Journal of Experimental Zoology Part B, Molecular and Developmental Evolution*, vol. 312b, no. 5, pp. 408–415, 2009.

[13] G. T. Huang, S. Gronthos, and S. Shi, "Mesenchymal stem cells derived from dental tissues vs. those from other sources: their biology and role in regenerative medicine," *Journal of Dental Research*, vol. 88, no. 9, pp. 792–806, 2009.

[14] N. Nuti, C. Corallo, B. M. Chan, M. Ferrari, and B. Gerami-Naini, "Multipotent differentiation of human dental pulp stem cells: a literature review," *Stem Cell Reviews*, vol. 12, no. 5, pp. 511–523, 2016.

[15] G. Papaccio, A. Graziano, R. d'Aquino et al., "Long-term cryopreservation of dental pulp stem cells (SBP-DPSCs) and their differentiated osteoblasts: a cell source for tissue repair," *Journal of Cellular Physiology*, vol. 208, no. 2, pp. 319–325, 2006.

[16] L. Spath, V. Rotilio, M. Alessandrini et al., "Explant-derived human dental pulp stem cells enhance differentiation and proliferation potentials," *Journal of Cellular and Molecular Medicine*, vol. 14, no. 6b, pp. 1635–1644, 2010.

[17] V. Tirino, F. Paino, A. RosaDe, and G. Papaccio, "Identification, isolation, characterization, and banking of human dental pulp stem cells," *Methods in Molecular Biology (Clifton, New Jersey)*, vol. 879, pp. 443–463, 2012.

[18] A. Arthur, G. Rychkov, S. Shi, S. A. Koblar, and S. Gronthos, "Adult human dental pulp stem cells differentiate toward functionally active neurons under appropriate environmental cues," *Stem Cells (Dayton, Ohio)*, vol. 26, no. 7, pp. 1787–1795, 2008.

[19] M. Kanafi, D. Majumdar, R. Bhonde, P. Gupta, and I. Datta, "Midbrain cues dictate differentiation of human dental pulp stem cells towards functional dopaminergic neurons," *Journal of Cellular Physiology*, vol. 229, no. 10, pp. 1369–1377, 2014.

[20] F. I. Young, V. Telezhkin, S. J. Youde et al., "Clonal heterogeneity in the neuronal and glial differentiation of dental pulp stem/progenitor cells," *Stem Cells International*, vol. 2016, Article ID 1290561, 10 pages, 2016.

[21] J. Zhang, M. Lian, P. Cao et al., "Effects of nerve growth factor and basic fibroblast growth factor promote human dental pulp stem cells to neural differentiation," *Neurochemical Research*, vol. 42, no. 4, pp. 1015–1025, 2016.

[22] G. Laino, R. d'Aquino, A. Graziano et al., "A new population of human adult dental pulp stem cells: a useful source of living autologous fibrous bone tissue (LAB)," *Journal of Bone and Mineral Research: The Official Journal of the American Society for Bone and Mineral Research*, vol. 20, no. 8, pp. 1394–1402, 2005.

[23] G. Mori, G. Brunetti, A. Oranger et al., "Dental pulp stem cells: osteogenic differentiation and gene expression," *Annals of the New York Academy of Sciences*, vol. 1237, pp. 47–52, 2011.

[24] G. Mori, M. Centonze, G. Brunetti et al., "Osteogenic properties of human dental pulp stem cells," *Journal of Biological Regulators and Homeostatic Agents*, vol. 24, no. 2, pp. 167–175, 2010.

[25] D. Menicanin, P. M. Bartold, A. C. Zannettino, and S. Gronthos, "Identification of a common gene expression signature associated with immature clonal mesenchymal cell populations derived from bone marrow and dental tissues," *Stem Cells and Development*, vol. 19, no. 10, pp. 1501–1510, 2010.

[26] S. Shi and S. Gronthos, "Perivascular niche of postnatal mesenchymal stem cells in human bone marrow and dental pulp," *Journal of Bone and Mineral Research: The Official Journal of the American Society for Bone and Mineral Research*, vol. 18, no. 4, pp. 696–704, 2003.

[27] S. Shi, P. G. Robey, and S. Gronthos, "Comparison of human dental pulp and bone marrow stromal stem cells by cDNA microarray analysis," *Bone*, vol. 29, no. 6, pp. 532–539, 2001.

[28] W. Huang, S. Yang, J. Shao, and Y. P. Li, "Signaling and transcriptional regulation in osteoblast commitment and differentiation," *Frontiers in Bioscience: A Journal and Virtual Library*, vol. 12, pp. 3068–3092, 2007.

[29] G. Mori, G. Brunetti, S. Colucci et al., "Alteration of activity and survival of osteoblasts obtained from human periodontitis patients: role of TRAIL," *Journal of Biological Regulators and Homeostatic Agents*, vol. 21, no. 3-4, pp. 105–114, 2007.

[30] J. N. GrandLe, L. Gonzalez-Cano, M. A. Pavlou, and J. C. Schwamborn, "Neural stem cells in Parkinson's disease: a role for neurogenesis defects in onset and progression," *Cellular and Molecular Life Sciences: CMLS*, vol. 72, no. 4, pp. 773–797, 2015.

[31] A. Jarmalaviciute, V. Tunaitis, E. Strainiene et al., "A new experimental model for neuronal and glial differentiation using stem cells derived from human exfoliated deciduous teeth," *Journal of Molecular Neuroscience: MN*, vol. 51, no. 2, pp. 307–317, 2013.

[32] D. Majumdar, M. Kanafi, R. Bhonde, P. Gupta, and I. Datta, "Differential neuronal plasticity of dental pulp stem cells from exfoliated deciduous and permanent teeth towards dopaminergic neurons," *Journal of Cellular Physiology*, vol. 231, no. 9, pp. 2048–2063, 2016.

[33] K. L. Yang, M. F. Chen, C. H. Liao, C. Y. Pang, and P. Y. Lin, "A simple and efficient method for generating Nurr1-positive neuronal stem cells from human wisdom teeth (tNSC) and the potential of tNSC for stroke therapy," *Cytotherapy*, vol. 11, no. 5, pp. 606–617, 2009.

[34] M. K. Lee, H. Choi, M. Gil, and V. M. Nikodem, "Regulation of osteoblast differentiation by Nurr1 in MC3T3-E1 cell line and mouse calvarial osteoblasts," *Journal of Cellular Biochemistry*, vol. 99, no. 3, pp. 986–994, 2006.

[35] F. Q. Pirih, A. Tang, I. C. Ozkurt, J. M. Nervina, and S. Tetradis, "Nuclear orphan receptor Nurr1 directly transactivates the osteocalcin gene in osteoblasts," *The Journal of Biological Chemistry*, vol. 279, no. 51, pp. 53167–53174, 2004.

[36] A. M. Rajalin and P. Aarnisalo, "Cross-talk between NR4A orphan nuclear receptors and beta-catenin signaling pathway in osteoblasts," *Archives of Biochemistry and Biophysics*, vol. 509, no. 1, pp. 44–51, 2011.

[37] J. Satoh and Y. Kuroda, "The constitutive and inducible expression of Nurr1, a key regulator of dopaminergic neuronal differentiation, in human neural and non-neural cell lines," *Neuropathology: Official Journal of the Japanese Society of Neuropathology*, vol. 22, no. 4, pp. 219–232, 2002.

[38] C. A. Altar, M. P. Vawter, and S. D. Ginsberg, "Target identification for CNS diseases by transcriptional profiling," *Neuropsychopharmacology: Official Publication of the American College of Neuropsychopharmacology*, vol. 34, no. 1, pp. 18–54, 2009.

[39] S. Vivekanantham, S. Shah, R. Dewji, A. Dewji, C. Khatri, and R. Ologunde, "Neuroinflammation in Parkinson's disease: role in neurodegeneration and tissue repair," *The International Journal of Neuroscience*, vol. 125, no. 10, pp. 717–725, 2015.

[40] A. R. Amini, C. T. Laurencin, and S. P. Nukavarapu, "Bone tissue engineering: recent advances and challenges," *Critical Reviews in Biomedical Engineering*, vol. 40, no. 5, pp. 363–408, 2012.

[41] X. Long, M. Olszewski, W. Huang, and M. Kletzel, "Neural cell differentiation in vitro from adult human bone marrow mesenchymal stem cells," *Stem Cells and Development*, vol. 14, no. 1, pp. 65–69, 2005.

[42] E. Bonucci, "Bone mineralization," *Frontiers in Bioscience (Landmark Edition)*, vol. 17, pp. 100–128, 2012.

[43] B. Clarke, "Normal bone anatomy and physiology," *Clinical Journal of the American Society of Nephrology: CJASN*, vol. 3, Supplement 3, pp. S131–S139, 2008.

[44] F. Posa, A. BenedettoDi, G. Colaianni et al., "Vitamin D effects on osteoblastic differentiation of mesenchymal stem cells from dental tissues," *Stem Cells International*, vol. 2016, Article ID 9150819, 9 pages, 2016.

[45] A. BenedettoDi, G. Brunetti, F. Posa et al., "Osteogenic differentiation of mesenchymal stem cells from dental bud: role of integrins and cadherins," *Stem Cell Research*, vol. 15, no. 3, pp. 618–628, 2015.

[46] A. BenedettoDi, C. Carbone, and G. Mori, "Dental pulp stem cells isolation and osteogenic differentiation: a good promise for tissue engineering," *Methods in Molecular Biology (Clifton, New Jersey)*, vol. 1210, pp. 117–130, 2014.

[47] C. A. Gregory, W. G. Gunn, A. Peister, and D. J. Prockop, "An Alizarin red-based assay of mineralization by adherent cells in culture: comparison with cetylpyridinium chloride extraction," *Analytical Biochemistry*, vol. 329, no. 1, pp. 77–84, 2004.

Hindawi
Stem Cells International
Volume 2017, Article ID 2416254, 15 pages
https://doi.org/10.1155/2017/2416254

Research Article

In Vitro and In Vivo Dentinogenic Efficacy of Human Dental Pulp-Derived Cells Induced by Demineralized Dentin Matrix and HA-TCP

Kyung-Jung Kang,[1] Min Suk Lee,[1] Chan-Woong Moon,[2] Jae-Hoon Lee,[2] Hee Seok Yang,[1] and Young-Joo Jang[1]

[1]*Department of Nanobiomedical Science and BK21 PLUS Global Research Center for Regenerative Medicine, Dankook University, 29 Anseo-Dong, Cheonan 330-714, Republic of Korea*
[2]*Department of Oral and Maxillofacial Surgery, College of Dentistry, Dankook University, 29 Anseo-Dong, Cheonan 330-714, Republic of Korea*

Correspondence should be addressed to Hee Seok Yang; hsyang@dankook.ac.kr and Young-Joo Jang; yjjang@dankook.ac.kr

Received 11 March 2017; Revised 26 April 2017; Accepted 3 May 2017; Published 28 June 2017

Academic Editor: Marco Tatullo

Human dental pulp cells have been known to have the stem cell features such as self-renewal and multipotency. These cells are differentiated into hard tissue by addition of proper cytokines and biomaterials. Hydroxyapatite-tricalcium phosphates (HA-TCPs) are essential components of hard tissue and generally used as a biocompatible material in tissue engineering of bone. Demineralized dentin matrix (DDM) has been reported to increase efficiency of bone induction. We compared the efficiencies of osteogenic differentiation and in vivo bone formation of HA-TCP and DDM on human dental pulp stem cells (hDPSCs). DDM contains inorganic components as with HA-TCP, and organic components such as collagen type-1. Due to these components, osteoinduction potential of DDM on hDPSCs was remarkably higher than that of HA-TCP. However, the efficiencies of in vivo bone formation are similar in HA-TCP and DDM. Although osteogenic gene expression and bone formation in immunocompromised nude mice were similar levels in both cases, dentinogenic gene expression level was slightly higher in DDM transplantation than in HA-TCP. All these results suggested that in vivo osteogenic potentials in hDPSCs are induced with both HA-TCP and DDM by osteoconduction and osteoinduction, respectively. In addition, transplantation of hDPSCs/DDM might be more effective for differentiation into dentin.

1. Introduction

Periodontal disease and dental caries cause periodontal bone defects, which will lead to tooth loss. The best way to treat periodontal bone defects is the induction of osteogenesis through reconstructive surgery. Recently, bone tissue engineering technology is known to be a promising clinical application for replacing wounded dental tissues [1–5]. Bone regeneration requires three components: stem cells, biological factors that can undergo and enhance osteogenic differentiation, and scaffolding materials that should be biocompatible and biodegradable [3]. Mesenchymal stem cells (MSCs) are regarded as a promising source for scaffold-based bone tissue engineering due to their self-renewal and osteogenic differentiation potentials [6–8]. Various dental tissues contain the populations of MSCs, and dental stem cells are identified from dental pulp tissue, periodontal ligament, apical papilla, and dental follicles [9–12]. Unlike other MSCs, dental stem cells including human dental pulp stem cells (hDPSCs) have the advantages of nonsurgical tissue collection and easy culture, which are essential for adult stem cell-based amplification. Of these, hDPSCs contain abilities of proliferation and multiple differentiations, and they have been applied for regeneration of dentin, periodontal ligament, and bone tissue in the oral maxillofacial regions [13–16]. At early stage of osteogenic

differentiation, DPSCs have shown higher alkaline phosphatase activity compared to bone marrow-derived MSCs in osteogenic medium [17]. DPSCs can be differentiated by osteoinductive bone factors such as bone morphogenetic proteins in both in vitro and in vivo studies [18–22]. However, using stem cell-based techniques for mature bone formation in large defect without additional cytokine or growth factor is still controversial, although they have potential for osteogenic differentiation. Possible reasons for conflict in stem cell therapy and tissue engineering might be a desertion of stem cells from the transplantation post and their heterogeneous differentiation properties. Inorganic-based scaffolds or carrier materials such as demineralized bone matrix, calcium phosphate scaffold, and hydroxyapatite-tricalcium phosphates (HA-TCP) have been used as platforms for cell delivery due to their osteoconductivity. In addition, they can serve as reservoirs for bioactive molecules. HA-TCP has excellent biocompatibility because their chemical and structural compositions are similar to those of inorganic-based components of natural bone tissue. These inorganic-based scaffolds have osteoconductivity and bone-bonding affinity site to enhance osteoblast differentiation and host bone cell recruitment. Nevertheless, inorganic-based scaffolds have limitations in that they have low mechanical process and that they lack bioactive molecules for osteogenic differentiation from intact host tissue [23–29]. There has been increasing interest in the development of demineralized or decellularized natural materials simultaneously having bioactive function as a solution to these problems. Many studies have been undertaken to investigate whether biological bone or dentin matrix with excellent biocompatibility and osteoconductivity could be used as biomaterial for stem cell attachment, proliferation, and osteogenic differentiation. Previous studies have shown that demineralized dentin matrix (DDM) is composed of approximately 55% inorganic minerals and 45% organic materials such as growth factors and cytokines. Based on the biochemical composition, DDM originated from animal induces bone formation potential in subcutaneous and intramuscular chambers in rodents [30] and has been used to treat bone defects by enhanced bone formation [31, 32]. DDM of enamel matrix derivative has been successfully used in clinics as bone graft and repair materials for several decades [33–36]. Biocompatible and bioactive materials for the purpose of bone tissue regeneration have been studied. Here, we show a method to isolate and culture human DPSCs and use them for in situ differentiation using inorganic scaffolds for ectopic bone regeneration without requiring additional stimuli. The first purpose of this investigation is to evaluate the osteoconductive activity of HA-TCP or osteoinductive human DDM in vitro with hDPSCs. The second purpose is to determine the abilities of hDPSCs with HA-TCP or human DDM to induce ectopic bone formation after transplanting them subcutaneously into athymic mice in vivo.

2. Materials and Methods

2.1. Culture of Human Dental Pulp Stem Cells and Transplantation Preparation. For primary culture of human dental pulp stem cells (hDPSCs), human third molars were collected from patients who were 15 to 27 years old under guidelines approved by the Institutional Review Board (IRB) of Dankook Dental Hospital (DKUDH IRB 2016-12-005). Human dental pulp tissue was obtained from the internal part of the tooth, chopped into small fragments, and enzymatically digested with 3 mg/mL collagenase type I (Millipore) and 4 mg/mL dispase (Sigma) at 37°C for 1 h. Cell suspension was incubated in α-MEM (HyClone) containing 20% fetal bovine serum (FBS, HyClone) and 1% antibiotics (Lonza) at 37°C in humidified atmosphere supplemented with 5% CO_2. To observe osteoinduction efficiency in vitro, 40,000 cells per well were cultured with 0.8 g of HA-TCP (0.5–1 mm, Q-Oss+, OSSTEM Implant) or DDM (0.5–1 mm, Korea Tooth Bank, Korea) in a hanging insert cell culture dish (SPL Life Sciences). For transplantation, 1×10^6 cells were resuspended in 100 μL of thrombin, and 40 mg of HA-TCP or DDM granules was added. Then, 100 μL of fibrinogen (TISSEEL, Baxter AG) was added and mixed immediately to allow polymerization at room temperature. Fibrin blocks of hDPSCs/HA-TCP or DDM were incubated in culture at 37°C in humidified atmosphere supplemented with 5% CO_2 till transplantation.

2.2. Characterization of HA-TCP and DDM. The crystallographic properties of HA-TCP and DDM were investigated to use X-ray diffraction (XRD, UltimaIV, Rigaku, Tokyo, Japan) measurement. The XRD was activated at 40 kV and 40 mA with Cu $K_{\alpha 1}$ radiation ($\lambda = 1.5405$ Å). The patterns of XRD were measured for step-scan of 0.02° and rate of 3° per minute over a 2θ range from 20 to 80°. Surface morphologies of HA-TCP and DDM were examined by scanning electronic microscopy (SEM, JSM-6510, JEOL Co., Tokyo, Japan). The HA-TCP and DDM were sputter-coated (Sputter Coater 108 Auto, Cressington, Watford, UK) with platinum and sliced to a thickness of 5 nm prior to SEM measurement. The pore size of DDM in SEM images was evaluated to use ImageJ software (NIH, Bethesda, MD, USA).

2.3. Preparation of DDM Extract and Western Analysis. Each HA-TCP (0.7 g) and DDM (0.7 g) granule was incubated with α-MEM (HyClone) without FBS at 37°C for 3 days to extract their components. Extracts were then concentrated. To detect cytokines and growth factors released from each inorganic granule, proteins in extracts were separated by SDS-PAGE, transferred to PVDF membrane, and probed with anti-collagen type-1 antibody (Santa Cruz Biotechnology) followed by incubation with horseradish peroxidase-(HRP-) conjugated secondary antibody. Protein signals were visualized by using ECL™ reagent (GE Healthcare).

2.4. Live/Dead Cell Survival Assay. Cell viability was determined using calcein-AM staining solution (Thermo Scientific). The fibrin blocks of hDPSCs/HA-TCP and hDPSCs/DDM were incubated in culture media for 4 days, washed with PBS, and incubated with 4 μM EthD-1 and 2 μM calcein-AM in PBS at room temperature for 45 min in the dark. The fluorescent signals were detected by using confocal microscope (LSM700, Carl Zeiss).

Table 1: Primers used for the quantitative real-time-PCR (qPCR).

Target gene	Primer sequences
Alkaline phosphatase (ALP)	For-5′-CTTGACCTCCTCGGAAGACACTC-3′ Rev-5′-CGCCCACCACCTTGTAGCC-3′
Bone sialophosphoprotein (BSP)	For-5′-TACCGAGCCTATGAAGATGA-3′ Rev-5′-CTTCCTGAGTTGAACTTCGA-3′
Osteopontin (OPN)	For-5′-GTGGGAAGGACAGTTATGAA-3′ Rev-5′-CTGACTTTGGAAAGTTCCTG-3′
Osteonectin (ONT)	For-5′-CTGTTGCCTGTCTCTAAACC-3′ Rev-5′-CACCATCATCAA ATTCTCCT-3′
Osteocalcin (OCN)	For-5′-TGAGTCCTGAGCAGCAG-3′ Rev-5′-TCTCTTCACTACCTCGCT-3′
Dentin matrix protein 1 (DMP1)	For-5′-GACTCTCAAGAAGACAGCAA-3′ Rev-5′-GACTCACTCACCACCTCT-3′
Dentin sialophosphoprotein (DSPP)	For-5′-CAGTACAGGATGAGTTAAATGCCAGTG-3′ Rev-5′-CCATTCCCTTCTCCCTTGTGACC-3’
GAPDH	For-5′-GTATGACAACAGCCTCAAGAT-3′ Rev-5′-CCTTCCACGATACCAAAGTT-3′

2.5. Subcutaneous Implantation of Fibrin Constructs in Immunocompromised Nude Mice for Ectopic Mineralized Tissue Formation. Twenty immunocompromised nude mice (female, 4 weeks old, Orient Bio, Korea) were used in this study. Animal study protocol was approved by the Institutional Animal Care and Use Committee of Dankook University. Two experimental groups were used in this study. Each group had 10 animals. Group 1 was used for fibrin gel with HA-TCP granule with or without hDPSCs. Group 2 was used for fibrin gel with DDM granule with or without hDPSCs. For transplantation, mice were anesthetized by intraperitoneal injection of a mixture of tiletamine/zolazepam (30 mg/kg, Zoletil 50®, Virbac) and xylazine (10 mg/kg, Rompun®, Bayer Korea Ltd.). Two subcutaneous 1 cm incisions were made in each flank pocket from the dorsal midline of mice. Prepared fibrin gels with granule with or without hDPSCs were placed into each pocket. After 1 week and 8 weeks, animals were sacrificed and implants were retrieved for further studies.

2.6. Microcomputer Tomography Examination (Micro-CT). Mineralization and bone formation were evaluated by micro-CT. Micro-CT images were obtained using a micro-CT scanner (SkyScan-1176, Skyscan) at a resolution of 15 μm pixel with a 0.5 mm aluminum filter and a rotation step of 0.4. Three readings were obtained for each sample. Bone volume was determined using a CT analyzer program (CT-An, Skyscan). 3D images were obtained using a 3D-visualization program. Statistical analyses for three readings were carried out using Student's t-test. Statistical significance was considered when p value was less than 0.05. Data are expressed as means with error bars representing standard error of the mean (SEM). Student's t-test was performed using GraphPad Prism 6 program.

2.7. Quantitative Real-Time Reverse-Transcription Polymerase Chain Reaction (qRT-PCR). Total RNAs of hDPSCs and frozen tissue were extracted by using Easy-spin™ Total RNA Extraction kit (Intron, Korea) and RNA Easy Mini Extraction kit (Qiagen), respectively. cDNA was synthesized from total RNA by using the ReverTra Ace™ qPCR RT kit (Toyobo Corporation), and the qRT-PCR was performed by using iTaq™ Universal SYBR™ Green Supermix (Bio-Rad) system. Used primers are listed in Table 1. The cycling parameters of qPCR were followed; 1 cycle for 30 sec at 95°C, 40 cycles for 15 sec at 95°C, and 1 minute at 55°C–64°C. During PCR, a dissociation curve was constructed in the range of 65°C to 95°C.

GAPDH was used as an internal control to normalize the variability in target gene expression. Statistical analyses on three readings were carried out using Student's t-test and p values of less than 0.05 were considered statistically significant. Data are expressed as means ($n = 3$) with error bars representing standard error of the mean (SEM). Student's t-test was performed using GraphPad Prism 6 program.

2.8. Histological Analysis. After 8 weeks, the retrieved samples from dorsal midline of athymic nude mice were fixed in 4% paraformaldehyde (PFA) overnight. The fixed samples were rinsed with PBS for removing residual PFA and dehydrated using 70% ethyl alcohol. And then, the dehydrated samples were decalcified using decalcifying solution-Lite (Sigma-Aldrich, St. Louis, MO, USA) for 16 hrs and embedded in paraffin wax. The embedded samples were transversely cut to obtain different cross-sectional images. The samples were sectioned with thickness of 6 μm by a microtome (RM2255, Leica, Bensheim, Germany). Sectioned samples were deparaffinized in xylene, hydrated with a series of graded ethanol, and stained with hematoxylin/eosin and Golder's trichrome staining. An optical microscope (CKX41, Olympus, Tokyo, Japan) was used to obtain images of the stained samples for confirming newly the deposition of mineralization by HA-TCP and DDM.

2.9. Immunohistochemical Analysis. Sectioned samples were selected randomly ($n = 6$ per group) and immersed in xylene and preceded a preconditioning process for double

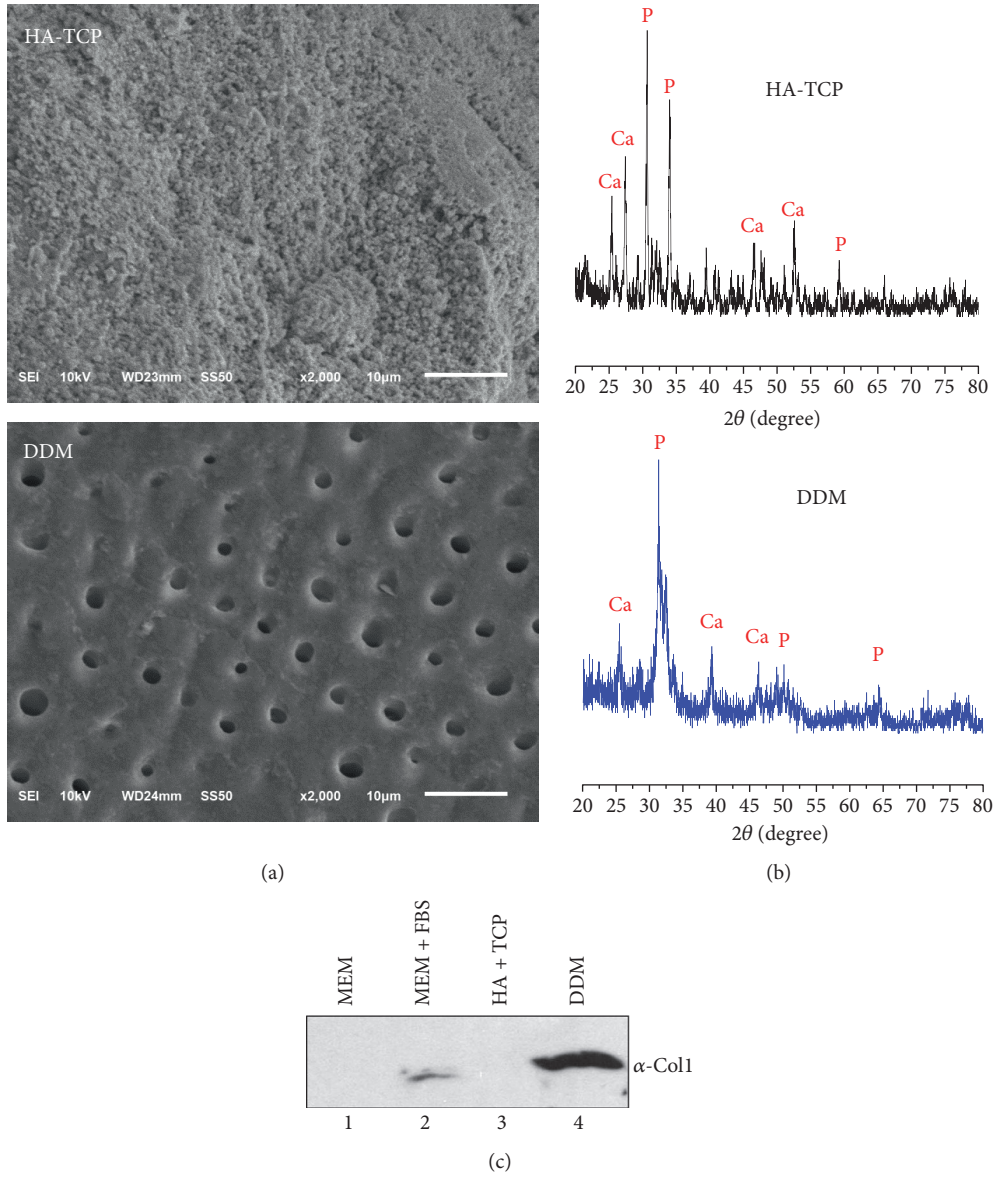

Figure 1: Characteristics of HA-TCP and human DDM scaffolds. (a) Surface structures of HA-TCP (upper panel) and DDM (lower panel) were examined by SEMs. Scale bars: 10 μm. (b) X-ray diffraction patterns of HA-TCP (upper graph) and DDM (lower graph). (c) Analysis of protein components in materials by immunoblot. The extracts of HA-TCP and DDM granules were concentrated, separated on SDS-PAGE, and immunoblotted with anti-type-1 collagen antibody. 1, α-MEM only; 2, α-MEM with 10% FBS; 3, HA-TCP extract in α-MEM; 4, DDM extract in α-MEM.

immunofluorescence staining of osteogenic and dentinogenic markers with human nuclear antigen (HNA). The samples were incubated in blocking buffer for 1 hr at room temperature. After blocking, samples were stained for 16 hrs with primary human specific antibodies; a 1 : 100 dilution of antibone sialoprotein antibody (Abcam), 1 : 200 dilutions of antihuman nuclear antigen (Abcam) and antiosteocalcin antibody (Abcam), a 1 : 500 dilution of antiosteopontin antibody (Abcam), a 1 : 1000 dilution of antiosteonectin antibody (Millipore), and 1 : 100 dilution of antidentin sialophosphoprotein antibody (Abcam). Fluorescein-isothiocyanate conjugated secondary antibodies (Jackson Immuno Research Laboratories, PA, USA) and 4′,6′-diamidino-2-phenylindole (DAPI, Vector Laboratories, Burlingame, CA, USA) were used to visualize the signals of the primary antibodies and nuclei, respectively. Samples were measured by using confocal microscope (LSM700, Carl Zeiss, Jena, Germany).

3. Results

3.1. Surface Analysis of HA-TCP and DDM Scaffolds. Demineralized dentin matrix (DDM) used in this study was a congeneric biomaterial produced from human dentin for this research. It was prepared by grinding, degreasing, and decalcification (performed by Korea Tooth Bank, Seoul, Korea). Two different specimens were randomly selected to determine their pore size and surface morphologies by SEM analysis. Results of SEM analysis are shown in Figure 1.

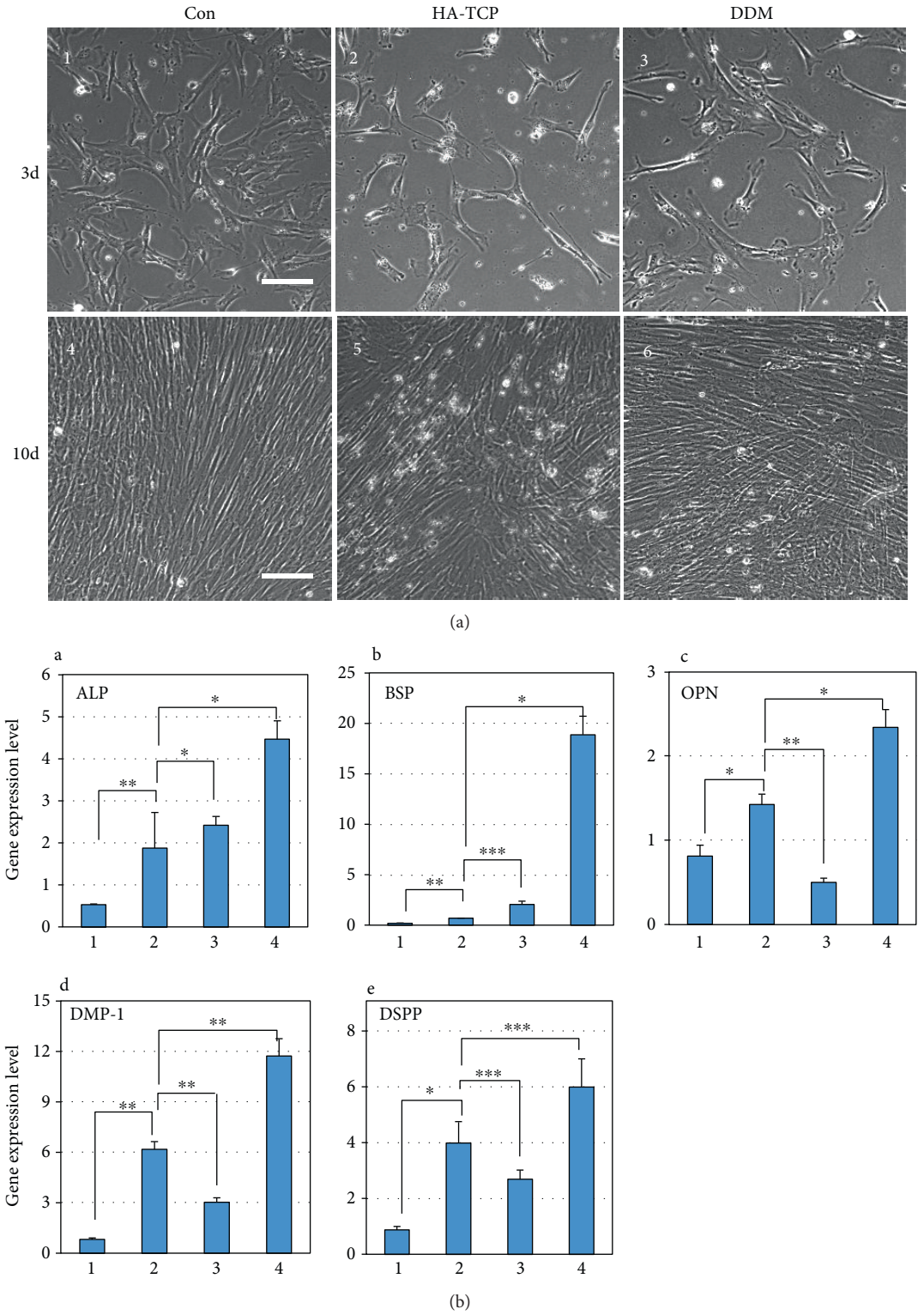

Figure 2: Osteoinduction potentials of HA-TCP and DDM on hDPSCs in vitro. (a) Morphology of hDPSCs cultured in the extracts of HA-TCP and DDM for 3 and 10 days. 1 and 4, hDPSCs cultured in α-MEM with 10% FBS, indicated as *Con*; 2 and 5, hPDSCs cultured in HA-TCP extract; 3 and 6, hDPSCs cultured in DDM extract. Scale bars: 100 μm. (b) Gene expression of osteogenic and dentinogenic markers in hDPSCs cultured in the extracts of HA-TCP and DDM. Gene expressions of ALP (A), BSP (B), OPN (C), DMP-1 (D), and DSPP (E) were analyzed by the qRT-PCR. 1, actively growing hDPSCs; 2, hDPSCs in the prolonged culture for 10 days; 3, hPDSCs cultured in HA-TCP extract for 10 days; 4, hDPSCs cultured in DDM extract for 10 days. Statistical analyses were carried out using Student's *t*-test. $^{*}p < 0.05$; $^{**}p < 0.01$; $^{***}p < 0.001$.

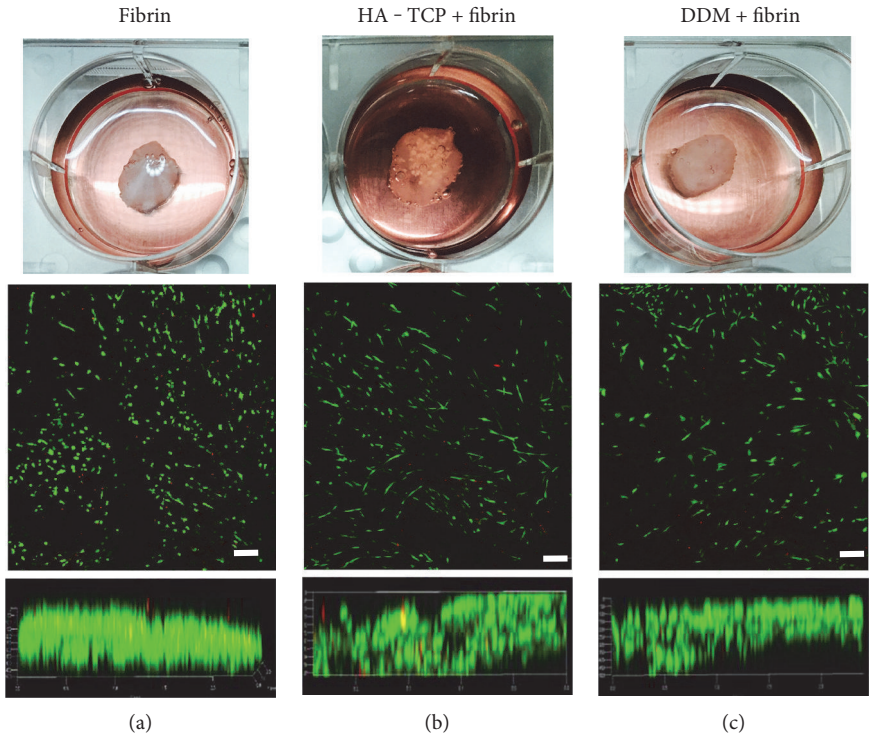

Figure 3: Cell viability of hDPSCs cultured in fibrin gel block. Cells were encapsulated with HA-TCP and DDM in fibrin and cultured in media for 4 days. Fibrin gen blocks were built at a certain size (upper panels). Scale bars: 1 cm. Cell viability was analyzed by using the live-dead viability assay kit. Live and dead cells were stained as green and red, respectively. Cells were detected on the surface of the block (middle panels) and in the interior of the blocks as a cross-sectional view of the block (lower panels). (a) Fibrin gel with hDPSCs. (b) HA-TCP/fibrin gel with hDPSCs. (c) DDM/fibrin gel with hDPSCs. Scale bar: 200 μm.

HA-TCP substrate was observed to have hydroxyapatite particles completely covering the surface of HA-TCP without pore or microtube structure (Figure 1(a), upper panel), while the surface of DDM exhibited a smear layer of enamel with continuous uniformly micro pores at diameter of $2.08 \pm 0.37\,\mu$m (Figure 1(a), lower panel). XRD analysis revealed several diffraction peaks produced by hydroxyapatite of HA-TCP (Figure 1(b), upper graph). Diffraction peaks at $2\ominus = 25.8$ (Ca), 31.9 (P), 37.2 (Ca), 45.5 (Ca), and 47.7 (P) corresponded well to expected spectra of the hydroxyapatite. Generally, the enamel layer on the tooth consists of pure hydroxyapatite composite. Because enamel was not completely removed from the sample tooth during demineralization, hydroxyapatite components such as phosphate and calcium were detected in the DDM used in this study. Peaks of the DDM showed a typical XRD pattern of synthesized hydroxyapatite, similar to the HA-TCP sample. XRD analysis for the DDM revealed numerous peaks of Ca and P, indicating the presence of enamel on the DDM surface (Figure 1(b), lower panel). In addition to inorganic components, dentin contains organic biomolecules. To detect protein component in materials, western blot analysis was performed using DDM and HA-TCP extracts. Indeed, collagen type-1 was detected in DDM extract (Figure 1(c), lanes 4). However, they were not detected in HA-TCP extract (Figure 1(c), lanes 3). Although very weak signals of these proteins were also detected in normal culture media containing 10% FBS (Figure 1(c), lanes 2), much higher amounts of collagen were released from the DDM.

3.2. In Vitro Osteoinduction Potentials of HA-TCP and DDM on hDPSCs. To determine the osteoinduction potential of HA-TCP or DDM, hDPSCs were cultured under the inserts with 800 mg of HA-TCP or DDM. Actively growing hDPSCs are generally detected as well-spreading and flat shapes (Figure 2(a), panel 1). Cell morphology was changed to a spinous and elongated phenotype, which aligned tightly and paralleled in confluent culture after 10 days (Figure 2(a), panel 4). Cells cultured with extracts of HA-TCP and DDM for 10 days also showed a similar phenotype as those under confluent culture condition (Figure 2(a), panels 5 and 6). The mRNA expression of osteogenic markers in these cells was then examined. The expression levels of alkaline phosphatase (ALP), bone sialophosphoprotein (BSP), osteopontin (OPN), dentin sialophosphoprotein (DSPP), and dentin matrix protein (DMP-1) were significantly increased in cells cultured after 10 days without addition of materials in comparison to those in actively growing cells after 3 days of culture (Figure 2(b), bars 1 and 2 in A–E), suggesting that hDPSCs could be differentiated into osteo/odontoblasts by themselves under the prolonged culture condition. Because the synthetic materials such as HA-TCP do not have osteoinduction potential, the osteo/dentinogenic markers in hDPSCs incubated with HA-TCP were not much increased in comparison to those in cells cultured for 10 days

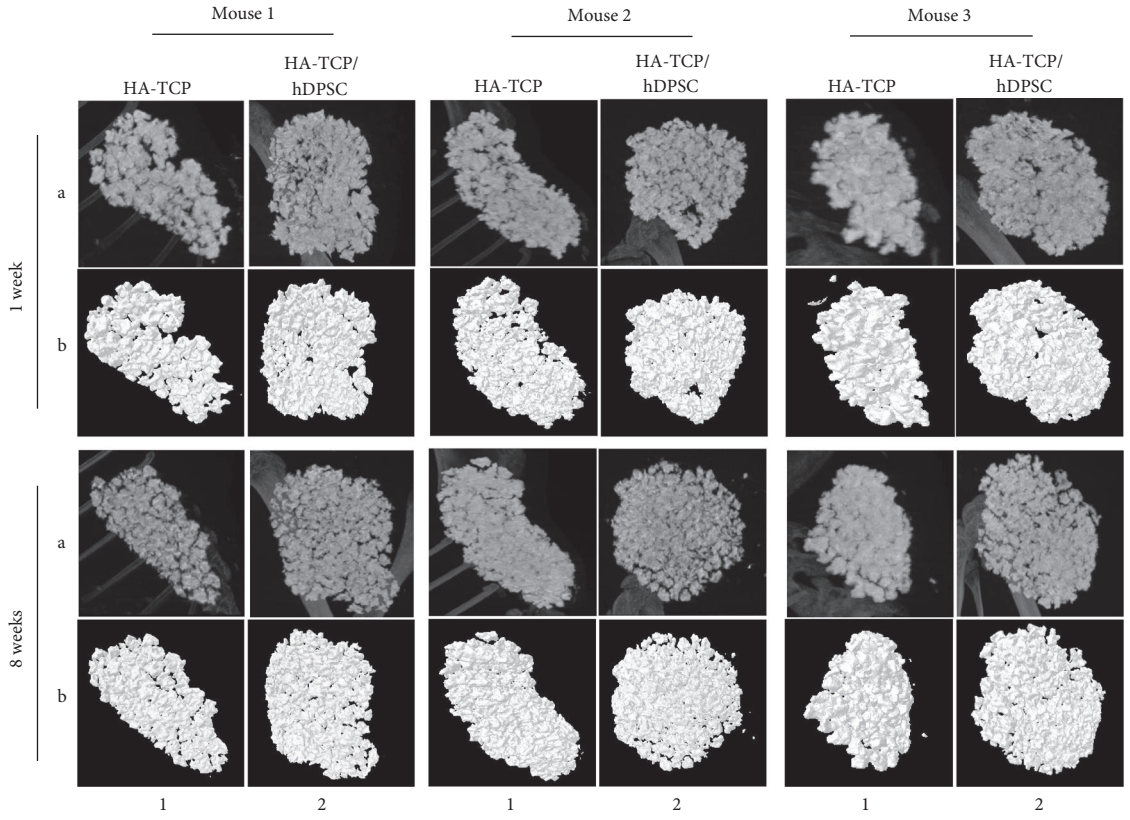

(a)

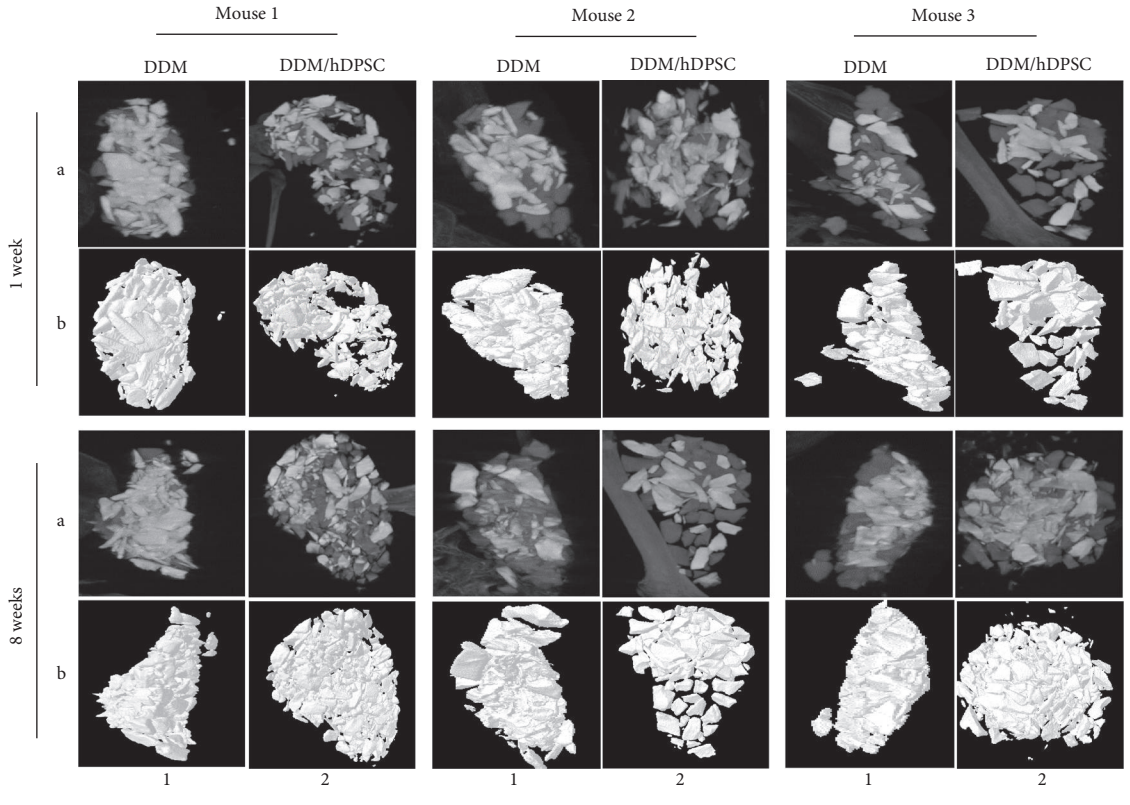

(b)

Figure 4: Continued.

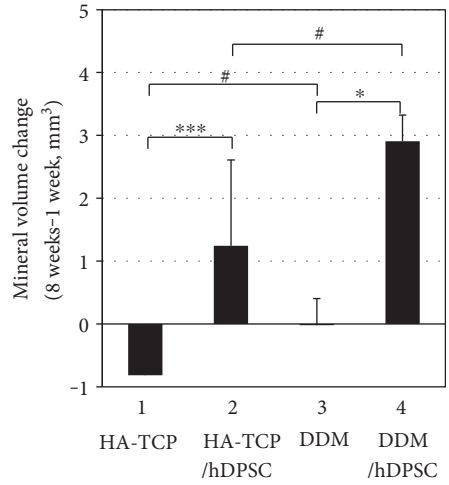

(c)

Figure 4: Ectopic bone-forming efficacy of hDPSCs transplanted with HA-TCP or DDM in athymic nude mice. Bone formations in the transplantation of HA-TCP (a) and DDM (b) were analyzed by micro-CT. The results were shown as X-ray images (A) and 3D-visualization image (B). (c) Quantification of mineral volume change over 1 week and 8 weeks. 1, transplantation of HA-TCP only; 2, transplantation of HA-TCP with hDPSCs; 3, transplantation of DDM only; 4, transplantation of DDM with hDPSCs. Statistical analyses were carried out using Student's t test. $^{*}p < 0.05$; $^{***}p < 0.001$; #, significant difference not be detected.

(Figure 2(b), bars 2 and 3 in A–E). Unlike HA-TCP, mRNA expression levels of osteogenic markers such as ALP, BSP, and OPN in hDPSCs with DDM extract were 2.4, 27.3, and 1.6 times higher, respectively, than those without the addition of DDM material (Figure 2(b), bars 2 and 4 in A–C). Regarding osteogenic markers, mRNA expression levels of two odontogenic markers DMP-1 and DSPP in hDPSCs cultured with DDM were 2.0 and 1.9 times higher, respectively, than those without the addition of DDM (Figure 2(b), bars 2 and 4 in D and E). These results indicate that DDM has better potential for osteoinduction in hDPSCs in vitro in comparison to synthetic hydroxyapatite materials such as HA-TCP.

3.3. Cell Viability of hDPSCs Cultured in Fibrin Gel Block with HA-TCP or DDM. For transplantation, hDPSCs were mixed with HA-TCP or DDM granules. To keep cells gathering in transplantation area and promote cell survival, it is necessary to encapsulate cells and biomaterial granules within fibrin gel. Culturing cells in a three-dimensional matrix is an important technique for tissue engineering as well as for studying cellular responses under culture conditions with biomaterials in vitro. hDPSCs were encapsulated with HA-TCP and DDM-fibrin gel, which had a similar size of 1 cm in width and 0.4 cm in height (Figures 3(a), 3(b), and 3(c), upper panels), and all samples were incubated in culture media. Cell viability of hDPSCs was analyzed by live and dead assay after 4 days of culture. These hDPSCs were viable inside the fibrin gel (Figures 3(a), 3(b), and 3(c)). Regardless whether HA-TCP or DDM was added, high cell viabilities were observed on the surface (Figure 3, middle panels) and in the interior of these gel constructs (Figure 3, lower panels).

3.4. Ectopic Bone-Forming Efficacy of hDPSCs Transplanted with HA-TCP or DDM in Subcutaneous of Athymic Mice. To determine the effect of HA-TCP or DDM on ectopic bone formation of hDPSCs, cells and materials encapsulated in fibrin blocks were implanted subcutaneously into athymic nude mice. After 1 week and 8 weeks of transplantation, samples implanted on the dorsal part were analyzed directly using micro-CT. The mice were under anesthesia during the analytic process. All sample groups of HA-TCP, hDPSC/HA-TCP, DDM, and hDPSC/DDM could be apparently seen subcutaneously on the dorsal area. They all kept their initial shapes, and hard tissue formations by mineralization were detected. Micro-CT images for retrieved transplants are shown in Figures 4(a) and 4(b). The differences of bone formation between 1 week and 8 weeks were evaluated as mineral volume change. In the samples without cells, bone volumes were not increased from 1 week to 8 weeks (Figure 4(c), bars 1 and 3). When hDPSCs were encapsulated, bone volumes of the HA-TCP group and the DDM group were increased as much as 1.24 mm^3 and 2.91 mm^3, respectively, at 8 weeks compared to those at 1 week (Figure 4(c), bars 2 and 4). Regarding materials transplanted, gene expression of BSP and OPN were enhanced in the transplant of hDPSC/HA-TCP, which were 3.5 and 1.3 times higher, respectively, compared to those in the transplant of hDPSC/DDM (Figure 5, bars 2 in A and B). Reversely, expression of ONT and OCN were slightly enhanced in hDPSCs/DDM transplant, compared to those in hDPSC/HA-TCP transplant (Figure 5, bars 2 in C and D). Only BSP expression level was significantly increased in HA-TCP transplant ($^{*}p < 0.001$), but the expression of other genes was not significantly different in between HA-TCP and DDM. Although DDM had higher osteoinduction potential than HA-TCP, osteoconduction ability of HA-TCP could

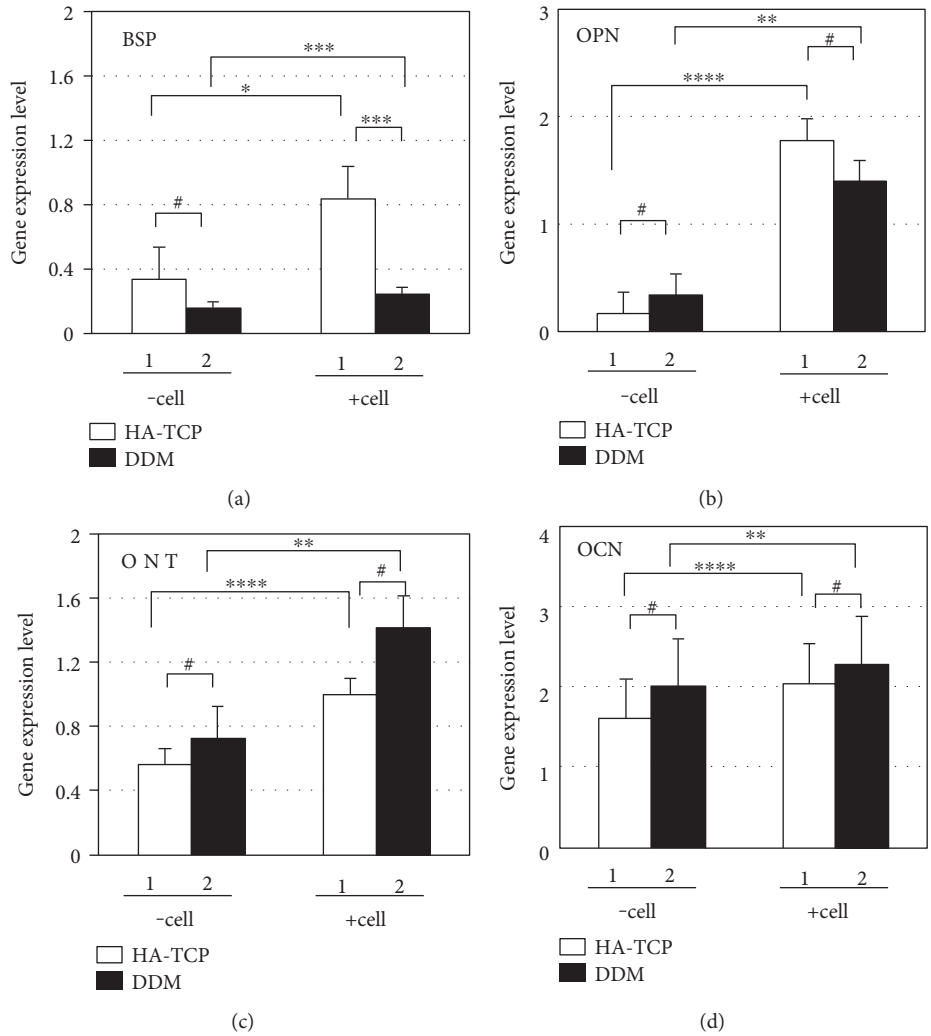

Figure 5: Analyses of gene expression of osteoblast markers in transplants. Fibrin blocks of HA-TCP/hDPSCs or DDM/hDPSCs were transplanted in athymic nude mice, and total RNA was isolated from transplant tissues after 8 weeks. Gene expressions of BSP (a), OPN (b), ONT (c), and OCN (d) were detected by qRT-PCR. 1, transplants with HA-TCP with or without hDPSCs; 2, transplants with DDM with or without hDPSCs. Transplantations with and without hDPSCs indicated as *–cell* and *+cell*, respectively. Statistical analyses were carried out using Student's *t*-test. $^{*}p < 0.05$; $^{**}p < 0.01$; $^{***}p < 0.001$; $^{****}p < 0.0001$; #, significant difference not be detected.

also be induced after in vivo transplantation experiment for 8 weeks. Goldner's trichrome staining results showed nearly no bone formation in implantation of HA-TCP or DDM without hDPSCs after 8 weeks of subcutaneous transplantation in mice. Implantation of HA-TCP or DDM resulted in regeneration of fibrous-like tissue (Figures 6(a) and 6(c)). However, osteoid formation around HA-TCP was observed in the transplantation group of HA-TCP with hDPSCs (Figure 6(b)). In newly formed bone (green color indicating mineralized bone), osteocytes in lacuna shape were observed in the group of HA-TCP and DDM with hDPSCs (Figures 6(b) and 6(d)). Ectopic bone formations were further supported by double immunofluorescent staining for bone-related markers and human nuclear antigen (HNA) as a marker for the detection of hDPSCs transplanted (Figure 7). A number of transplanted hDPSCs were found on the lining of the surface of coencapsulated HA-TCP and DDM granules at mineralized sites. Osteogenic marker proteins OPN, OCN, ONT, and BSP were expressed on the coincident area lined with cells (Figures 7(a), 7(b), 7(c), and 7(d)). Interestingly, DSPP, one of the dentin markers, was strongly detected in hDPSCs lined on the surface of DDM (Figure 7(e)) than those on the surface of HA-TCP transplanted. These results suggest that both HA-TCP and DDM induced in vitro osteogenic differentiation potential of hDPSCs transplanted, and they enhanced ectopic bone tissue formation. Inflammation was not observed in any histological section at the implanted site.

4. Discussion

Generally, human dental pulp stem cells are cultured from pulp tissues extracted from wisdom and deciduous teeth. They can be differentiated into various lineage types such as odontoblast, osteoblast, chondrocyte, adipocyte, and neural cells [22, 37–43]. To analyze osteogenesis and odontogenesis

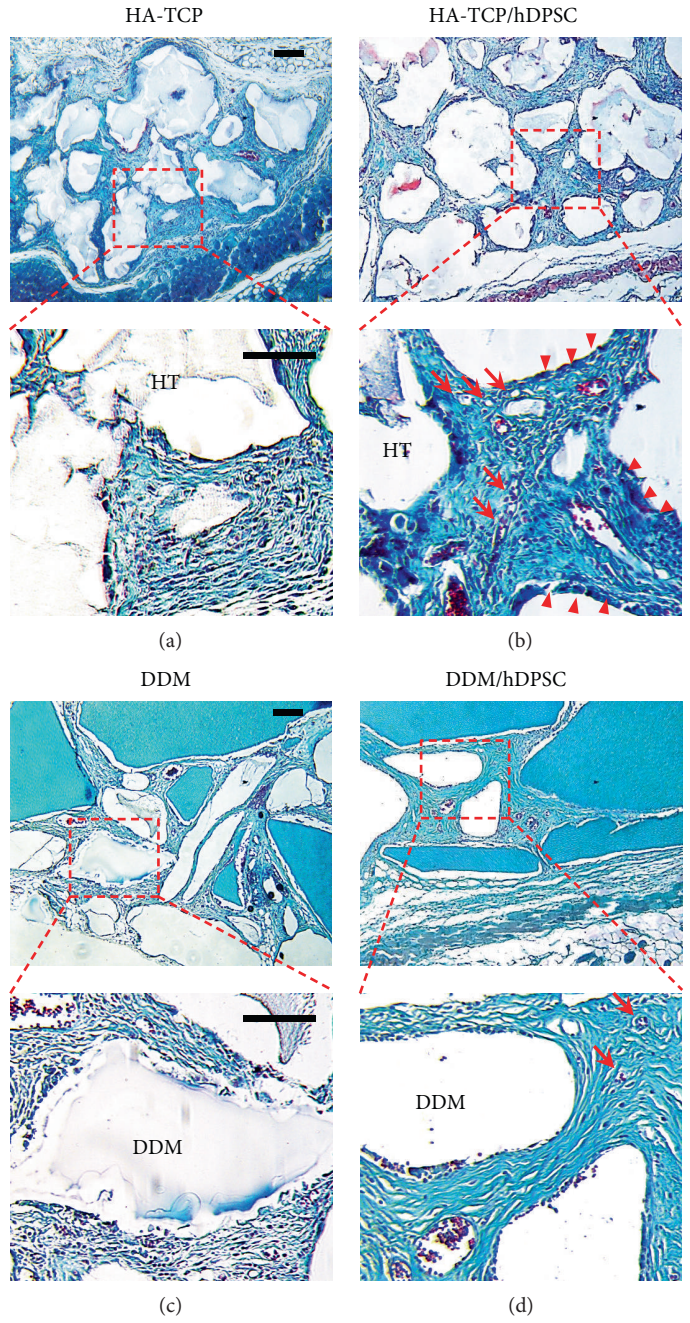

Figure 6: Histological analysis of bone-like tissue formed in transplants. Bone formation in vivo in athymic nude mice was examined by Goldner's trichrome staining of paraffin sections of transplants. (a) Transplants of HA-TCP only. (b) Transplants of HA-TCP with hDPSCs. (c) Transplants of DDM only. (d) Transplants of DDM with hDPSCs. Osteoid and lacuna structures were indicated as arrow heads (►) and arrows (→), respectively. Scale bar: 100 μm.

of hDPSCs, we compared inorganic based HA-TCP and human DDM under both in vitro and in vivo conditions. Primary culture of isolated hDPSCs on both biocompatible inorganic materials was performed and used in in vitro studies. For in vivo ectopic bone regeneration, both inorganic materials and hDPSCs were transplanted subcutaneously to athymic mice. Although characterization of osteoconductivity or osteoinductivity of biomaterials remains a challenge in the field of tissue engineering, osteoinductive DDM has excellent benefit for reconstructive surgery due to multiple trauma and craniofacial deformities. It is also beneficial for oncological surgery and periodontal surgery due to its osteoinductive properties. SEM analysis was performed in this study to examine surface characteristics of inorganic HA-TCP and DDM. Highly porous surface of DDM was revealed by SEM analysis, showing similarity to bony structure. The morphometrically high porous (pore size: 2.08 ± 0.37 μm) DDM might also be useful as a promising scaffold in bone substitution. Furthermore, microsized pores are expected to be able to efficiently supply nutrients and oxygen in vivo (Figure 1(a), lower panel).

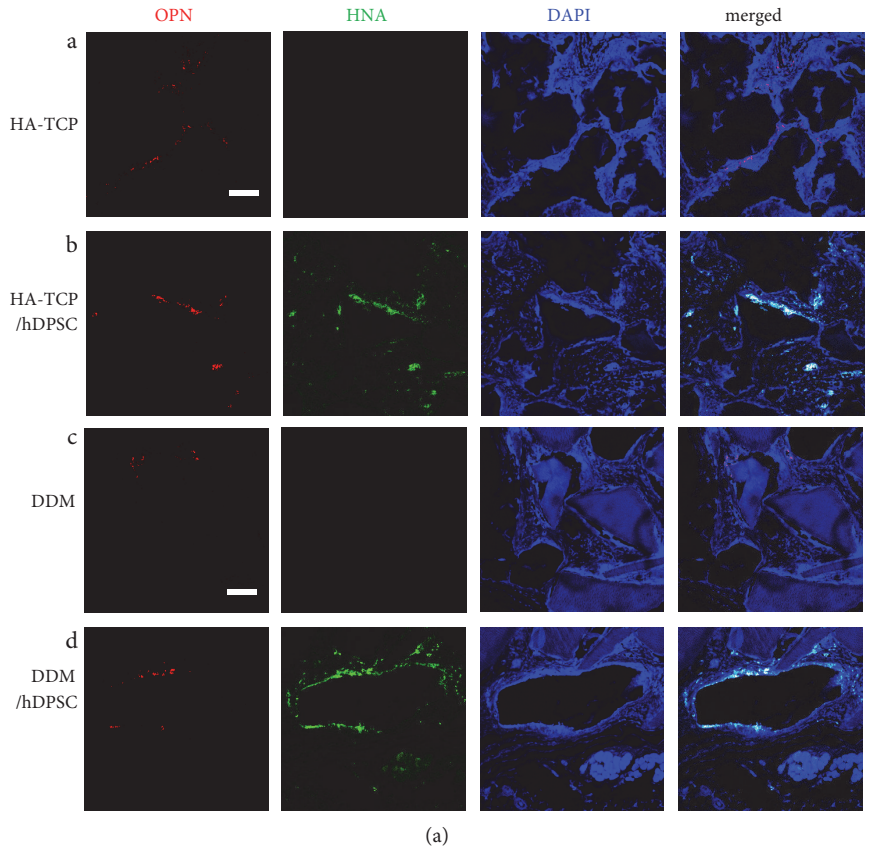

(a)

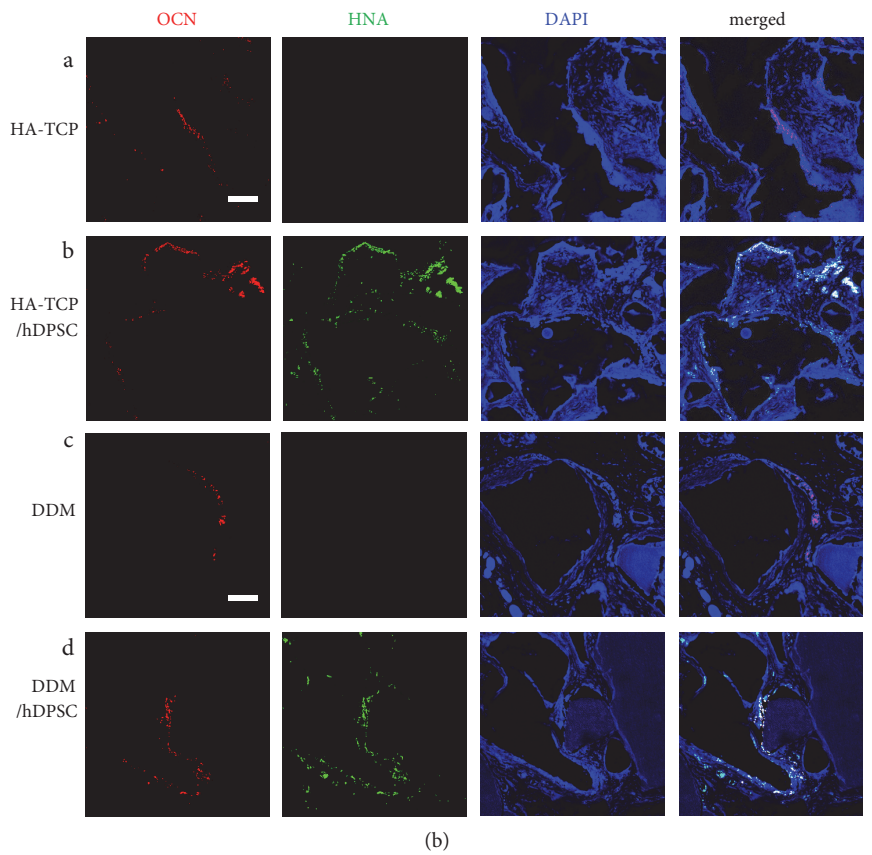

(b)

Figure 7: Continued.

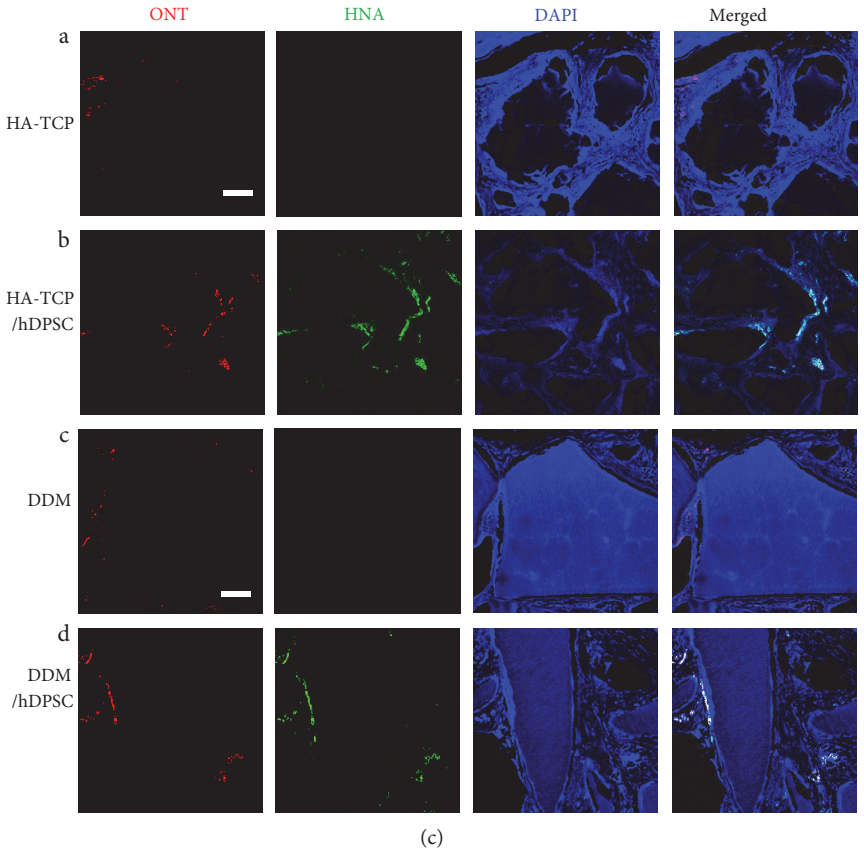

(c)

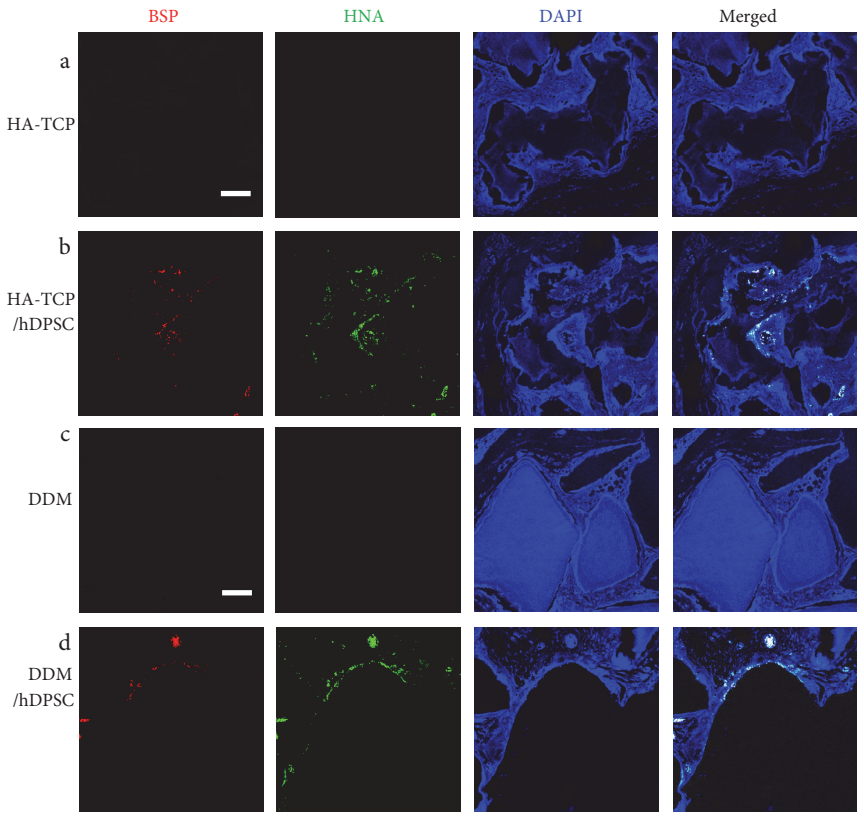

(d)

Figure 7: Continued.

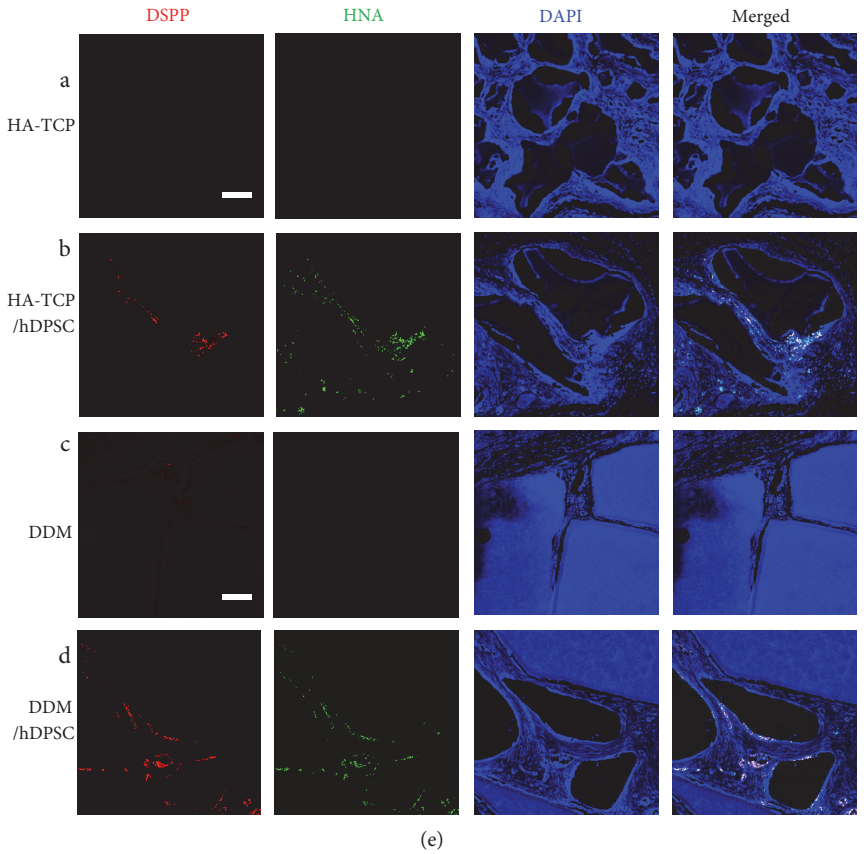

Figure 7: Immunohistochemical localization of osteogenic and dentinogenic markers. Paraffin sections of the transplants were incubated with anti-OPN antibody (a), anti-OCN antibody (b), anti-ONT antibody (c), anti-BSP antibody (d), and anti-DSPP antibody (e). Signal of markers was shown as red. Nuclei of human cells and DNA in tissues were stained by anti-HNA antibody (green) and DAPI (blue), respectively. (A), transplants of HA-TCP only; (B), transplants of HA-TCP with hDPSCs; (C), transplants of DDM only; (D), transplants of DDM with hDPSCs. Scale bar: 100 μm.

In analysis of minerals by XRD, both HA-TCP and DDM contained large amount of calcium and phosphate (Figure 1(b)) [44]. In general thoughts, DDM should not contain minerals in its component, because they were prepared by demineralization. However, because dentin tissue used in this study for preparation of DDM was mixed with the enamel part at a certain amount, calcium and phosphate were detected in DDM even after demineralization [45]. Expression levels of osteogenic and dentinogenic markers were significantly increased in hDPSCs cultured in the extract of DDM in comparison with those in hDPSCs cultured in HA-TCP extract, suggesting that HA-TCP alone might have no effect on osteoinduction in in vitro cell culture. DDM could induce osteogenic and dentinogenic differentiation due to its osoteoinduction property (Figure 2(b)). hDPSCs transplanted with HA-TCP and DDM showed incomparable ectopic bone formation efficacy in vivo. After transplantation of HA-TCP and DDM in nude mice, both biomaterials failed to show apparent ectopic bone formation on hDPSCs after 8 weeks. Because HA-TCP itself has time-dependent resorbability without osteoinductivity [46], bone volume of HA-TCP was even slightly decreased in comparison with that of DDM. However, mineral volumes in transplants of HA-TCP/hDPSCs and DDM/hDPSCs were increased by 15.3% and by 28.7%, respectively, in comparison with those of control without cells (Figures 4(a), 4(b), and 4(c)). Expression levels of late osteogenic markers such as ONT and OCN in transplants of DDM/hDPSCs were higher than those in transplants of HA-TCP/hDPSCs (Figures 5(c) and 5(d)). Reversely, expression levels of early osteogenic markers in transplants of HA-TCP/hDPSCs were higher than those in transplants of DDM/hDPSCs (Figures 5(a) and 5(b)), demonstrating that inorganic ions released from HA-TCP could stimulate the adhesion and proliferation of marginal osteoblasts due to osteoconduction ability [47, 48]. Indeed, more osteoids were formed in transplant of HA-TCP/hDPSCs than those in DDM/hDPSCs based on histological analysis (Figure 6(b)), and lacuna structure and immature bone formed in both transplants were similar to each other (Figures 6(b) and 6(d)). Finally, the osteoconduction potential of HA-TCP in in vivo transplantation of this study seemed to be as good as that of DDM, and there was no significant difference in calcium deposition or osteogenesis after 8 weeks of transplantation between the two groups. Interestingly, the expression level of dentin-specific marker DSPP was highly detected in DDM/hDPSCs transplant, but not in HA-TCP/hDPSCs transplant (Figure 7(e)), indicating that DDM might have a better effect on dentin regeneration than HA-TCP. In conclusion, the transplantation with hDPSCs could improve the osteogenic or/and dentinogenic potential of biomaterials. This study also showed that HA-TCP and DDM might have similar

effects on ectopic bone formation in in vivo animal model, although they showed the different efficacy in in vitro cellular differentiation. Additional studies are needed to determine whether hDPSC transplantation combined with osteoconduction and osteoinduction materials, which could be used in dentin regeneration. Human DDM could lead to the development of cost-effective stem cell therapy for bone tissue regeneration in clinical trials with minimal surgical operations. In addition, both biocompatible and inorganic materials might be useful for in situ osteogenic differentiation and transplantation by local delivery of hDPSCs without causing adverse effects.

5. Conclusion

Human dental pulp stem cells have been known to be able to form hard tissues through osteo/dentinogenesis. In current studies, HA-TCP and DDM have been used for regeneration of dentin or bone in tissue engineering. Here, we investigated the effect of osteo/dentinogenic potential of hDPSCs on DDM compared to that on HA-TCP in vitro and in vivo. Osteoinduction effect of DDM was clearly observed in vitro, but osteogenic potential was similar in both cases in in vivo transplantation. Interestingly, dentinogenic potential was detected in a higher efficacy in transplantation of DDM/hDPSCs, suggesting that DDM might be more effective than HA-TCP on dentin regeneration of hDPSCs.

Conflicts of Interest

The authors have no relevant affiliations or financial involvement with any organization or entity with a financial interest in or conflict with the subject matter or materials discussed in the article.

Authors' Contributions

Kyung-Jung Kang and Min Suk Lee contributed equally to this work.

Acknowledgments

This research was supported by the Bio & Medical Technology Development Program of the NRF funded by the Korean government, MSIP (NRF-2015M3A9C6029130) (to Young-Joo Jang) and by the Basic Science Research Program of the NRF funded by the Korean government, the Ministry of Education (2016R1D1A1B03931163) (to Hee Seok Yang).

References

[1] D. Marolt, M. Knezevic, and G. V. Novakovic, "Bone tissue engineering with human stem cells," *Stem Cell Research & Therapy*, vol. 1, no. 2, p. 10, 2010.

[2] M. Riccio, T. Maraldi, A. Pisciotta et al., "Fibroin scaffold repairs critical-size bone defects in vivo supported by human amniotic fluid and dental pulp stem cells," *Tissue Engineering. Part A*, vol. 18, no. 9-10, pp. 1006–1013, 2012.

[3] R.F. Service, "Tissue engineers build new bone," *Science*, vol. 289, no. 5484, pp. 1498–1500, 2000.

[4] Y. Yamada, M. Ueda, T. Naiki, and T. Nagasaka, "Tissue-engineered injectable bone regeneration for osseointegrated dental implants," *Clinical Oral Implants Research*, vol. 15, no. 5, pp. 589–597, 2004.

[5] D. Schwartz-Arad, L. Levin, and L. Sigal, "Surgical success of intraoral autogenous block onlay bone grafting for alveolar ridge augmentation," *Implant Dentistry*, vol. 14, no. 2, pp. 131–138, 2005.

[6] S. Annibali, D. Bellavia, L. Ottolenghi et al., "Micro-CT and PET analysis of bone regeneration induced by biodegradable scaffolds as carriers for dental pulp stem cells in a rat model of calvarial "critical size" defect: preliminary data," *Journal of Biomedical Materials Research. Part B, Applied Biomaterials*, vol. 102, no. 4, pp. 815–825, 2014.

[7] F. P. Barry and J. M. Murphy, "Mesenchymal stem cells: clinical applications and biological characterization," *The International Journal of Biochemistry & Cell Biology*, vol. 36, no. 4, pp. 568–584, 2004.

[8] S. Srouji, T. Kizhner, E. Suss-Tobi, E. Livne, and E. Zussman, "3-D Nanofibrous electrospun multilayered construct is an alternative ECM mimicking scaffold," *Journal of Materials Science. Materials in Medicine*, vol. 19, no. 3, pp. 1249–1255, 2008.

[9] S. Gronthos, M. Mankani, J. Brahim, P. G. Robey, and S. Shi, "Postnatal human dental pulp stem cells (DPSCs) in vitro and in vivo," *Proceedings of the National Academy of Sciences of the United States of America*, vol. 97, no. 25, pp. 13625–13630, 2000.

[10] B. M. Seo, M. Miura, S. Gronthos et al., "Investigation of multipotent postnatal stem cells from human periodontal ligament," *Lancet*, vol. 364, no. 9429, pp. 149–155, 2004.

[11] W. Sonoyama, Y. Liu, T. Yamaza et al., "Characterization of the apical papilla and its residing stem cells from human immature permanent teeth: a pilot study," *Journal of Endodontics*, vol. 34, no. 2, pp. 166–171, 2008.

[12] S. Yao, F. Pan, V. Prpic, and G. E. Wise, "Differentiation of stem cells in the dental follicle," *Journal of Dental Research*, vol. 87, no. 8, pp. 767–771, 2008.

[13] A. Khorsand, M. B. Eslaminejad, M. Arabsolghar et al., "Autologous dental pulp stem cells in regeneration of defect created in canine periodontal tissue," *The Journal of Oral Implantology*, vol. 39, no. 4, pp. 433–443, 2013.

[14] A. Woloszyk, S. H. Dircksen, N. Bostanci, R. Müller, S. Hofmann, and T. A. Mitsiadis, "Influence of the mechanical environment on the engineering of mineralised tissues using human dental pulp stem cells and silk fibroin scaffolds," *PloS One*, vol. 9, no. 10, article e111010, 2014.

[15] J. Jensen, D. C. Kraft, H. Lysdahl et al., "Functionalization of polycaprolactone scaffolds with hyaluronic acid and β-TCP facilitates migration and osteogenic differentiation of human dental pulp stem cells *in vitro*," *Tissue Engineering. Part A*, vol. 21, no. 3-4, pp. 729–739, 2015.

[16] B. Tran Hle and V. N. Doan, "Human dental pulp stem cells cultured onto dentin derived scaffold can regenerate dentin-like tissue in vivo," *Cell and Tissue Banking*, vol. 16, no. 4, pp. 559–568, 2015.

[17] D. L. Alge, D. Zhou, L. L. Adams et al., "Donor-matched comparison of dental pulp stem cells and bone marrow-derived mesenchymal stem cells in a rat model," *Journal of Tissue Engineering and Regenerative Medicine*, vol. 4, no. 1, pp. 73–81, 2010.

[18] A. Graziano, R. d'Aquino, G. Laino, and G. Papaccio, "Dental pulp stem cells: a promising tool for bone regeneration," *Stem Cell Reviews*, vol. 4, no. 1, pp. 21–26, 2008.

[19] T. Yasui, Y. Mabuchi, H. Toriumi et al., "Purified human dental pulp stem cells promote osteogenic regeneration," *Journal of Dental Research*, vol. 95, no. 2, pp. 206–214, 2016.

[20] M. Monti, A. Graziano, S. Rizzo et al., "In vitro and in vivo differentiation of progenitor stem cells obtained after mechanical digestion of human dental pulp," *Journal of Cellular Physiology*, vol. 232, no. 3, pp. 548–555, 2017.

[21] J. K. Choi, H. I. Hwang, and Y. J. Jang, "The efficiency of the in vitro osteo/dentinogenic differentiation of human dental pulp cells, periodontal ligament cells and gingival fibroblasts," *International Journal of Molecular Medicine*, vol. 35, no. 1, pp. 161–168, 2015.

[22] N. Nuti, C. Corallo, B. M. Chan, M. Ferrari, and B. Gerami-Naini, "Multipotent differentiation of human dental pulp stem cells: a literature review," *Stem Cell Reviews*, vol. 12, no. 5, pp. 511–523, 2016.

[23] S. B. Sulaiman, T. K. Keong, C. H. Cheng, A. B. Saim, and R. B. Idrus, "Tricalcium phosphate/hydroxyapatite (TCP-HA) bone scaffold as potential candidate for the formation of tissue engineered bone," *The Indian Journal of Medical Research*, vol. 137, no. 6, pp. 1093–1101, 2013.

[24] T. Okuda, K. Ioku, I. Yonezawa et al., "The effect of the microstructure of β-tricalcium phosphate on the metabolism of subsequently formed bone tissue," *Biomaterials*, vol. 28, no. 16, pp. 2612–2621, 2007.

[25] M. Mastrogiacomo, A. Papadimitropoulos, A. Cedola, F. Peyrin et al., "Engineering of bone using bone marrow stromal cells and a silicon-stabilized tricalcium phosphate bioceramic: evidence for a coupling between bone formation and scaffold resorption," *Biomaterials*, vol. 28, no. 7, pp. 1376–1384, 2007.

[26] L. E. Ling, L. Feng, H. C. Liu et al., "The effect of calcium phosphate composite scaffolds on the osteogenic differentiation of rabbit dental pulp stem cells," *Journal of Biomedical Materials Research. Part A*, vol. 103, no. 5, pp. 1732–1745, 2015.

[27] P. Janicki, P. Kasten, K. Kleinschmidt, R. Luginbuehl, and W. Richter, "Chondrogenic pre-induction of human mesenchymal stem cells on β-TCP: enhanced bone quality by endochondral heterotopic bone formation," *Acta Biomaterialia*, vol. 6, no. 8, pp. 3292–3301, 2010.

[28] Y. F. Feng, L. Wang, X. Li et al., "Influence of architecture of β-tricalcium phosphate scaffolds on biological performance in repairing segmental bone defects," *PLoS One*, vol. 7, no. 11, article e49955, 2012.

[29] P. Kasten, J. Vogel, R. Luginbühl et al., "Ectopic bone formation associated with mesenchymal stem cells in a resorbable calcium deficient hydroxyapatite carrier," *Biomaterials*, vol. 26, no. 29, pp. 5879–5889, 2005.

[30] G. Bang and M. R. Urist, "Bone induction in excavation chambers in matrix of decalcified dentin," *Archives of Surgery*, vol. 94, no. 6, pp. 781–789, 1967.

[31] G. S. Oliveira, M. N. Miziara, E. R. da Silva, E. L. Ferreira, A. P. Biulchi, and J. B. Alves, "Enhanced bone formation during healing process of tooth sockets filled with demineralized human dentine matrix," *Australian Dental Journal*, vol. 58, no. 3, pp. 326–332, 2013.

[32] N. Bakhshalian, S. Hooshmand, N. Bakhshalian et al., "Biocompatibility and microstructural analysis of osteopromotive property of allogenic demineralized dentin matrix," *The International Journal of Oral & Maxillofacial Implants*, vol. 28, no. 6, pp. 1655–1662, 2013.

[33] R. D. Finkelman, S. Mohan, J. C. Jennings, A. K. Taylor, S. Jepsen, and D. J. Baylink, "Quantitation of growth factors IGF-I, SGF/IGF-II, and TGF-β in human dentin," *Journal of Bone and Mineral Research*, vol. 5, no. 7, pp. 717–723, 1990.

[34] N. Cassidy, M. Fahey, S. S. Prime, and A. J. Smith, "Comparative analysis of transforming growth factor-β isoforms 1-3 in human and rabbit dentine matrices," *Archives of Oral Biology*, vol. 42, no. 3, pp. 219–223, 1997.

[35] D. J. Roberts-Clark and A. J. Smith, "Angiogenic growth factors in human dentine matrix," *Archives of Oral Biology*, vol. 45, no. 11, pp. 1013–1016, 2000.

[36] G. Liu, G. Xu, Z. Gao et al., "Demineralized dentin matrix induces odontoblastic differentiation of dental pulp stem cells," *Cells, Tissues, Organs*, vol. 201, no. 1, pp. 65–76, 2016.

[37] N. Kawashima, "Characterisation of dental pulp stem cells: a new horizon for tissue regeneration?" *Archives of Oral Biology*, vol. 57, no. 11, pp. 1439–1458, 2012.

[38] J. M. Seong, B. C. Kim, J. H. Park, I. K. Kwon, A. Mantalaris, and Y. S. Hwang, "Stem cells in bone tissue engineering," *Biomedical Materials*, vol. 5, no. 6, article 062001, 2010.

[39] W. Zhang, X. F. Walboomers, S. Shi, M. Fan, and J. A. Jansen, "Multilineage differentiation potential of stem cells derived from human dental pulp after cryopreservation," *Tissue Engineering*, vol. 12, no. 10, pp. 2813–2823, 2006.

[40] H. Yamazaki, M. Tsuneto, M. Yoshino, K. I. Yamamura, and S. I. Hayashi, "Potential of dental mesenchymal cells in developing teeth," *Stem Cells*, vol. 25, no. 1, pp. 78–87, 2007.

[41] A. Pisciotta, G. Carnevale, S. Meloni et al., "Human dental pulp stem cells (hDPSCs): isolation, enrichment and comparative differentiation of two sub-populations," *BMC Developmental Biology*, vol. 15, p. 14, 2015.

[42] G. Carnevale, A. Pisciotta, M. Riccio et al., "Human dental pulp stem cells expressing STRO-1, c-kit and CD34 markers in peripheral nerve regeneration," *Journal of Tissue Engineering and Regenerative Medicine*, 2017.

[43] S. Goorha and L. T. Reiter, "Culturing and neuronal differentiation of human dental pulp stem cells," *Current Protocols in Human Genetics*, vol. 92, pp. 21–26, 2017.

[44] D. D. Tavares, L. D. Castro, G. D. Soares, G. G. Alves, and J. M. Granjeiro, "Synthesis and cytotoxicity evaluation of granular magnesium substituted β-tricalcium phosphate," *Journal of Applied Oral Science*, vol. 21, no. 1, pp. 37–42, 2013.

[45] T. Wang, S. Yang, L. Wang, and H. Feng, "Use of poly (amidoamine) dendrimer for dentinal tubule occlusion: a preliminary study," *PLoS One*, vol. 10, no. 4, article e0124735, 2015.

[46] S. Ibrahim, S. Sabudin, S. Sahid et al., "Bioactivity studies and adhesion of human osteoblast (hFOB) on silicon-biphasic calcium phosphate material," *Saudi Journal of Biological Sciences*, vol. 23, no. 1, pp. S56–S63, 2016.

[47] J. H. Kim, N. T. Linh, Y. K. Min, and B. T. Lee, "Surface modification of porous polycaprolactone/biphasic calcium phosphate scaffolds for bone regeneration in rat calvaria defect," *Journal of Biomaterials Applications*, vol. 29, no. 4, pp. 624–635, 2014.

[48] C. N. Cornell and J. M. Lane, "Current understanding of osteoconduction in bone regeneration," *Clinical Orthopaedics and Related Research*, Supplement 355, pp. S267–S273, 1998.

Hindawi
Stem Cells International
Volume 2017, Article ID 8920356, 14 pages
https://doi.org/10.1155/2017/8920356

Research Article

Cellular Responses in Human Dental Pulp Stem Cells Treated with Three Endodontic Materials

Alejandro Victoria-Escandell,[1] José Santiago Ibañez-Cabellos,[2,3,4] Sergio Bañuls-Sánchez de Cutanda,[4,5] Ester Berenguer-Pascual,[3] Jesús Beltrán-García,[3] Eva García-López,[3] Federico V. Pallardó,[2,3,4] José Luis García-Giménez,[2,3,4] Antonio Pallarés-Sabater,[1] Ignacio Zarzosa-López,[1] and Manuel Monterde[1]

[1]*Department of Endodontics, Faculty of Medicine and Dentistry, Catholic University of Valencia "San Vicente Mártir", C/Quevedo, 2, 46001 Valencia, Spain*
[2]*Center for Biomedical Network Research on Rare Diseases (CIBERER), CIBER-ISCIII, Valencia, Spain*
[3]*Department of Physiology, Faculty of Medicine and Dentistry, University of Valencia, Av. Blasco Ibañez 15, 46010 Valencia, Spain*
[4]*INCLIVA Health Research Institute, Av. de Menéndez y Pelayo 4, 46010 Valencia, Spain*
[5]*Cell Culture Laboratory, Central Unit of Research in Medicine (UCIM), University of Valencia, Av. Blasco Ibañez 15, 46010 Valencia, Spain*

Correspondence should be addressed to Alejandro Victoria-Escandell; alejandro.victoria@ucv.es

Received 17 January 2017; Revised 22 March 2017; Accepted 12 April 2017; Published 24 May 2017

Academic Editor: Andrea Ballini

Human dental pulp stem cells (HDPSCs) are of special relevance in future regenerative dental therapies. Characterizing cytotoxicity and genotoxicity produced by endodontic materials is required to evaluate the potential for regeneration of injured tissues in future strategies combining regenerative and root canal therapies. This study explores the cytotoxicity and genotoxicity mediated by oxidative stress of three endodontic materials that are widely used on HDPSCs: a mineral trioxide aggregate (MTA-Angelus white), an epoxy resin sealant (AH-Plus cement), and an MTA-based cement sealer (MTA-Fillapex). Cell viability and cell death rate were assessed by flow cytometry. Oxidative stress was measured by OxyBlot. Levels of antioxidant enzymes were evaluated by Western blot. Genotoxicity was studied by quantifying the expression levels of DNA damage sensors such as ATM and RAD53 genes and DNA damage repair sensors such as RAD51 and PARP-1. Results indicate that AH-Plus increased apoptosis, oxidative stress, and genotoxicity markers in HDPSCs. MTA-Fillapex was the most cytotoxic oxidative stress inductor and genotoxic material for HDPSCs at longer times in preincubated cell culture medium, and MTA-Angelus was less cytotoxic and genotoxic than AH-Plus and MTA-Fillapex at all times assayed.

1. Introduction

Progress in dentistry is associated with advancements in dental materials and the design of new regenerative therapies. Both are relevant in the design of restorative biocompatible endodontic materials, which should not affect the cells until the repair of injured tissue has started. Regenerative therapy using human dental pulp stem cells (HDPSCs) is currently acquiring interest because of the potential of these cells to differentiate into odontoblasts and osteoblasts [1–3], both of which have the ability to replace injured bone and dentin pulp tissues with healthy tissue and thus restore functionality of the tooth [4]. HDPSCs can migrate to the pulp lesion sites to replace damaged cells and in turn contribute to the healing process [5]. Therefore, it is recommended that materials used during odontological interventions do not interfere in cellular signaling mediated by HDPSCs.

Biocompatibility is one of the most important requirements for endodontic materials. In vitro studies evaluating biocompatibility by means of cytotoxicity analysis of

endodontic materials have been a previous focus for research. Endodontic materials can produce oxidative stress [6, 7] contributing to genotoxicity. However, there are few studies on how these materials can damage DNA and the DNA damage signaling response mediated by them [8].

Among the materials used for endodontics, root canal sealers (RCSs) are used as root filling material in classical endodontic therapy. However, RCSs can extrude to the periarticular area through the apical foramen or the lateral and accessory canals. In this way, they can establish direct contact with periapical tissues where they can stimulate an inflammatory reaction [9, 10] and delay the healing process [11]. Even if there is no extrusion, these materials can permit the release of soluble substances [12] that can be toxic to the periapical tissues and affect the local bone metabolism and the wound healing process [13].

AH-Plus, an RCS widely used in endodontics, contains epoxy resins and amines [14, 15] which can mediate cytotoxicity and genotoxicity [16]. MTA-Fillapex is an RCS containing MTA and a synthetic disalicylate resin. It was created in an effort to combine a material with excellent biocompatibility and bioactive potential such as MTA with another material with very good physical properties such as synthetic resins. However, recent research has provided contradictory results for this sealer regarding cytotoxicity and genotoxicity [17–20].

Mineral trioxide aggregate MTA-Angelus is a root repair material composed of calcium silicate-based hydraulic cement, which has been described as biocompatible and has been commonly used in the repair of pulp exposures and root perforations, among other applications [21]. Previous studies have demonstrated that MTA-Angelus is not genotoxic over short periods of time [22]. However, it lacks the appropriate physical properties to be used as an RCS since it does not have adequate fluidity and it is difficult to manipulate and transport inside the conduct [23].

We propose the use of HDPSCs to characterize cytotoxicity and genotoxicity mediated by oxidative stress produced by endodontic materials, because of their special capability to regenerate injured tissues and for their relevance in stem cell-based regenerative therapy. Moreover, HDPSCs can be used in regenerative therapy of pulp tissue by cell transplantation into the root canal or pulp chamber, reinforcing the necessity of evaluating the effect of these materials on HDPSCs.

In this study, we examined cytotoxicity, DNA damage responses (DDR), and oxidative stress produced by three endodontic materials (MTA-Angelus, AH-Plus, and MTA-Fillapex) in HDPSCs. Apoptosis and necrosis were evaluated by flow cytometry, the expression of genes participating in DDR by qRT-PCR, and oxidative stress and antioxidant enzyme levels by Western blot.

2. Materials and Methods

2.1. Sample Preparation. Each endodontic sealer (MTA-Angelus, AH-Plus, and MTA-Fillapex) was prepared as indicated in the manufacturer's instructions. The composition of each endodontic material is shown in Supplementary Table S1 available online at https://doi.org/10.1155/2017/8920356 (Supplementary Materials). Test samples consisting of preconditioned cell culture medium were prepared according to ISO 10993-12:2007 [24]. Briefly explained, 100 mg of each freshly mixed RCS (AH-Plus and MTA-Fillapex) and 100 mg of MTA-Angelus powder were immersed in 1 mL of serum-free low-glucose DMEM (Biowest, ref: L0060-500), supplemented with antibiotics and fungicides. These samples were incubated for different time periods comprising 24 h, 48 h, 7 days, 15 days, and 30 days in an incubator at 37°C and under hypoxic conditions of 3% O_2 and 5% CO_2. The obtained extracts were filtered using 0.40 μm filters and stored until their use. The original samples were considered 100% stock medium. Prior to their use in the experiments, preconditioned media were supplemented with 10% fetal bovine serum. For each experiment performed, 1 : 2 dilutions of the stock medium were used. The pH of each preconditioned medium was measured using a pH meter (Consort C1010, Cleaver Scientific Ltd., Warwickshire, UK). Triplicates of each preconditioned medium were prepared independently in order to perform three independent replicates for each assay.

2.2. Cell Culture. HDPSCs were provided by Marya El Alami and Prof. Juan Gambini (Department of Physiology, Medicine and Dentistry School, University of Valencia). HDPSCs were obtained from extracted teeth of healthy subjects after signing an informed consent and getting approval from the ethics committee of the University of Valencia that the study fulfilled the Declaration of Helsinki principles. HDPSCs were characterized by positive mesenchymal pluripotency markers such as STRO1, OCT1, CD133, CD34, and nestin and by a negative signal for CD45, confirming that the cells conserved mesenchymal stem cell properties [25]. HDPSCs were grown in low-glucose DMEM (Biowest, ref: L0060-500), supplemented with 10% fetal bovine serum (HyClone, ref: SV30160.03), 100 μg/mL penicillin, 100 μg/mL streptomycin, and 0.25 μg/mL amphotericin in a cell culture incubator at 37°C and under hypoxia conditions of 3% O_2 and 5% CO_2. To perform cytotoxicity and genotoxicity experiments, HDPSCs were incubated with mediums prepared with endodontic materials described in the sample preparation section. The group defined as the control was exposed only to supplemented DMEM culture medium.

2.3. Cytotoxicity Assay. The cytotoxicity of each endodontic material was assessed using the sulforhodamine B (SRB) assay. The protocol was described previously by Vichai and Kirtikara [26]. Briefly explained, HDPSCs were cultured for 24 h in a 96-well plate. Afterwards, the cells were exposed for 24 additional hours to the 1 : 2 dilution of medium preconditioned with endodontic materials as described in the previous section. Cell viability was calculated based on the measurement of the basic amino acid content using 0.4% SRB in 1% acetic acid with the absorbance measurement at 492 nm, subtracting the background measurement at 620 nm. Each condition was tested by triplicate in three independent samples.

2.4. Flow Cytometry. Apoptosis was determined with the Annexin V kit (Immunostep, Salamanca, Spain) following

the manufacturer's specifications. 10^6 cells were resuspended in 100 μL of diluted 1X Annexin V binding buffer (Annexin V Binding Buffer, 10X, 0.1 M HEPES NaOH (pH 7.4), 1.4 M NaCl, and 25 mM CaCl2) and stained with 5 μL Annexin V-FITC and 5 μL propidium iodide (PI) for 15 minutes at room temperature in the dark. After the incubation period, 400 μL of 1X Annexin V binding buffer was added. For each sample, 4000 stained cells were analyzed by flow cytometry using a FACS-Verse cytometer (Becton Dickinson, San Jose, CA, USA) and Infinicyt software (Cytognos, Santa Marta de Tormes, Salamanca, Spain). Each condition was tested in triplicate.

2.5. Oxidized Protein Analysis by OxyBlot Technique. To determine protein carbonyl groups, we performed the procedure proposed by Shacter et al. [27]. Briefly explained, 10 μg of proteins was denatured and derivatized using 10 mM DNPH in acid solution. The reaction mixture was neutralized and separated by SDS/PAGE and transferred onto a nitrocellulose membrane.

Finally, the membrane reacted to the anti-DNP antibody as described by the manufacturer of the OxyBlot kit (OxyBlot Protein Oxidation Detection kit, Millipore Inc., Billerica, MA. USA). Western blot and OxyBlot experiments were repeated twice.

2.6. Antioxidant Enzyme Expression by Western Blot. MnSOD and catalase protein levels were studied by Western blotting, using 20 μg of total protein extracts obtained after cell lysis, as previously described by us in previous papers [28]. The antibodies used were anti-catalase (Sigma, St. Louis, USA) and anti-MnSOD (Stressgen, Ann Arbor, MI, USA) at a dilution of 1 : 1000 in 1% (*w*/*v*) nonfat dry milk TBS-Tween overnight at 4°C. β-actin (1 : 1000, Santa Cruz BioTech, USA) was used as a loading control and secondary antibody, and anti-rabbit IgG (Calbiochem, San Diego, CA, USA) was conjugated to horseradish peroxidase at a dilution of 1 : 2500 in 1% (*w*/*v*) nonfat dry milk for 1 h at room temperature. The detection procedure was performed using Amersham RPN 2106 ECL Western Blotting Detection Reagent (GE Healthcare Bio-Sciences AB, Uppsala, Sweden). Images were captured using a GE Healthcare LAS-4000 system.

2.7. Gene Expression Analysis Using the qRT-PCR Method. Total RNA was isolated from cells using the PARIS™ (Protein and RNA Isolation System) Kit (Ambion, Austin, TX, USA). For reverse transcription (RT) reactions, 400 ng of the purified RNA was reverse-transcribed using random hexamers with the High-Capacity cDNA Reverse Transcription Kit (P/N 4322171, Applied Biosystems, Foster City, USA).

The mRNA levels were determined by quantitative real-time PCR analysis using an ABI Prism 7900HT Fast Real-Time PCR System (Applied Biosystems, Foster City, CA, USA). The gene-specific primer pairs and probes of TaqMan Gene Expression Assays (Thermo Fisher)were the following: ATM (Hs01112355_g1, Applied Biosystems), RAD53 or CHEK2 (Hs00200485_m1, Applied Biosystems), RAD51 (Hs00947967_m1, Applied Biosystems), PARP-1 (Hs00242302_m1; Applied Biosystems), and GAPDH (Hs02758991_g1, Applied Biosystems), and were used together with the TaqMan Universal PCR Master Mix (P/N 4304437) and reverse-transcribed sample RNA in 20 μL reaction volumes. PCR conditions were 10 min at 95°C for enzyme activation, followed by 40 two-step cycles (15 s at 95°C; 1 min at 60°C). The levels of GAPDH expression were measured in all samples to normalize differences in RNA input, RNA quality, and reverse transcription efficiency. Each sample was analyzed in triplicate, and relative expression was calculated according to the $2^{-\Delta\Delta Ct}$ method [29].

2.8. Statistics. Data from three independent experiments, resulting in nine independent samples, are expressed as the mean ± standard deviation (SD). For experiments with three or more groups, comparisons were made using the one-way analysis of variance (ANOVA) to determine the difference between groups (flow cytometry and gene expression by qRT-PCR). When an interaction effect was found, multiple comparisons using the Student-Newman-Keuls post hoc test were performed. Differences were considered statistically significant for *p*values < 0.05. GraphPad Software v6.0 was used for statistical analysis and graphic representations.

3. Results

3.1. HDPSC Apoptosis Is Increased in Presence of AH-Plus and MTA-Fillapex. Flow cytometry was used to analyze cell viability and cell death in HDPSCs in the presence of 3 different preconditioned mediums and the control group, as described in the Material and Methods section.

The average of apoptotic cells after incubating samples with preconditioned mediums for 24 hours was significantly different between the 4 groups compared (one-way ANOVA, $p = 0.007$) (Figure 1(a)). As shown in Table 1, when multiple comparisons were performed, the most cytotoxic medium at 24 h was AH-Plus, with significantly increased early apoptosis (ea. 19.9 ± 2.1) and late apoptosis (la. 25.5 ± 1.1) observed, compared to the control group (ea. 2.5 ± 1.2; la. 10.0 ± 1.8), MTA-Angelus (ea. 6.5 ± 0.7; la. 12.9 ± 0.3), and MTA-Fillapex (ea. 3.5 ± 0.2; la. 11.6 ± 0.7).

For longer periods of treatment (48 h and 7, 15, and 30 days), cytometry results revealed that MTA-Fillapex became the most cytotoxic preconditioned medium with higher averages of apoptotic cells (Table 1) and with statistically significant differences in comparison to the other conditions assessed (Figures 1(b), 1(c), 1(d), and 1(e)).

For all conditions assayed, MTA-Angelus was the least cytotoxic endodontic material and showed the highest cell viability values at all times studied (Table 1).

Cell viability and apoptosis of HDPSCs could be related to changes in the pH of the cell culture medium produced by the endodontic materials. Therefore, the pH values were measured at different times during sample preparation (Table 2). Our results indicated that the most basic pH was obtained for MTA-Angelus (pH 8.6 ± 0.5) and MTA-Fillapex (pH 8.6 ± 0.4) at 24 h. The pH of AH-Plus remained near its physiological pH at all times analyzed (pH 7.8 ± 0.3). Results suggest that cell death was not directly affected by

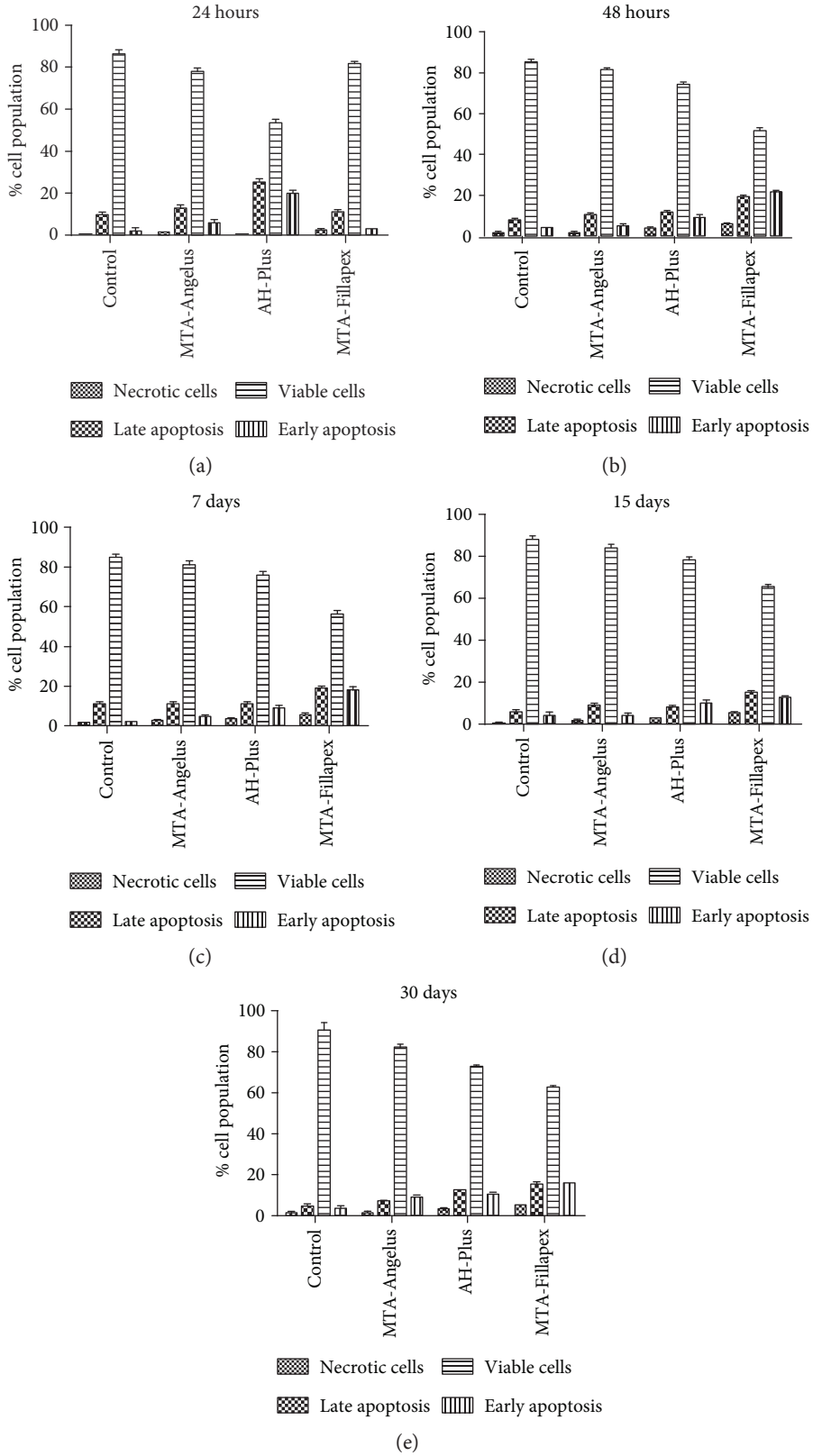

Figure 1: Cytotoxicity induced on HDPSCs assessed using flow cytometry by 1 : 2 dilutions of preconditioned cell culture medium with endodontic materials at 24 hours. Graphs show cell population as viable cells, early apoptotic cells, late apoptotic cells, and necrotic cells at (a) 24 hours, (b) 48 hours, (c) 7 days, (d) 15 days, and (e) 30 days. Each condition was tested by triplicate in three independent samples. The statistical test used was ANOVA with a post hoc Newman-Keuls test to analyze changes in viable, apoptotic, and necrotic cells in each condition. In Table 1, the values of statistical significance for each comparison are shown.

Table 1: Cell viability, apoptosis, and necrosis in HDPSCs at different times of treatment with endodontic materials.

Condition	Group	Viable cells				Early Apoptosis				Necrosis				Late apoptosis			
		Mean	SD		p	Mean	SD		p	Mean	SD		p	Mean	SD		p
Endodontic materials (50%) 24 h	Control	86.8	2.8	—		2.5	1.2	—		0.9	0.1	—		10.0	1.8	—	
	MTA-Angelus	78.5	1.2	C	0.036	6.5	0.7	C	n.s	2.0	0.2	C	0.09	12.9	0.3	C	n.s
				AH-Plus	0.001			AH-Plus	0.002			AH-Plus	0.003			AH-Plus	0.002
				MTA-Fillapex	n.s			MTA-Fillapex	n.s			MTA-Fillapex	n.s			MTA-Fillapex	n.s
	AH-Plus	54.0	0.9	C	<0.0001	19.9	2.1	C	0.001	0.5	0.1	C	n.s	25.5	1.1	C	0.001
				MTA-Angelus	0.001			MTA-Angelus	0.002			MTA-Angelus	0.003			MTA-Angelus	0.002
				MTA-Fillapex	<0.0001			MTA-Fillapex	0.001			MTA-Fillapex	0.001			MTA-Fillapex	0.001
	MTA-Fillapex	82.2	1.1	C	n.s	3.5	0.2	C	n.s	2.7	0.2	C	0.002	11.6	0.7	C	n.s
				MTA-Angelus	n.s			MTA-Angelus	n.s			MTA-Angelus	n.s			MTA-Angelus	n.s
				AH-Plus	<0.0001			AH-Plus	0.001			AH-Plus	0.001			AH-Plus	0.001
Endodontic materials (50%) 48 h	Control	85.9	0.7	—		4.4	0.2	—		1.5	0.9	—		8.1	1.4	—	
	MTA-Angelus	81.8	0.8	C	n.s	5.5	0.6	C	n.s	1.7	0.6	C	n.s	10.9	0.8	C	n.s
				AH-Plus	0.016			AH-Plus	0.012			AH-Plus	n.s			AH-Plus	n.s
				MTA-Fillapex	<0.0001			MTA-Fillapex	<0.0001			MTA-Fillapex	0.018			MTA-Fillapex	0.006
	AH-Plus	74.5	1.6	C	0.03	9.6	1.0	C	0.005	3.9	0.6	C	n.s	11.9	1.2	C	n.s
				MTA-Angelus	0.016			MTA-Angelus	0.012			MTA-Angelus	n.s			MTA-Angelus	n.s
				MTA-Fillapex	<0.0001			MTA-Fillapex	<0.0001			MTA-Fillapex	n.s			MTA-Fillapex	0.01
	MTA-Fillapex	51.9	1.4	C	<0.0001	22.6	0.1	C	<0.0001	6.2	0.8	C	0.015	19.6	0.7	C	0.002
				MTA-Angelus	<0.0001			MTA-Angelus	<0.0001			MTA-Angelus	0.018			MTA-Angelus	0.006
				AH-Plus	<0.0001			AH-Plus	<0.0001			AH-Plus	n.s			AH-Plus	0.01
Endodontic materials (50%) 7 d	Control	85.4	1.5	—		1.8	0.3	—		1.6	0.3	—		11.1	1.4	—	
	MTA-Angelus	81.4	3.1	C	n.s	4.7	1.1	C	n.s	2.7	0.7	C	n.s	11.2	1.2	C	n.s
				AH-Plus	n.s			AH-Plus	n.s			AH-Plus	n.s			AH-Plus	n.s
				MTA-Fillapex	0.005			MTA-Fillapex	0.017			MTA-Fillapex	0.016			MTA-Fillapex	0.012
	AH-Plus	76.1	2.9	C	n.s	8.9	2.6	C	n.s	3.5	0.6	C	n.s	11.3	0.9	C	n.s
				MTA-Angelus	n.s			MTA-Angelus	n.s			MTA-Angelus	n.s			MTA-Angelus	n.s
				MTA-Fillapex	0.013			MTA-Fillapex	n.s			MTA-Fillapex	0.041			MTA-Fillapex	0.013
	MTA-Fillapex	56.5	3.9	C	0.003	17.9	3.3	C	0.009	6.3	0.6	C	0.006	19.2	1.2	C	0.011
				MTA-Angelus	0.005			MTA-Angelus	0.017			MTA-Angelus	0.016			MTA-Angelus	0.012
				AH-Plus	0.013			AH-Plus	n.s			AH-Plus	0.041			AH-Plus	0.013
Endodontic materials (50%) 15 d	Control	88.0	3.8	—		4.6	2.3	—		1.2	0.1	—		6.1	1.4	—	
	MTA-Angelus	84.1	2.8	C	n.s	4.7	0.8	C	n.s	1.9	0.8	C	n.s	9.2	1.2	C	n.s
				AH-Plus	n.s			AH-Plus	n.s			AH-Plus	n.s			AH-Plus	n.s
				MTA-Fillapex	0.009			MTA-Fillapex	0.019			MTA-Fillapex	0.015			MTA-Fillapex	0.027

Table 1: Continued.

Condition	Group	Viable cells				Early Apoptosis				Necrosis				Late apoptosis			
		Mean	SD		*p*	Mean	SD		*p*	Mean	SD		*p*	Mean	SD		*p*
				C	n.s			C	n.s			C	n.s			C	n.s
	AH-Plus	78.5	1.3	MTA-Angelus	n.s	10.6	1.5	MTA-Angelus	n.s	2.9	0.5	MTA-Angelus	n.s	8.3	1.3	MTA-Angelus	n.s
				MTA-Fillapex	0.033			MTA-Fillapex	n.s			MTA-Fillapex	0.044			MTA-Fillapex	0.018
				C	0.005			C	0.018			C	0.008			C	0.007
	MTA-Fillapex	65.4	1.6	MTA-Angelus	0.009	13.3	0.1	MTA-Angelus	0.019	5.7	0.8	MTA-Angelus	0.015	15.6	0.7	MTA-Angelus	0.027
				AH-Plus	0.033			AH-Plus	n.s			AH-Plus	0.044			AH-Plus	0.018
	Control	88.8	7.8	—		3.4	2.7	—		1.5	0.7	—		4.7	2.3	—	
				C	n.s			C	n.s			C	n.s			C	n.s
	MTA-Angelus	82.4	1.9	AH-Plus	n.s	8.9	1.6	AH-Plus	n.s	1.8	0.5	AH-Plus	n.s	693	1.0	AH-Plus	n.s
				MTA-Fillapex	0.04			MTA-Fillapex	n.s			MTA-Fillapex	0.009			MTA-Fillapex	0.015
Endodontic materials (50%) 30 d				C	0.07			C	0.049			C	0.042			C	0.02
	AH-Plus	72.9	0.8	MTA-Angelus	n.s	10.6	1.1	MTA-Angelus	n.s	3.8	0.4	MTA-Angelus	n.s	12.7	0.1	MTA-Angelus	n.s
				MTA-Fillapex	n.s			MTA-Fillapex	n.s			MTA-Fillapex	n.s			MTA-Fillapex	n.s
				C	0.015			C	0.007			C	0.007			C	0.007
	MTA-Fillapex	63.1	1.1	MTA-Angelus	0.04	15.9	0.2	MTA-Angelus	n.s	5.4	0.3	MTA-Angelus	0.009	15.6	1.2	MTA-Angelus	0.015
				AH-Plus	n.s			AH-Plus	n.s			AH-Plus	n.s			AH-Plus	n.s

Table 2: Mean and standard deviations of the pH value for preconditioned medium at the different time periods.

	After DMEM preparation	24 h	48 h	72 h	7 days	15 days	28 days
Control	7.4 ± 0.2	7.4 ± 0.3	7.4 ± 0.2	7.5 ± 0.3	7.6 ± 0.4	7.4 ± 0.3	7.5 ± 0.1
MTA-Angelus	8.7 ± 0.5	8.6 ± 0.5	8.1 ± 0.3	8.0 ± 0.4	7.8 ± 0.2	8.0 ± 0.4	7.9 ± 0.4
AH-Plus	7.6 ± 0.4	7.8 ± 0.3	7.8 ± 0.4	7.6 ± 0.2	7.4 ± 0.3	7.6 ± 0.3	7.5 ± 0.3
MTA-Fillapex	8.8 ± 0.5	8.8 ± 0.4	8.3 ± 0.5	8.0 ± 0.3	8.0 ± 0.2	8.1 ± 0.3	8.1 ± 0.4

the pH of preconditioned DMEM because AH-Plus had the most similar physiological pH and the highest apoptosis at 24 h. Furthermore, pH values for MTA-Angelus and MTA-Fillapex were similar at all times analyzed; however, apoptosis was higher for MTA-Fillapex than for MTA-Angelus, suggesting that pH was not involved in cell cytotoxicity.

3.2. Endodontic Materials Induce Oxidative Stress in HDPSCs. Oxidative stress induced by endodontic materials in HDPSCs was analyzed using the OxyBlot technique. We chose those experimental conditions in which increased apoptosis was observed at 24 h for AH-Plus and MTA-Fillapex. When HDPSCs were incubated in preconditioned medium with endodontic materials AH-Plus and MTA-Fillapex for 24 h, oxidized protein levels increased compared to those in control conditions. Furthermore, a low signal was observed for oxidized proteins for MTA-Angelus, suggesting that this material did not produce oxidative stress at 24 h (Figure 2(a)).

Due to the observed increase in apoptosis in HDPSCs when cells were incubated with MTA-Angelus for 7 days, we also decided to explore oxidative stress in these conditions. We found that MTA-Angelus produced oxidative stress at the same level as AH-Plus and MTA-Fillapex, which may explain the increase in apoptosis observed in these conditions (Figure 2(b)). Furthermore, the concentration of MTA-Angelus in the cell culture media was increased to evaluate the effect of higher concentrations of this endodontic material by observing how oxidized protein levels increased.

All these results suggest that MTA-Angelus was the endodontic material that induced less oxidative stress in HDPSCs.

3.3. Endodontic Materials Alter the Expression of Antioxidant Enzymes. Afterwards, we wondered if the oxidative stress induced by endodontic materials in HDPSCs was produced as a consequence of inhibition of key antioxidant enzymes. Using Western blot, we proceeded to evaluate the protein levels of MnSOD and catalase as antioxidant enzymes involved in the detoxification of superoxide radicals and peroxides, respectively (Figure 2(c)). When HDPSCs were incubated in preconditioned medium with the endodontic materials AH-Plus and MTA-Fillapex for 24 h, both catalase and MnSOD were downregulated compared to those in control conditions and MTA-Angelus. Furthermore, we did not observe changes in MnSOD and catalase expression between MTA-Angelus 50% and MTA-Angelus 100%, therefore indicating that this endodontic material did not alter the expression of antioxidant enzymes (Figure 2(c)).

All these results suggest that HDPSCs were underprotected against oxidative stress in the presence of AH-Plus and MTA-Fillapex, while MTA-Angelus did not affect the antioxidant shield in HDPSCs.

3.4. Endodontic Materials Affect DNA Damage Responses in HDPSCs. Since the major effects of cytotoxicity analyzed by flow cytometry were found in cell culture medium preincubated for 24 h for AH-Plus and it was also observed that MTA-Fillapex at 48 h of incubation also produced apoptosis, we decided to study the DNA damage responses only at these times.

Among the different types of damage produced in DNA, double-strand breaks (DSBs) and single-strand breaks (SSBs) have mutagenic potential because they can seriously affect the integrity of DNA [30]. DSBs are detected by complex signal transduction mechanisms in which different enzymatic machineries participate, one of the most important being ATM kinase (Ataxia-telangiectasia-mutated protein kinase) [31]. Another component of DNA damage response is the activation of serine/threonine kinase effectors, Rad53 (*Saccharomyces cerevisiae*) being one of the most relevant enzymes or Chk2 (which is its counterpart in humans) [32]. SSBs are detected by PARP-1 [33] which signals the process for repair [34]. In DSB repair, protein Rad51, also known as FANCR, is involved in the guidance of the DNA strands during homologous recombination (HR) [35].

At 24 h, the results show that protein kinase RAD53 (1.7 ± 0.3) (Figure 3(a)) and the ATM kinase (2.0 ± 0.2) (Figure 3(b)) were overexpressed when HDPSCs were incubated with AH-Plus medium compared to the control group. Increased expression of the ATM gene was also observed for the other biomaterials (MTA-Angelus 1.4 ± 0.1 and MTA-Fillapex 1.3 ± 0.3) compared to the control group (1.0 ± 0.1) although the main effect was further increased when the medium preincubated with AH-Plus was used (2.0 ± 0.2). In addition, when the genes participating in DNA repair were analyzed, increased expression of RAD51 was observed when HDPSCs were incubated with AH-Plus (1.9 ± 0.1) and MTA-Fillapex (1.3 ± 0.3) compared to control (1.0 ± 0.1) and MTA-Angelus (1.3 ± 0.4) (Figure 3(c)) and increased expression for PARP-1 was seen when HDPSCs were incubated with AH-Plus (1.8 ± 0.1) compared to other conditions in which relative expression of PARP-1 was similar to the control group (1.0 ± 0.1) (Figure 3(d)) at 24 h. The results suggest that AH-Plus induced both DSBs and SSBs, while MTA-Fillapex only produced the activation of DSB repair.

However, at 48 h, when cells were incubated with the medium preconditioned with endodontic materials, increased expression of these genes was observed for cells incubated with MTA-Fillapex (and to a lesser extent for AH-Plus and MTA-Angelus (Figure 4)).

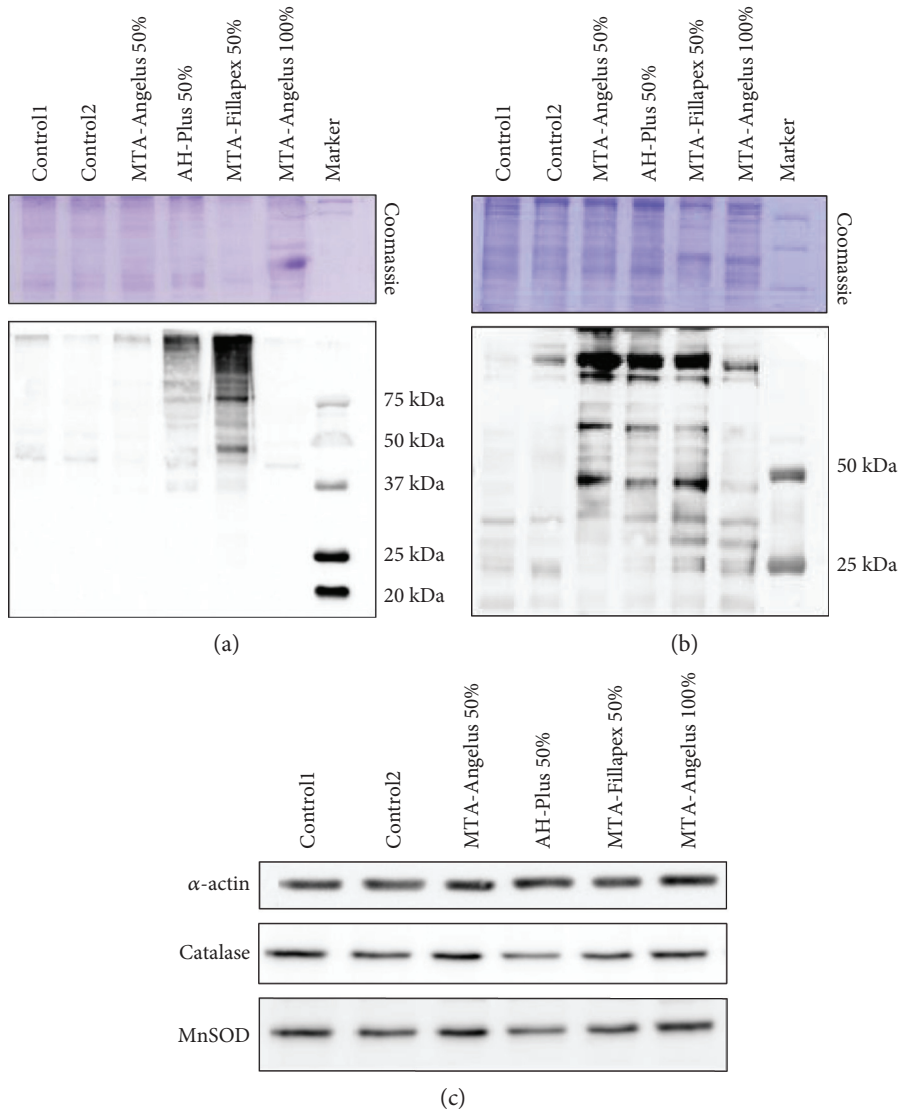

Figure 2: Oxidative stress and antioxidant responses in HDPSCs incubated with endodontic materials. Immunoblots are representative images of two independent analyses in HDPSCs incubated with MTA-Angelus, AH-Plus, and MTA-Fillapex. (a) OxyBlot analysis for the detection of carbonylated proteins from total extracts of HDPSCs incubated with endodontic materials for 24 h. (b) OxyBlot analysis for the detection of carbonylated proteins from total extracts of HDPSCs incubated with endodontic materials for 7 days. (c) Western blot analysis of two antioxidant enzymes, catalase and MnSOD, from total extracts of HDPSCs incubated with endodontic materials for 24 h. For OxyBlots, Coomassie gel staining was used as a loading control. In immunoassays for detecting the levels of antioxidant enzymes, β-actin was used as a reference and loading control.

These results indicate that endodontic materials activate DNA repair mechanisms for both DSBs and SSBs. However, the highest activation of DNA damage sensors Rad53 (2.1 ± 0.7) and ATM (1.9 ± 0.5) was found for MTA-Fillapex when results were compared to those of control and other conditions. In line with these results, the highest effector signaling for DNA repair (mediated by Rad51 and PARP-1) was also found for MTA-Fillapex (Rad51 3.5 ± 0.5; PARP-1 1.7 ± 0.3). Relative expression found for these genes in other groups was lower than that found for MTA-Fillapex, control (Rad51 (1.0 ± 0.2), PARP-1 (1.0 ± 0.2)), MTA-Angelus (Rad51 (1.2 ± 0.0), PARP-1 (1.4 ± 0.0)), and AH-Plus (Rad51 (1.5 ± 0.0), PARP-1 (1.4 ± 0.1)). All in all, the results suggest that MTA-Fillapex was the most genotoxic material for HDPSCs.

4. Discussion

In our study, we used mesenchymal stem cells from dental pulp (HDPSCs), which have the advantage over other cell lines of being able to differentiate into odontoblasts [1] and osteoblasts [2]. HDPSC is a cell model with physiological properties which are homologous to the primary tissue where the endodontic materials are in contact. Furthermore, HDPSCs have other advantages such as a large capacity for proliferation, the ability to maintain their cellular phenotype for a long time period, and

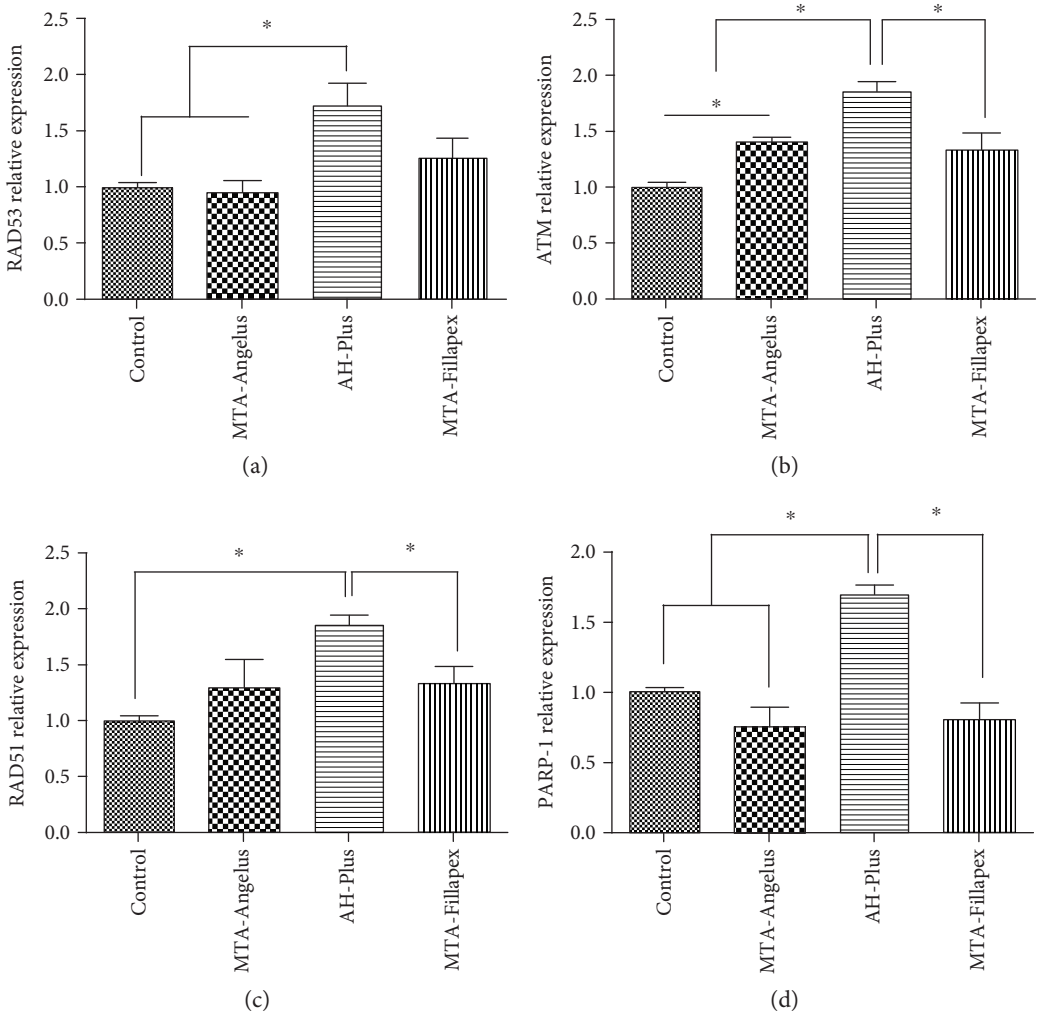

Figure 3: Analysis of expression of DNA damage responses and repair genes in HDPSCs incubated with endodontic materials at 24 hours, by the technique of real-time polymerase chain reaction (qRT-PCR) for (a) RAD53, (b) ATM, (c) RAD51, and (d) PARP-1. The statistical test used was ANOVA with a post hoc Newman-Keuls test to analyze changes in the relative expression of DNA damage response and DNA repair genes. $*$ indicates significant differences between groups compared ($p < 0.05$). Each sample was analyzed in triplicate.

the sensitivity of response to toxins [36, 37]. Additionally, HDPSCs are promising cell lines that can be used in regenerative medicine to repair damaged tissue, and they have potential applicability in dental tissue engineering and regenerative therapy of dental tissues [38]. For these above-mentioned reasons, HDPSCs can be considered a relevant cellular model to evaluate the effect of endodontic materials.

The results obtained by flow cytometry indicated that MTA-Angelus was the least cytotoxic material over time, compared to AH-Plus and MTA-Fillapex. Our results are similar to those obtained by Zhou et al. [39]. These authors studied the effect of MTA in human gingival fibroblasts using flow cytometry and observed that MTA in a diluted medium did not increase apoptosis or necrosis. In contrast, Petrovic et al. [40] found that MTA-Angelus was cytotoxic using 50% diluted medium in an MRC5 cell line consisting of human lung fibroblasts. In our experiments, we observed maximal apoptosis for mediums prepared with AH-Plus at 24 h and MTA-Fillapex at 48 h. Regarding AH-Plus, some studies have shown that this endodontic material increased cytotoxicity at 24 h [41, 42], probably due to the presence of amines in its composition [43]. MTA-Fillapex was the most cytotoxic endodontic material, in agreement with Zhou et al. [44] who observed that MTA-Fillapex was cytotoxic for human gingival fibroblasts using 50% diluted medium preincubated with this material for periods of 1 to 4 weeks.

Oxidative stress can mediate cytotoxicity and genotoxicity, and distinct endodontic materials have demonstrated their ability to generate oxidative stress [6, 45]. Therefore, we were interested in evaluating the oxidative damage and antioxidant defenses in order to assess the oxidative stress in our samples.

The results of our study indicated that MTA-Angelus did not induce oxidative stress in HDPSCs after 24 h of incubation. However, AH-Plus and MTA-Fillapex under these conditions increased oxidative stress in HDPSCs. Coinciding with our results, a study by Camargo et al. [46] evaluated the production of reactive oxygen species (ROS) by white and

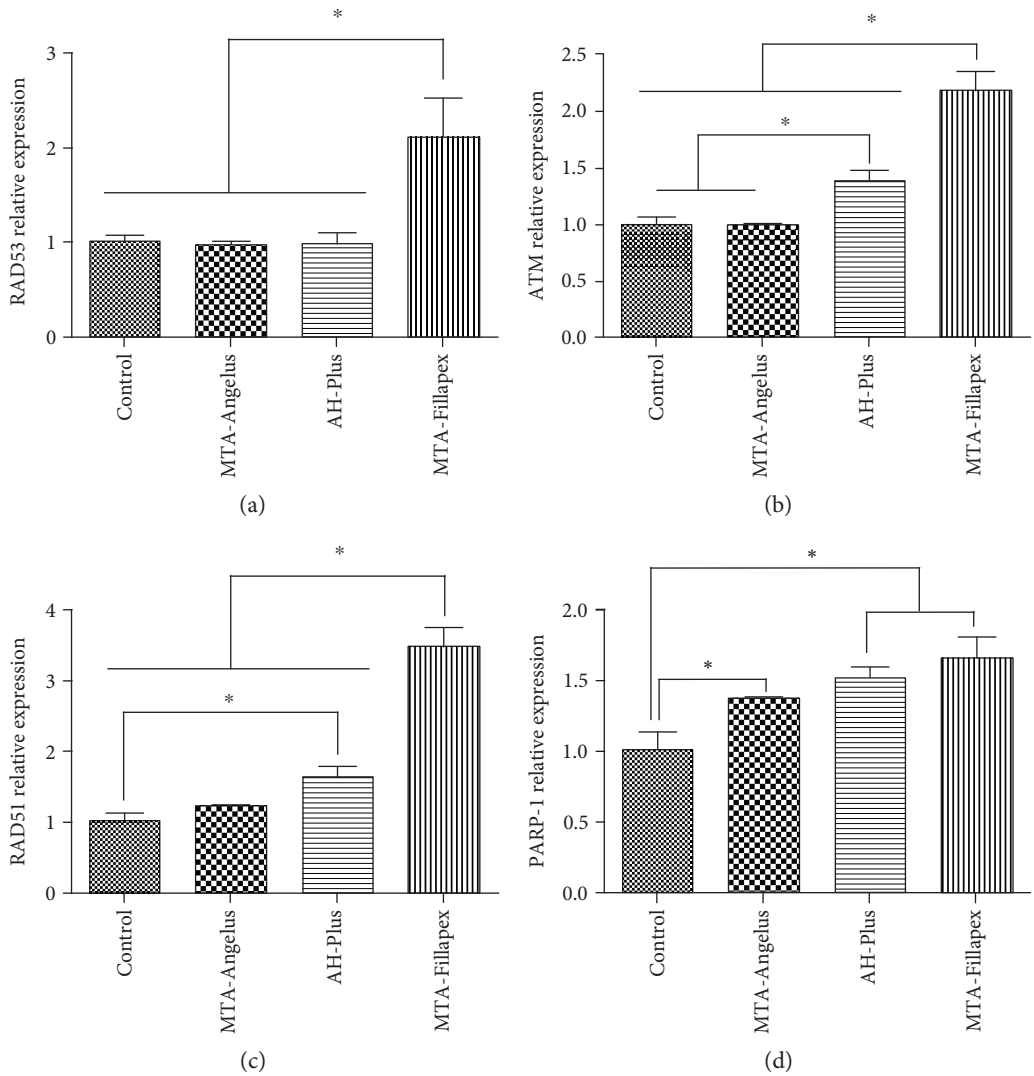

Figure 4: Analysis of expression of DNA damage responses and repair genes in HDPSCs incubated with endodontic materials at 48 hours, by the technique of real-time polymerase chain reaction (qRT-PCR) for (a) RAD53, (b) ATM, (c) RAD51, and (d) PARP-1. The statistical test used was ANOVA with a post hoc Newman-Keuls test to analyze changes in the relative expression of DNA damage response and DNA repair genes. $*$ indicates significant differences between groups compared ($p < 0.05$). Each sample was analyzed in triplicate.

grey MTA on transfected HDPSCs. The results of ROS production by the cells exposed to the 1 : 1 extracts for 1 hour showed that both white and gray MTA did not cause an increase in ROS production. However, a study by Chang et al. [47] on the ability of MTA-Angelus and other endodontic calcium silicate-based materials to induce the formation of ROS and activate the endogenous antioxidant defenses demonstrated that MTA-Angelus induced production of ROS after 3 days of incubation in an immortalized cell line of human dental pulp. AH-Plus contains bisphenol A diglycidyl ether (BADGE), and some controversial results can be found in the literature suggesting that BADGE can release small amounts of bisphenol A (BPA) [48–51]. However, although no released BPA was the origin of cytotoxicity, it can be considered that BADGE can mediate cytotoxic effects on different cellular models, such as lymphocytes [52] and Caco-2 cells [53].

A study by Kim et al. [54] obtained similar results to those obtained by us, when studying the cytotoxicity of AH-Plus and its ability to produce ROS in an MC-3T3 E1 mouse osteoblast cell line, which was cultured in a medium supplemented with AH-Plus at 30% concentration for 24 hours.

In addition, Camargo et al. [55] analyzed the cytotoxic effect generated by AH-Plus at 50% concentration and mediated by ROS on a fibroblast cell line from human dental pulp.

The mechanisms by which 50% MTA-Fillapex produces oxidative stress and genotoxicity may be mediated by the presence of titanium dioxide (TiO2) in its composition, which has been shown to produce ROS that leads to oxidative damage in DNA [56]. An in vivo study by Zmener et al. [57] evaluated the inflammatory response induced by MTA-Fillapex after subcutaneous implantation of this biomaterial in Wistar rats. The results showed a severe reaction after 10

days that was maintained at 30 days and 90 days. These authors speculate that cytotoxicity may be due to the leaching of toxic elements due to the high solubility of MTA-Fillapex.

Our results showed that in HDPSCs treated with AH-Plus and MTA-Fillapex for 24 h, both catalase and MnSOD were downregulated compared to those in control conditions and MTA-Angelus. Villeneuve et al. have described the fine balance between cell viability and death by controlling ROS levels via Nrf2 and p21 [58]. The authors propose that in mild oxidative stress conditions (such as may occur for MTA-Angelus in our study), cells can respond activating Nrf2 expression and downstream gene targets (such as antioxidant enzymes catalase and MnSOD). However, at high levels of oxidative stress (such as may occur for AH Plus and MTA Fillapex) (Figure 2(c)), one may speculate that the Nrf2 antioxidant response pathway must be suppressed to induce apoptosis, because apoptosis requires the accumulation of ROS (Figures 2(a) and 2(b)). Other plausible explanation is that the Nrf2 system is activated in any case but oxidative stress exceeds the capacities of enzymatic antioxidants, when cells are treated with AH-Plus and MTA-Fillapex.

Therefore, since these materials can produce oxidative stress, it is crucial to evaluate the mechanisms of genotoxicity. In this regard, we studied the expression of different genes mediating cellular response and DNA repair after DNA damage induction. We analyzed sensors and effectors of DNA damage response such as ATM, RAD53, RAD51, and PARP-1.

The cellular medium prepared with AH-Plus for 24 h was the most genotoxic for HDPSCs and produced the overexpression of ATM and RAD53 (Figure 3). AH-Plus also induced the overexpression of RAD51 and PARP-1 in the same conditions. Our results are in agreement with the results we obtained by flow cytometry, confirming a genotoxic effect for AH-Plus. The results for this endodontic material are probably related to the release of formaldehyde during polymerization [59], which is extremely reactive and can cause crosslinks between biomolecules [60]. Our results agree with those obtained by Candeiro et al. in a model of human gingival fibroblasts [61] and also with results obtained by Camargo et al. [16] for this endodontic material. Interestingly, Van Landuyt et al. [62] studied the genotoxicity and cytotoxicity effect mediated by AH-Plus in a model of gingival fibroblasts, in which they did not observe increased levels of gamma-H2AX (a marker for DNA double-strand breaks). However, they found increased cytotoxicity for 1 : 3 and 1 : 10 dilutions of medium preconditioned with AH-Plus. In our study, AH-Plus was able to induce DNA damage and DNA repair activation for both DSBs and SSBs, which were detected by the overexpression of RAD51 and PARP-1, respectively.

When we used medium preincubated with endodontic materials for 48 h, our results demonstrated that MTA-Fillapex further increased the expression of the DNA damage signaling pathways mediated by the ATM and RAD53 sensors and the PARP-1 and RAD51 effectors for DNA repair genes, suggesting that MTA-Fillapex can produce SSBs and DSBs. The results also coincide with the results obtained by flow cytometry and indicate the cytotoxic and genotoxic potential of MTA-Fillapex. The genotoxicity of MTA-Fillapex could be related to the content of TiO2, which has been previously demonstrated to induce the formation of micronuclei [56] and the presence of salicylates in its composition, which were shown to induce DNA damage and apoptosis in vitro in fibrosarcoma cell lines [63]. Bin et al. [64] demonstrated genotoxicity and cytotoxicity for MTA-Fillapex in vitro using V79 fibroblasts and lower concentrations of MTA-Fillapex than those used in our study.

Our results point out the relevance of using an appropriate cell line to study the cytotoxicity, genotoxicity, and biocompatibility of endodontic materials. Particularly, MTA has a wide range of possibilities in endodontic treatments [65] because of its clinical use involving the direct contact of this biomaterial with periradicular and pulpal tissues, contributing not only to cytotoxicity, genotoxicity, and proliferation but also to the differentiation of odontoblasts and osteoblasts [66, 67].

5. Conclusions

AH-Plus and MTA-Fillapex were the most cytotoxic and genotoxic materials for HDPSCs in this study. Genotoxicity is mediated by an increase in oxidative stress and downregulation of the antioxidant defense shield. On the other hand, MTA-Angelus was the least cytotoxic and genotoxic material at all assayed times in which antioxidant enzyme expression levels were not altered. This is of special relevance in characterizing the biocompatibility and the cytotoxic and genotoxic effects of the biomaterials on a relevant source of cells for regenerative therapy.

Conflicts of Interest

The authors declare that there is no conflict of interests regarding the publication of this paper.

Authors' Contributions

Alejandro Victoria-Escandell and José Santiago Ibañez-Cabellos contributed equally to this work.

Acknowledgments

José Luis García-Giménez and Federico V. Pallardó are supported by the Ministry of Economy and Competitiveness and the Institute of Health Carlos III through CIBERER (the Center for Biomedical Network Research on Rare Diseases and the Ingenio 2010 Initiative cofinanced by FEDER funds from the European Union), as well as by grants from the University of Valencia (1090569000) and the Spanish National Plan for Scientific and Technical Research and Innovation (AIB2010-SE-00333). José Santiago Ibañez-Cabellos is an "Atracció de Talent" fellow (University of Valencia).

References

[1] S. Gronthos, M. Mankani, J. Brahim, P. G. Robey, and S. Shi, "Postnatal human dental pulp stem cells (DPSCs) in vitro and in vivo," *Proceedings of the National Academy of Sciences*

of the United States of America, vol. 97, no. 25, pp. 13625–13630, 2000.

[2] F. Carinci, G. Papaccio, G. Laino et al., "Comparison between genetic portraits of osteoblasts derived from primary cultures and osteoblasts obtained from human pulpar stem cells," *The Journal of Craniofacial Surgery*, vol. 19, no. 3, pp. 616–627, 2008.

[3] E. Piva, S. A. Tarlé, J. E. Nör et al., "Dental pulp tissue regeneration using dental pulp stem cells isolated and expanded in human serum," *Journal of Endodontia*, vol. 43, no. 4, pp. 568–574, 2017.

[4] M. Nakashima and A. Akamine, "The application of tissue engineering to regeneration of pulp and dentin in endodontics," *Journal of Endodontics*, vol. 31, no. 10, pp. 711–718, 2005.

[5] M. Fitzgerald, D. J. Chiego Jr., and D. R. Heys, "Autoradiographic analysis of odontoblast replacement following pulp exposure in primate teeth," *Archives of Oral Biology*, vol. 35, no. 9, pp. 707–715, 1990.

[6] C. W. Pires, G. Botton, F. C. Cadoná et al., "Induction of cytotoxicity, oxidative stress and genotoxicity by root filling pastes used in primary teeth," *International Endodontic Journal*, vol. 49, no. 8, pp. 737–745, 2016.

[7] A. A. Eid, J. L. Gosier, C. M. Primus et al., "In vitro biocompatibility and oxidative stress profiles of different hydraulic calcium silicate cements," *Journal of Endodontia*, vol. 40, no. 2, pp. 255–260, 2014.

[8] J. S. Bertram, "The molecular biology of cancer," *Molecular Aspects of Medicine*, vol. 21, no. 6, pp. 167–223, 2000.

[9] R. K. Scarparo, F. S. Grecca, and E. V. F. Fachin, "Analysis of tissue reactions to methacrylate resin-based, epoxy resin-based, and zinc oxide–eugenol endodontic sealers," *Journal of Endodontics*, vol. 35, no. 2, pp. 229–232, 2009.

[10] O. Zmener, G. Banegas, and C. H. Pameijer, "Bone tissue response to a methacrylate-based endodontic sealer: a histological and histometric study," *Journal of Endodontics*, vol. 31, no. 6, pp. 457–459, 2005.

[11] D. Ricucci, I. N. Rôças, F. R. Alves, S. Loghin, and J. F. Siqueira Jr, "Apically extruded sealers: fate and influence on treatment outcome," *Journal of Endodontia*, vol. 42, no. 2, pp. 243–249, 2016.

[12] E. Schäfer and T. Zandbiglari, "Solubility of root-canal sealers in water and artificial saliva," *International Endodontic Journal*, vol. 36, no. 10, pp. 660–669, 2003.

[13] C. Rodrigues, J. Costa-Rodrigues, J. A. Capelas, and M. H. Fernandes, "Behaviour of co-cultured human osteoclastic and osteoblastic cells exposed to endodontic sealers' extracts," *Clinical Oral Investigations*, vol. 18, no. 2, pp. 479–488, 2014.

[14] J. Santos, L. Tjäderhane, C. Ferraz et al., "Long-term sealing ability of resin-based root canal fillings," *International Endodontic Journal*, vol. 43, no. 6, pp. 455–460, 2010.

[15] L. Vasiliadis, K. Kodonas, N. Economides, C. Gogos, and C. Stavrianos, "Short-and long-term sealing ability of Guttaflow and AH-Plus using an ex vivo fluid transport model," *International Endodontic Journal*, vol. 43, no. 5, pp. 377–381, 2010.

[16] C. H. R. Camargo, T. R. Oliveira, G. O. Silva, S. B. Rabelo, M. C. Valera, and B. N. Cavalcanti, "Setting time affects in vitro biological properties of root canal sealers," *Journal of Endodontics*, vol. 40, no. 4, pp. 530–533, 2014.

[17] M. Z. Scelza, A. B. Linhares, L. E. da Silva, J. M. Granjeiro, and G. G. Alves, "A multiparametric assay to compare the cytotoxicity of endodontic sealers with primary human osteoblasts," *International Endodontic Journal*, vol. 45, no. 1, pp. 12–18, 2012.

[18] C. V. Bin, M. C. Valera, S. E. Camargo et al., "Cytotoxicity and genotoxicity of root canal sealers based on mineral trioxide aggregate," *Journal of Endodontia*, vol. 38, no. 4, pp. 495–500, 2012.

[19] S. W. Chang, S. Y. Lee, S. K. Kang, K. Y. Kum, and E. C. Kim, "In vitro biocompatibility, inflammatory response, and osteogenic potential of 4 root canal sealers: Sealapex, Sankin apatite root sealer, MTA Fillapex, and iRoot SP root canal sealer," *Journal of Endodontics*, vol. 40, no. 10, pp. 1642–1648, 2014.

[20] E. Assmann, D. E. Böttcher, C. B. Hoppe, F. S. Grecca, and P. M. Kopper, "Evaluation of bone tissue response to a sealer containing mineral trioxide aggregate," *Journal of Endodontics*, vol. 41, no. 1, pp. 62–66, 2015.

[21] M. Parirokh and M. Torabinejad, "Mineral trioxide aggregate: a comprehensive literature review–part III: clinical applications, drawbacks, and mechanism of action," *Journal of Endodontia*, vol. 36, no. 3, pp. 400–413, 2010.

[22] E. Zeferino, C. E. Bueno, L. M. Oyama, and D. A. Ribeiro, "Ex vivo assessment of genotoxicity and cytotoxicity in murine fibroblasts exposed to white MTA or white Portland cement with 15% bismuth oxide," *International Endodontic Journal*, vol. 43, no. 10, pp. 843–848, 2010.

[23] G. Bogen and S. Kuttler, "Mineral trioxide aggregate obturation: a review and case series," *Journal of Endodontia*, vol. 35, no. 6, pp. 777–790, 2009.

[24] International Organization for Standardization ISO 10993, "Biological evaluation of medical devices," *Part 12: Sample preparation and reference materials*.

[25] M. El Alami, J. Viña-Almunia, J. Gambini et al., "Activation of p38, p21, and NRF-2 mediates decreased proliferation of human dental pulp stem cells cultured under 21% O2," *Stem Cell Reports*, vol. 3, no. 4, pp. 566–573, 2014.

[26] V. Vichai and K. Kirtikara, "Sulforhodamine B colorimetric assay for cytotoxicity screening," *Nature Protocols*, vol. 1, no. 3, pp. 1112–1116, 2006.

[27] E. Shacter, J. A. Williams, M. Lim, and R. L. Levine, "Differential susceptibility of plasma proteins to oxidative modification: examination by western blot immunoassay," *Free Radical Biology & Medicine*, vol. 17, no. 5, pp. 429–437, 1994.

[28] J. L. Garcia-Gimenez, A. Gimeno, P. Gonzalez-Cabo et al., "Differential expression of PGC-1alpha and metabolic sensors suggest age-dependent induction of mitochondrial biogenesis in Friedreich ataxia fibroblasts," *PloS One*, vol. 6, no. 6, article e20666, 2011.

[29] K. Litvak and T. Schmittgen, "Analysis of relative gene expression data using real-time quantitative PCR and the 2 (-delta delta C (T)) method," *Methods*, vol. 25, no. 4, pp. 402–408, 2001.

[30] D. Hanahan and R. A. Weinberg, "Hallmarks of cancer: the next generation," *Cell*, vol. 144, no. 5, pp. 646–674, 2011.

[31] T. T. Su, "Cellular responses to DNA damage: one signal, multiple choices," *Annual Review of Genetics*, vol. 40, pp. 187–208, 2006.

[32] A. Pellicioli and M. Foiani, "Signal transduction: how Rad53 kinase is activated," *Current Biology*, vol. 15, no. 18, pp. R769–R771, 2005.

[33] K. Caldecott, "Protein ADP-ribosylation and the cellular response to DNA strand breaks," *DNA Repair*, vol. 19, pp. 108–113, 2014.

[34] P. Jagtap and C. Szabó, "Poly (ADP-ribose) polymerase and the therapeutic effects of its inhibitors," *Nature Reviews Drug Discovery*, vol. 4, no. 5, pp. 421–440, 2005.

[35] Z. Chen, H. Yang, and N. P. Pavletich, "Mechanism of homologous recombination from the RecA–ssDNA/dsDNA structures," *Nature*, vol. 453, no. 7194, pp. 489–494, 2008.

[36] E. Ledesma-Martinez, V. M. Mendoza-Nunez, and E. Santiago-Osorio, "Mesenchymal stem cells derived from dental pulp: a review," *Stem Cells International*, vol. 2016, Article ID 4709572, p. 12, 2016.

[37] T. Gong, B. C. Heng, E. C. Lo, and C. Zhang, "Current advance and future prospects of tissue engineering approach to dentin/pulp regenerative therapy," *Stem Cells International*, vol. 2016, Article ID 9204574, p. 13, 2016.

[38] M. Nakashima, K. Iohara, and M. Murakami, "Dental pulp stem cells and regeneration," *Endodontic Topics*, vol. 28, no. 1, pp. 38–50, 2013.

[39] H.-m. Zhou, Y. Shen, Z. J. Wang et al., "In vitro cytotoxicity evaluation of a novel root repair material," *Journal of Endodontics*, vol. 39, no. 4, pp. 478–483, 2013.

[40] V. Petrovic, V. Opačić-Galić, S. Živković et al., "Biocompatibility of new nanostructural materials based on active silicate systems and hydroxyapatite: in vitro and in vivo study," *International Endodontic Journal*, vol. 48, no. 10, pp. 966–975, 2015.

[41] E. Silva, T. Accorsi-Mendonça, J. F. Almeida, C. C. Ferraz, B. P. Gomes, and A. A. Zaia, "Evaluation of cytotoxicity and up-regulation of gelatinases in human fibroblast cells by four root canal sealers," *International Endodontic Journal*, vol. 45, no. 1, pp. 49–56, 2012.

[42] A. Eldeniz, K. Mustafa, D. Ørstavik, and J. E. Dahl, "Cytotoxicity of new resin-, calcium hydroxide- and silicone-based root canal sealers on fibroblasts derived from human gingiva and L929 cell lines," *International Endodontic Journal*, vol. 40, no. 5, pp. 329–337, 2007.

[43] I. Miletić, N. Devcić, I. Anić, J. Borcić, Z. Karlović, and M. Osmak, "The cytotoxicity of RoekoSeal and AH plus compared during different setting periods," *Journal of Endodontics*, vol. 31, no. 4, pp. 307–309, 2005.

[44] H. M. Zhou, S. Y. Du TF, Z. J. Wang, Y. F. Zheng, and M. Haapasalo, "In vitro cytotoxicity of calcium silicate–containing endodontic sealers," *Journal of Endodontics*, vol. 41, no. 1, pp. 56–61, 2015.

[45] S. Krifka, G. Spagnuolo, G. Schmalz, and H. Schweikl, "A review of adaptive mechanisms in cell responses towards oxidative stress caused by dental resin monomers," *Biomaterials*, vol. 34, no. 19, pp. 4555–4563, 2013.

[46] S. Camargo, C. H. Camargo, K. A. Hiller, S. M. Rode, H. Schweikl, and G. Schmalz, "Cytotoxicity and genotoxicity of pulp capping materials in two cell lines," *International Endodontic Journal*, vol. 42, no. 3, pp. 227–237, 2009.

[47] S. W. Chang, S. Y. Lee, H. J. Ann, K. Y. Kum, and E. C. Kim, "Effects of calcium silicate endodontic cements on biocompatibility and mineralization-inducing potentials in human dental pulp cells," *Journal of Endodontics*, vol. 40, no. 8, pp. 1194–1200, 2014.

[48] T. Hanaoka, N. Kawamura, K. Hara, and S. Tsugane, "Urinary bisphenol A and plasma hormone concentrations in male workers exposed to bisphenol A diglycidyl ether and mixed organic solvents," *Occupational and Environmental Medicine*, vol. 59, no. 9, pp. 625–628, 2002.

[49] I. J. Climie, D. H. Hutson, and G. Stoydin, "Metabolism of the epoxy resin component 2,2-bis [4-(2,3-epoxypropoxy) phenyl] propane, the diglycidyl ether of bisphenol A (DGEBPA) in the mouse. Part II. Identification of metabolites in urine and faeces following a single oral dose of 14C-DGEBPA," *Xenobiotica*, vol. 11, no. 6, pp. 401–424, 1981.

[50] D. H. Han, M. J. Kim, E. J. Jun, and J. B. Kim, "Salivary bisphenol-A levels due to dental sealant/resin: a case-control study in Korean children," *Journal of Korean Medical Science*, vol. 27, no. 9, pp. 1098–1104, 2012.

[51] G. Schmalz, A. Preiss, and D. Arenholt-Bindslev, "Bisphenol-A content of resin monomers and related degradation products," *Clinical Oral Investigations*, vol. 3, no. 3, pp. 114–119, 1999.

[52] S. Suarez, R. A. Sueiro, and J. Garrido, "Genotoxicity of the coating lacquer on food cans, bisphenol A diglycidyl ether (BADGE), its hydrolysis products and a chlorohydrin of BADGE," *Mutation Research*, vol. 470, no. 2, pp. 221–228, 2000.

[53] G. Ramilo, I. Valverde, J. Lago, J. M. Vieites, and A. G. Cabado, "Cytotoxic effects of BADGE (bisphenol A diglycidyl ether) and BFDGE (bisphenol F diglycidyl ether) on Caco-2 cells in vitro," *Archives of Toxicology*, vol. 80, no. 11, pp. 748–755, 2006.

[54] T. G. Kim, Y. H. Lee, N. H. Lee et al., "The antioxidant property of pachymic acid improves bone disturbance against AH plus-induced inflammation in MC-3T3 E1 cells," *Journal of Endodontia*, vol. 39, no. 4, pp. 461–466, 2013.

[55] C. H. Camargo, S. E. Camargo, M. C. Valera, K. A. Hiller, G. Schmalz, and H. Schweikl, "The induction of cytotoxicity, oxidative stress, and genotoxicity by root canal sealers in mammalian cells," *Oral Surgery, Oral Medicine, Oral Pathology, Oral Radiology, and Endodontics*, vol. 108, no. 6, pp. 952–960, 2009.

[56] R. K. Shukla, V. Sharma, A. K. Pandey, S. Singh, S. Sultana, and A. Dhawan, "ROS-mediated genotoxicity induced by titanium dioxide nanoparticles in human epidermal cells," *Toxicology in Vitro*, vol. 25, no. 1, pp. 231–241, 2011.

[57] O. Zmener, R. Martinez Lalis, C. H. Pameijer, C. Chaves, G. Kokubu, and D. Grana, "Reaction of rat subcutaneous connective tissue to a mineral trioxide aggregate–based and a zinc oxide and eugenol sealer," *Journal of Endodontics*, vol. 38, no. 9, pp. 1233–1238, 2012.

[58] N. F. Villeneuve, Z. Sun, W. Chen, and D. D. Zhang, "Nrf2 and p21 regulate the fine balance between life and death by controlling ROS levels," *Cell Cycle*, vol. 8, no. 20, pp. 3255–3256, 2009.

[59] M. R. Leonardo, L. A. Bezerra da Silva, M. T. Filho, and R. Santana da Silva, "Release of formaldehyde by 4 endodontic sealers," *Oral Surgery, Oral Medicine, Oral Pathology, Oral Radiology, and Endodontology*, vol. 88, no. 2, pp. 221–225, 1999.

[60] S. Pfuhler and H. Uwe Wolf, "Detection of DNA-crosslinking agents with the alkaline comet assay," *Environmental and Molecular Mutagenesis*, vol. 27, no. 3, pp. 196–201, 1996.

[61] G. Candeiro, C. Moura-Netto, R. S. D'Almeida-Couto et al., "Cytotoxicity, genotoxicity and antibacterial effectiveness of a bioceramic endodontic sealer," *International Endodontic Journal*, vol. 49, no. 9, pp. 858–864, 2015.

[62] K. L. Van Landuyt, B. Geebelen, M. Shehata et al., "No evidence for DNA double-strand breaks caused by endodontic sealers," *Journal of Endodontics*, vol. 38, no. 5, pp. 636–641, 2012.

[63] J. Mahdi, M. A. Alkarrawi, A. J. Mahdi, I. D. Bowen, and D. Humam, "Calcium salicylate-mediated apoptosis in human HT-1080 fibrosarcoma cells," *Cell Proliferation*, vol. 39, no. 4, pp. 249–260, 2006.

[64] C. V. Bin, M. C. Valera, S. E. Camargo et al., "Cytotoxicity and genotoxicity of root canal sealers based on mineral trioxide aggregate," *Journal of Endodontics*, vol. 38, no. 4, pp. 495–500, 2012.

[65] M. Parirokh and M. Torabinejad, "Mineral trioxide aggregate: a comprehensive literature review—part III: clinical applications, drawbacks, and mechanism of action," *Journal of Endodontics*, vol. 36, no. 3, pp. 400–413, 2010.

[66] M. Kuratate, K. Yoshiba, Y. Shigetani, N. Yoshiba, H. Ohshima, and T. Okiji, "Immunohistochemical analysis of nestin, osteopontin, and proliferating cells in the reparative process of exposed dental pulp capped with mineral trioxide aggregate," *Journal of Endodontia*, vol. 34, no. 8, pp. 970–974, 2008.

[67] B. N. Lee, K. N. Lee, J. T. Koh et al., "Effects of 3 endodontic bioactive cements on osteogenic differentiation in mesenchymal stem cells," *Journal of Endodontia*, vol. 40, no. 8, pp. 1217–1222, 2014.